

University of Rhode Island

DigitalCommons@URI

Open Access Master's Theses

1985

A GEOPHYSICAL INVESTIGATION OF SALT WATER INTRUSION INTO A COASTAL AQUIFER SOUTH DARTMOUTH, MASSACHUSETTS

Richard Kowalski

University of Rhode Island

Follow this and additional works at: <https://digitalcommons.uri.edu/theses>

Terms of Use

All rights reserved under copyright.

Recommended Citation

Kowalski, Richard, "A GEOPHYSICAL INVESTIGATION OF SALT WATER INTRUSION INTO A COASTAL AQUIFER SOUTH DARTMOUTH, MASSACHUSETTS" (1985). *Open Access Master's Theses*. Paper 2011. <https://digitalcommons.uri.edu/theses/2011>

This Thesis is brought to you by the University of Rhode Island. It has been accepted for inclusion in Open Access Master's Theses by an authorized administrator of DigitalCommons@URI. For more information, please contact digitalcommons-group@uri.edu. For permission to reuse copyrighted content, contact the author directly.

A GEOPHYSICAL INVESTIGATION OF
SALT WATER INTRUSION
INTO A
COASTAL AQUIFER
SOUTH DARTMOUTH, MASSACHUSETTS
BY
RICHARD G. KOWALSKI

A THESIS SUBMITTED IN PARTIAL FULFILLMENT OF THE
REQUIREMENTS FOR THE DEGREE OF
MASTER OF SCIENCE
IN
GEOLOGY

UNIVERSITY OF RHODE ISLAND

1985

ABSTRACT

The withdrawal of fresh groundwater from a coastal aquifer may induce the flow of salt water from the sea towards the well. This migration of salt water into a fresh water aquifer is known as salt water intrusion.

The single most important design factor of a fresh water supply well in a coastal area is the depth to the salt/fresh water interface. In many cases salt water intrusions could probably be minimized if the position of the salt/fresh water interface could be determined before a domestic or municipal well is installed. In some highly developed coastal areas the position of the salt/fresh water interface has been determined in numerous boreholes. The extensive field data collected was then used to predict how various pumping schemes would affect the position of the interface with the use of computer modeling. Pinder and Page (1976) used this type of approach for a study on Long Island. However, on a smaller scale, the drilling of boreholes may be prohibitively expensive and the use of computer modeling out of the question.

In this study the depth to the salt/fresh water interface was determined adjacent to a deep borehole by performing a Vertical Electrical Sounding (VES). The depth to the interface as determined by the VES was in agreement with the observed depth in the borehole.

Vertical Electrical Soundings were also made in other areas in order to determine if the method could be successfully applied to determine the depth to the salt/fresh water interface in locations without deep boreholes. In order to make this evaluation the depths to the salt/fresh water interface as determined from the VES curve interpretations in these areas were compared with the water quality data obtained in shallow wells and with the results of applying three theoretical methods. The three methods, described by Kashef (1983), Todd (1980) and Glover (1959), all provide solutions for the depth to a salt/fresh water under natural (nonpumping) conditions.

The depth to the salt/fresh water interface as determined by the Vertical Electrical Soundings was in agreement with the theoretical calculations in the areas where the position of the interface was not greatly affected by the pumping of fresh water from the aquifer. However, in the areas where the position of the salt/fresh water interface was known to have been affected by pumping, the depth to the interface interpreted from the VES curves was always less than predicted by the three theoretical methods.

ACKNOWLEDGEMENTS

I welcome the opportunity to thank those associated with this study and its development throughout my years at the University of Rhode Island. The research was supported by a grant from the Katherine Nordell Lloyd Center for Environmental Studies.

I am particularly grateful to Dr. Reinhard K. Frohlich for giving freely of his time and providing valuable guidance and suggestions during the study. His avid pursuit of the development of the electrical resistivity method in groundwater studies provided the incentive for this research.

Appreciation is extended to Dr. Daniel W. Urish for detailed explanations of his work in salt water intrusion.

I am indebted to the Rhode Island Water Resources Center and Dr. William E. Kelly for assisting in the funding of my graduate studies.

The assistance of my fellow graduate students is greatly appreciated throughout these years, especially David Sanders, Tim Pac, and Murray Rosenberg.

Finally, I must thank my wife, Lisa C. Duhaime for her inspiration, support, unending encouragement and understanding throughout this undertaking.

TABLE OF CONTENTS

	PAGE
ABSTRACT	ii
ACKNOWLEDGEMENTS	iii
TABLE OF CONTENTS	iv
LIST OF FIGURES	vii
LIST OF TABLES	x
1.0 INTRODUCTION	1
2.0 THE SALT/FRESH WATER INTERFACE IN A COASTAL AQUIFER	7
2.1 The Ghyben-Herzberg Relation	7
2.2 Theoretical Approaches to Salt Water Intrusion	9
2.3 The Analytical Solutions Applied in this Investigation	12
2.4 The Disturbance of a Natural Salt/Fresh Water Interface	22
2.5 Previous Applications of the Electrical Resistivity Method to the Problem of Salt Water Intrusion	26
3.0 GEOLOGY AND HYDROGEOLOGY OF THE STUDY AREA	28
3.1 Surficial and Bedrock Geology	28
3.2 Hydrogeologic Characteristics of the Study Area	33
4.0 GEOPHYSICAL DEFINITION OF THE SALT/FRESH WATER INTERFACE	40
4.1 Theory of Direct Current Electrical Resistivity	40
4.2 Methodology	41
4.3 Interpretation of Vertical Electrical Soundings	43
4.31 Archie's law and the formation factor	52
4.4 Limitations on the Interpretation of VES Curves	55
4.5 Instrumentation	57
4.6 Location of the Test Sites	60
4.7 Data Interpretations	63
5.0 DISCUSSION OF RESULTS	64
5.1 Vertical Electrical Sounding #1	64
5.2 Vertical Electrical Sounding #2	74
5.3 Vertical Electrical Sounding #3	79
5.4 Vertical Electrical Sounding #4	84

5.5	Vertical Electrical Sounding #5	88
5.6	Vertical Electrical Sounding #6	93
5.7	Vertical Electrical Sounding #7	97
5.8	Vertical Electrical Sounding #8	103
5.9	Vertical Electrical Sounding #9	108
5.10	Vertical Electrical Sounding #10	112
5.11	Vertical Electrical Sounding #11	114
6.0	SUMMARY	117
7.0	REFERENCES	122

APPENDICES

A:	Kashef's Modification of the Ghyben-Herzberg Equation	127
B:	Glover's Solution for the Pattern of Fresh Water Flow in a Coastal Aquifer	137
C:	Todd's Solution for a Fresh Water Lens Under an Oceanic Island	142
D:	Tide Gauge Data for the Determination of Mean Sea Level	154
E:	Well Elevation Survey Data	159
F:	Well Gauging Data	164
G:	Determining Aquifer Hydraulic Conductivity by the Tidal Method	167
H:	Salinity, Temperature and Specific Conductivity Measurements	177
I:	Constant Head Soil Permeability Test	182
J:	Soil Porosity	187
K:	Vertical Electrical Sounding Field Data	190
L:	Computer Program For VES Curve Interpretation	201

LIST OF FIGURES

1.	Examples of salt/fresh water interfaces in three coastal aquifers	2
2.	Study area location map	5
3.	Schematic of the Ghyben-Herzberg relation	8
4.	Ghyben-Herzberg interface for a nearly horizontal water table surface	10
5.	Difference between the Ghyben-Herzberg interface and the true interface	14
6.	Difference between the Ghyben-Herzberg interface and the interface as determined by Kashef	17
7.	Flow net used by Glover to determine the depth to a salt/fresh water interface	19
8.	Configuration of an interface beneath an oceanic island as determined by Todd	21
9.	Induced upconing of a salt/fresh water interface	25
10.	Study area bedrock geology	29
11.	Rose diagram of the strike orientations of the surface bedrock fractures in the study area	31
12.	Location map of wells and fracture measurements	32
13.	Idealized cross-section of part of study area	35
14.	Electrode configurations for vertical electrical soundings	42
15.	Example plot of field data obtained from a vertical electrical sounding	44
16.	Example of a Resistivity-Depth model	45
17.	First step of interpretation of field data using Master Curves	48
18.	Second step of interpretation of field data using Master Curves	50

LIST OF FIGUREScontinued

19. Summary of the two step Master Curve interpretation of the curve in figures 17 and 18 51

20. Electrical resistivity equipment schematic 58

21. VES location map, northern section of study area 61

22. VES location map, southern section of study area 62

23a. VES 1 field data with best match theoretical curve 66

 b. Depth to the salt/fresh water interface as measured by VES 1 and as theoretically calculated 69

24a. VES 2 field data with best match theoretical curve 75

 b. Depth to the salt/fresh water interface as measured by VES 2 and as theoretically calculated 76

25a. VES 3 field data with best match theoretical curve 80

 b. Depth to the salt/fresh water interface as measured by VES 3 and as theoretically calculated 82

26a. VES 4 field data with best match theoretical curve 85

 b. Depth to the salt/fresh water interface as measured by VES 4 and as theoretically calculated 86

27a. VES 5 field data with best match theoretical curve 89

 b. Two possible Resistivity-Depth models for the interpretation of VES 5 90

 c. Depth to the salt/fresh water interface as measured by VES 5 and as theoretically calculated 92

28a.	VES 6 field data with best match theoretical curve	94
	b. Depth to the salt/fresh water interface as measured by VES 6 and as theoretically calculated	95
29a.	VES 7 field data with best match theoretical curve	98
	b. Depth to the salt/fresh water interface as measured by VES 7 and as theoretically calculated	101
30a.	VES 8 field data with best match theoretical curve	104
	b. Depth to the salt/fresh water interface as measured by VES 8 and as theoretically calculated	105
31a.	VES 9 field data with best match theoretical curve	109
	b. Depth to the salt/fresh water interface as measured by VES 9 and as theoretically calculated	110
32.	VES 10 field data	113
33.	VES 11 field data	115
34.	Explanation of symbols used in Todd's method .	143
35.	Tide gauge chart recording	155
36.	Chart recording of water level fluctuations in Well 2	173
37.	Calibration curve for the salinity meter . . .	178

LIST OF TABLES

1.	Measured hydrogeologic parameters	37
2.	Resistivity-Depth models for VES 1	68
3.	Formation Factors	73
4.	Resistivity-Depth models for VES 7	100
5.	Theoretical and Measured Depths to a Salt/Fresh Water Interface: Chaypee Hill .	118
6.	Theoretical and Measured Depths to a Salt/Fresh Water Interface: Plummer and Berg Properties	119
7.	Theoretical and Measured Depths to a Salt/Fresh Water Interface: Potomska Point	120
8.	Depths to the interface using Glover's method .	141
9.	Well gauging data	165
10.	Tidal method data	175
11.	Salinity, temperature and specific conductivity data	180
12.	VES 1 field data	190
13.	VES 2 field data	191
14.	VES 3 field data	192
15.	VES 4 field data	193
16.	VES 5 field data	194
17.	VES 6 field data	195
18.	VES 7 field data	196
19.	VES 8 field data	197
20.	VES 9 field data	198
21.	VES 10 field data	199
22.	VES 11 field data	200

1.0 INTRODUCTION

Salt water intrusion, which is defined as the displacement or mixing of fresh ground water with saline water, is the most common form of fresh ground water contamination. The phenomenon generally occurs due to activities of man. Salt water intrusion can occur in deep aquifers with the upward advance of saline waters of geologic origin, in shallow aquifers from surface waste discharges, and in coastal aquifers from an invasion of sea water. It has been found that salt water intrusion has occurred in localities of most parts of the United States. However, the problem of sea water intrusion along coasts has received the most attention (Todd, 1980).

Under natural conditions, fresh groundwater is continually discharged to the ocean in most coastal areas of the world. This underground flow of fresh water seaward tends to balance the underground flow of salt water landward. Due to the difference in density between the fresh and salt water a curvilinear interface usually forms as shown in Figure 1. However, when private or municipal wells tap the fresh water in coastal aquifers, the seaward flow of fresh groundwater may be decreased or even reversed. The continued pumping of fresh water beyond some critical point may induce a flow of salt water from the sea toward the well. Once the sea water travels inland to the well field, the underground aquifer will become

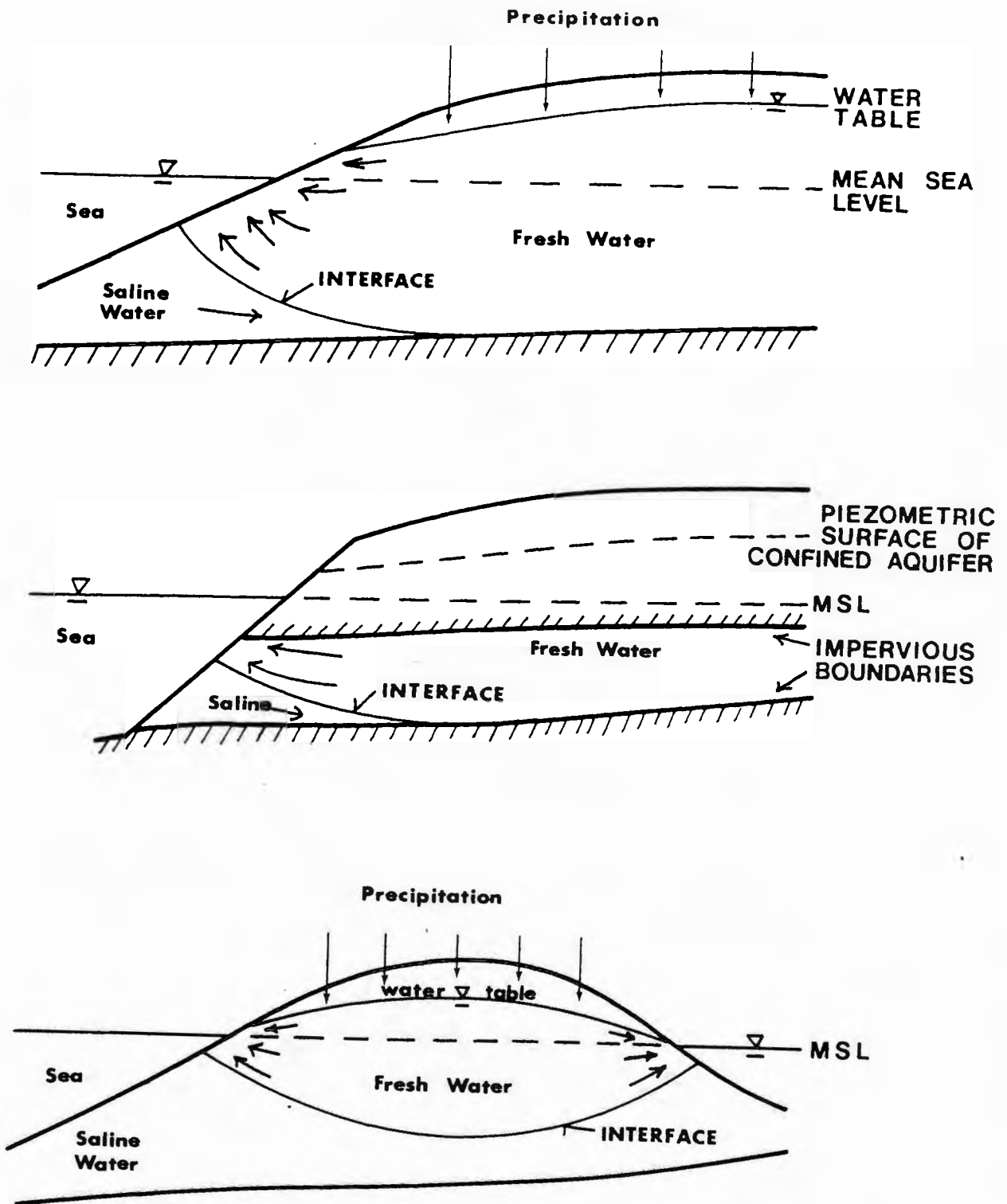


Figure 1. Examples of salt/fresh water interfaces in three coastal aquifers; top, unconfined aquifer, middle, confined aquifer, and bottom, unconfined aquifer on an island. After Bear, 1979.

contaminated and it may take years to displace the salt from the aquifer even if adequate fresh ground water is available.

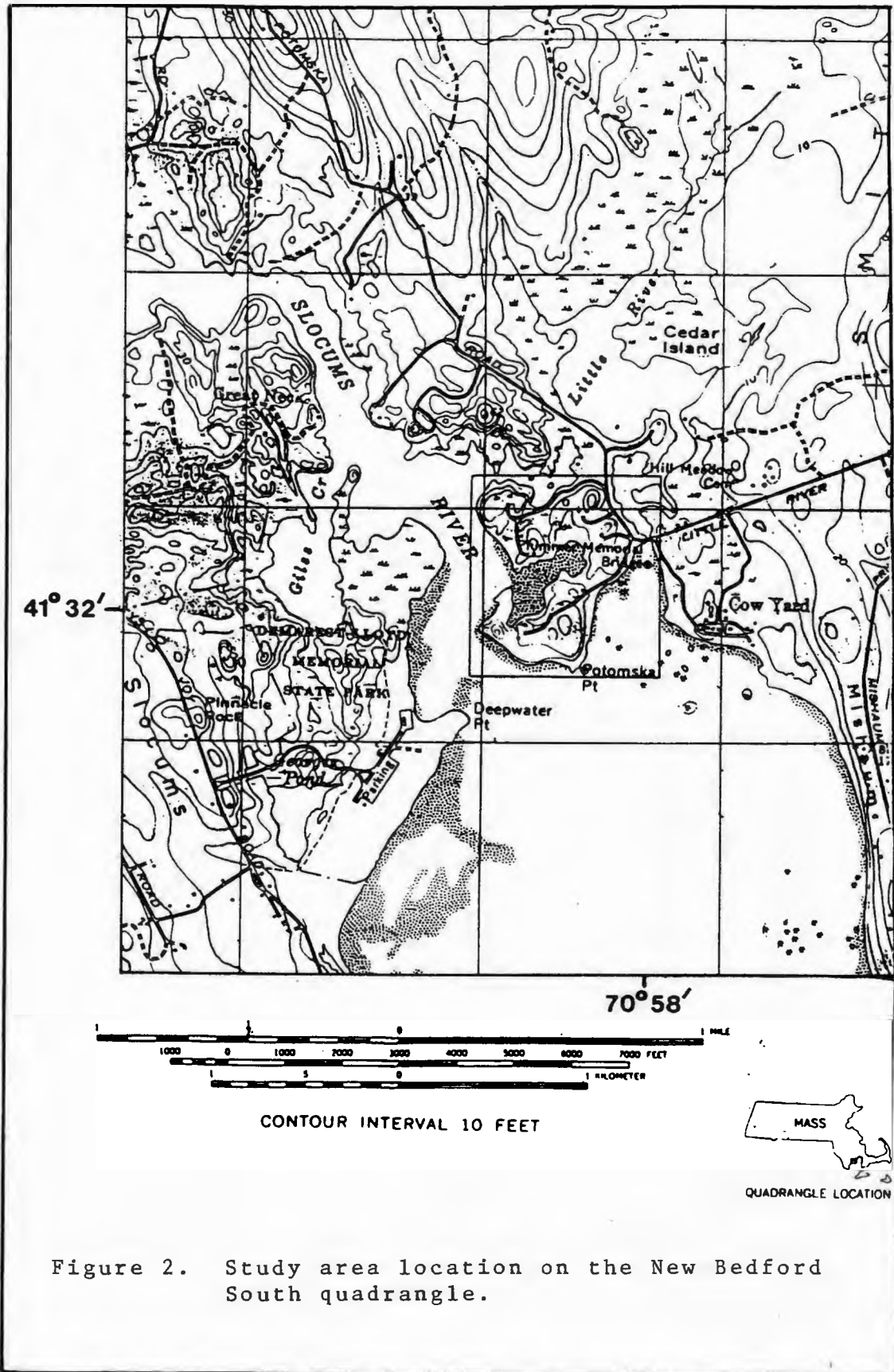
When a well is designed for the purpose of providing fresh water in a coastal area, the single most important design factor is the depth to the salt water - fresh water interface. In many cases salt water intrusions could probably be minimized if the position of the salt - fresh water interface could be determined before a domestic or municipal well is installed. In some highly developed coastal areas the position of the salt - fresh water interface has been determined in numerous boreholes for planning purposes. In one case, extensive field data collected from boreholes has been used to predict how various pumping schemes would affect the position of a salt - fresh water interface using a complex computer model. (Pinder and Page, 1976).

The development of computer numerical techniques has made possible the implementation of successful water management schemes in areas susceptible to salt water intrusion. However, in the area under investigation the use of exploratory boreholes and computer modeling techniques would not be practical. The study area is typical of many coastal resorts in that fresh water is supplied by individual wells with the peak demand for water falling in the dry summer months. The site under

investigation is located in South Dartmouth, Massachusetts. The study area, shown in Figure 2, is an irregularly shaped peninsula which extends into an estuary. Local residents have been experiencing difficulties in obtaining fresh ground water for at least the past fifty years. Since the area is virtually surrounded on all sides by salt water and does not receive any influx of fresh groundwater from the mainland, it is not surprising that the residents have had to abandon wells which have drawn in salt water. The only 'solution' which is typically applied is the drilling or excavation of a new well in another area and pumping that well until it too has to be abandoned.

The need for a method which can provide reasonably accurate information on the position of salt - fresh water interfaces in situations which involve the small-scale development of a coastal aquifer is obvious from the situation described above. If the depth to the salt - fresh water interface could be determined before a well was installed for a private fresh water supply, the well could be properly designed and managed to best suit the situation.

The electrical resistivity method is well suited for the delineation of a salt - fresh water interface. The method has been successfully employed in this capacity by other workers, but in all of the cases reviewed there have been numerous deep boreholes available for the calibration



of the Vertical Electrical Sounding (VES) curves. Therefore, the main objective of this investigation will be to determine if the depth to a salt - fresh water interface can be measured using the electrical resistivity method along with the use of only limited shallow wells. Also to be determined will be the effect that the withdrawal of fresh groundwater has had on the availability of potable groundwater in this aquifer. In order to make these determinations, the values for the depth to the salt/ fresh water interface as determined by the electrical resistivity method will be compared with the results of three theoretical calculations for the depth to the interface. These three methods, all of which are based on the Ghyben-Herzberg relation (Ghyben, 1889 and Herzberg, 1901), yield values for the depth to the salt/fresh water interface under nonpumping conditions. When these theoretical calculations are compared with the depths to the interface as determined from the VES curve interpretations, the amount of salt water intrusion which has occurred may be determined.

2.0 THE SALT/FRESH WATER INTERFACE IN A COASTAL AQUIFER

2.1 The Ghyben-Herzberg Relation

Two investigators working independently, Ghyben (1889) and Herzberg (1901), were the first to recognize that fresh groundwater floats above salt water in coastal aquifers because of its lower density. These two investigators found that salt water occurred underground along the coast not at sea level but, at a depth below sea level of about forty times the height of the fresh groundwater above sea level. The equation derived by Ghyben and Herzberg explains the distribution of salt and fresh water in coastal aquifers based on the hydrostatic equilibrium which exists between two fluids of different densities. The Ghyben-Herzberg relation yields a value for the depth to a salt water interface below sea level, z :

$$z = [p_f / (p_s - p_f)] H_f \quad (1)$$

where p_f and p_s are the densities of fresh and salt water and z and h_f are as shown in Figure 3. It must be emphasized that this figure is based on a hydrostatic balance and is therefore highly idealized. In actual coastal situations there is a hydrodynamic balance between the fresh and salt water because fresh water flows toward the sea and is discharged through a seepage face as shown in Figure 1. Note that there is no seepage face in Figure 3. From density considerations alone, without fresh water

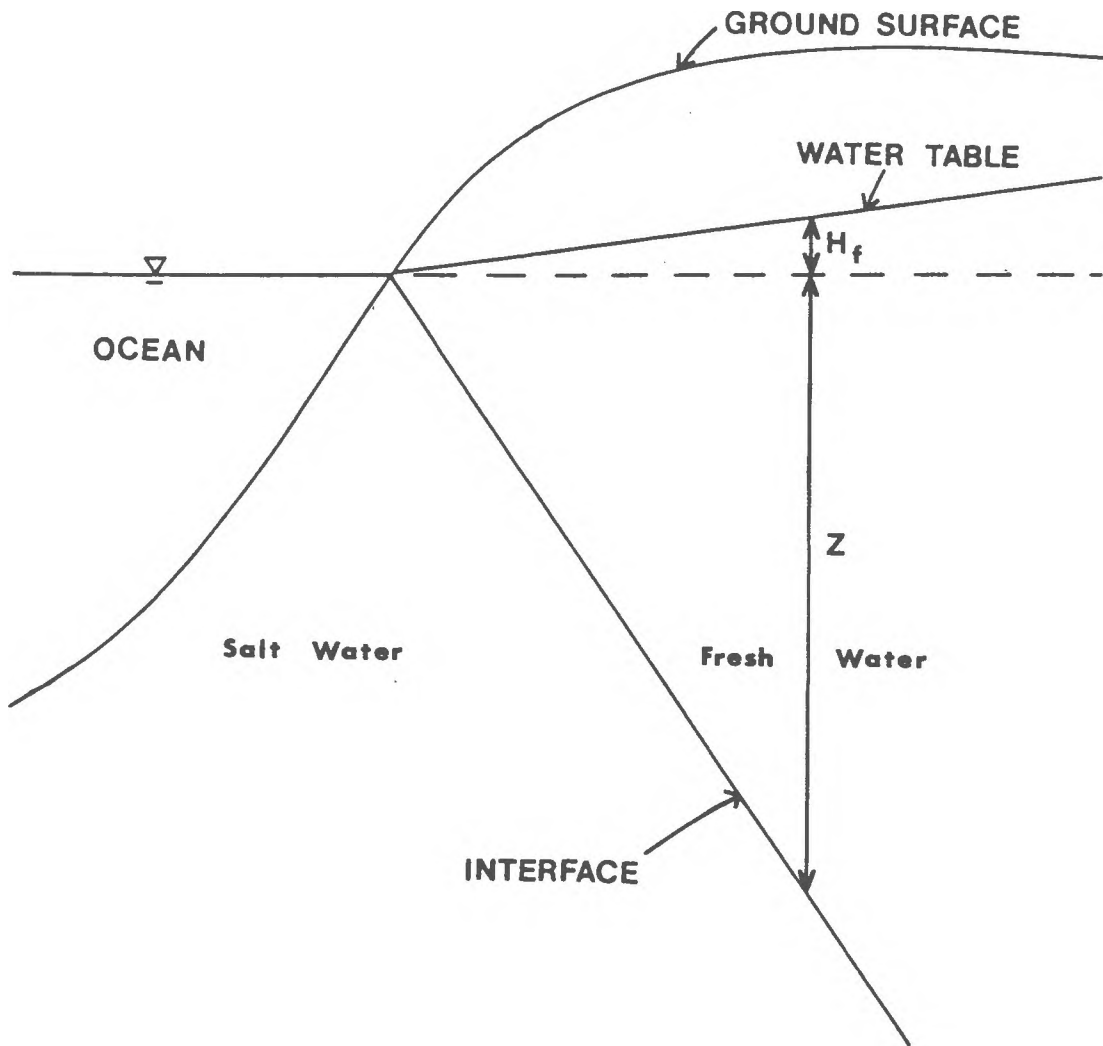


Figure 3. Idealized sketch of fresh and salt water distributions in an unconfined coastal aquifer according to the Ghyben-Herzberg relation.

flow, a horizontal interface would develop with fresh water everywhere floating above salt water as depicted in Figure 4. It has been shown that where the flow is nearly horizontal, the Ghyben-Herzberg relation gives satisfactory results. Only near the shoreline, where upward vertical flow components are greatest (see figure 1a), do significant errors in the position of the interface occur.

2.2 Theoretical Approaches to Salt Water Intrusion

During the last four decades, the use of the Ghyben-Herzberg relation to determine the position of the salt/fresh water interface in coastal aquifers has been questioned by many investigators. Hubbert (1940) was the first to recognize that the position of the salt/fresh water interface could be influenced by the movement of the water. He also proved the analogy between the interface in salt water intrusion problems and the free surface in a two-dimensional gravity flow system. Later, various investigators (Glover, 1959; Henry, 1959; Cooper, 1959; and Fetter, 1972), developed analytic solutions which took into account the hydrodynamic effects, each with the use of different mathematical procedures. With the advent of the computer era, the various numerical solutions are now more practical and have been extensively refined. Computer models which numerically simulate salt/fresh water interfaces have been developed for parts of Long Island

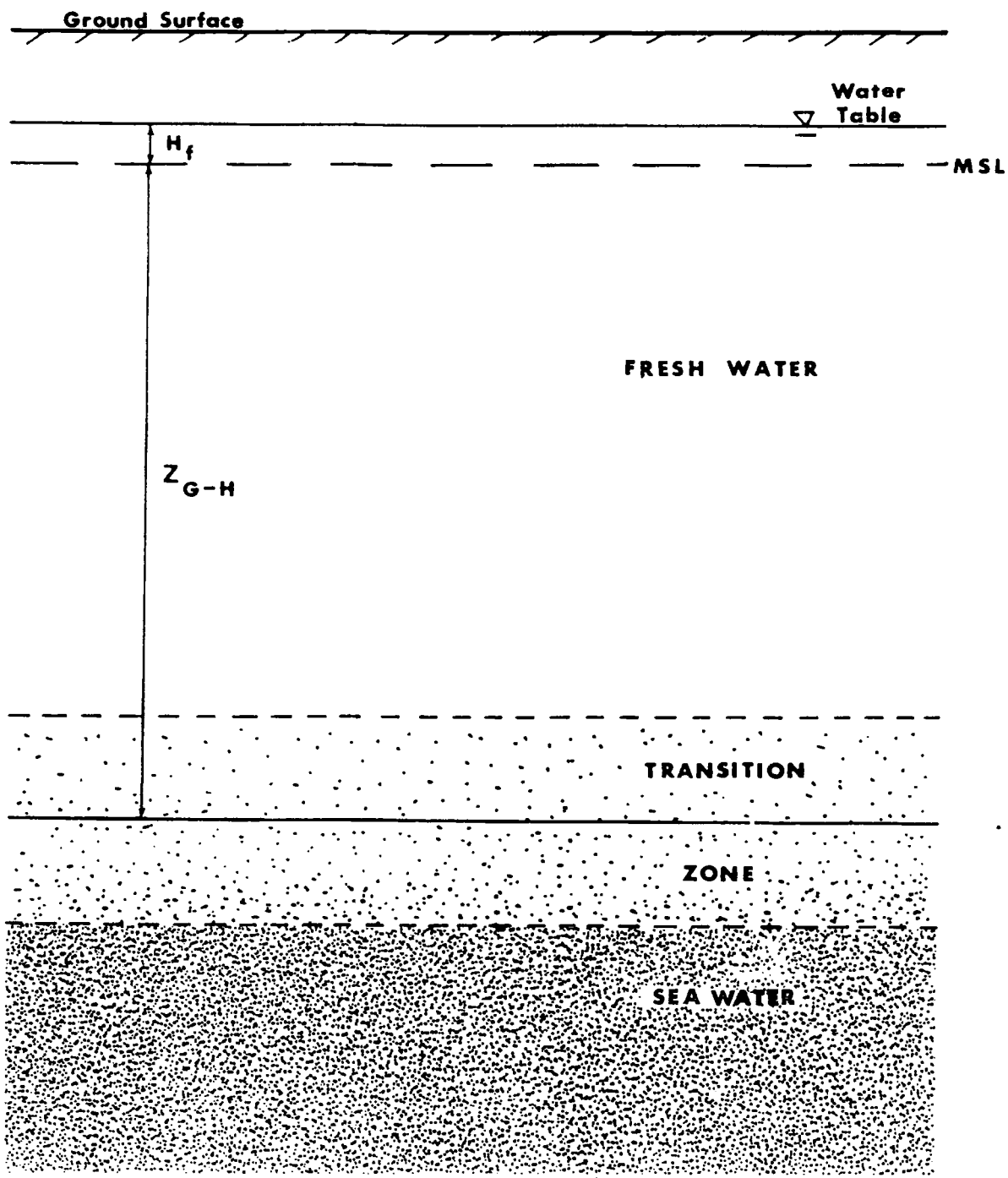


Figure 4. The calculated depth to the interface using the Ghyben-Herzberg relation (Z_{G-H}) is most accurate when both the water table and the interface are nearly horizontal.

(Pinder and Page, 1976), Hawaii (Liu et al, 1983) and other areas.

There are several approaches to the study of sea water intrusion. In most cases the fresh water and salt water in the aquifer is assumed to be immiscible and a sharp interface exists between the two fluids. However, a sharp interfacial boundary between fresh and salt water does not occur under field conditions. Instead, a zone of brackish water of finite thickness separates the two fluids as shown in Figure 4. This zone develops from dispersion by flow of the fresh water plus unsteady displacements of the interface by external influences such as tides, recharge, and the pumping of wells (Cooper, 1964).

The importance of the transition zone in the realm of coastal groundwater management is a current area of controversy. Although numerous investigations have been conducted, the results are still inconclusive and cannot be applied by ground water managers. However, the results of the investigations on the transition zone which have been completed do seem to indicate that the importance of the transition zone depends on the specific hydrogeologic conditions which exist in the area of concern (Kashef, 1977). Consequently, only a few researchers have developed solutions for the movement of the salt/fresh water interface in coastal aquifers which include the effect of dispersion of salts into a transition zone. Pinder and

Cooper (1970) were successful in their attempt to combine the equations of ground water with those of hydrodynamic dispersion using a numerical technique.

In general, most of the theoretical approaches that have been developed are capable of predicting the depth to a salt/fresh water interface under ideal conditions. These analytical solutions are of value only if they include the most probable ranges of natural conditions. Because salt/fresh water interfaces are affected by so many factors, any method used must introduce some idealized assumptions in order to develop or solve equations under specific hydraulic and geometric boundary conditions. A summary of the methods used and the assumptions made by the various investigators in arriving at their solutions appears in an article by Kashef (1977).

2.3 The Analytical Solutions Applied in this Investigation

In order to check the results obtained using the electrical resistivity method, three theoretical methods have been applied by this investigator. The three methods are all based on the Ghyben-Herzberg relation but, each method relies on the use of different assumed idealized conditions.

The equation used in the first method is written in terms of the Ghyben-Herzberg solution with the addition of

a correction factor. This equation was developed by Kashef, who in 1983 reviewed the most refined and acceptable of the highly complex solutions already developed and compared them with the Ghyben-Herzberg results under a wide range of natural conditions. He found that the Ghyben-Herzberg principle is valid for most practical purposes and that the difference between the location of the interface predicted by the Ghyben-Herzberg relation and those determined by the more complex methods may be less than the difference resulting from small errors in the field measurements of water table elevations.

The correction factors included in Kashef's equations listed on the following pages allow for more precision within zones close to the shore. This correction was found to be necessary because the Ghyben-Herzberg solution does not take into account the movement of the fresh water and therefore always underestimates the depth to the true interface, as shown by Figure 5. The method is simply applied by using field measurements of water levels in observation wells.

The method employs the use of two equations which yield values for the depth to an interface below sea level assuming that either a horizontal or a vertical fresh water outflow face exists. The two equations from Kashef (1983) are:

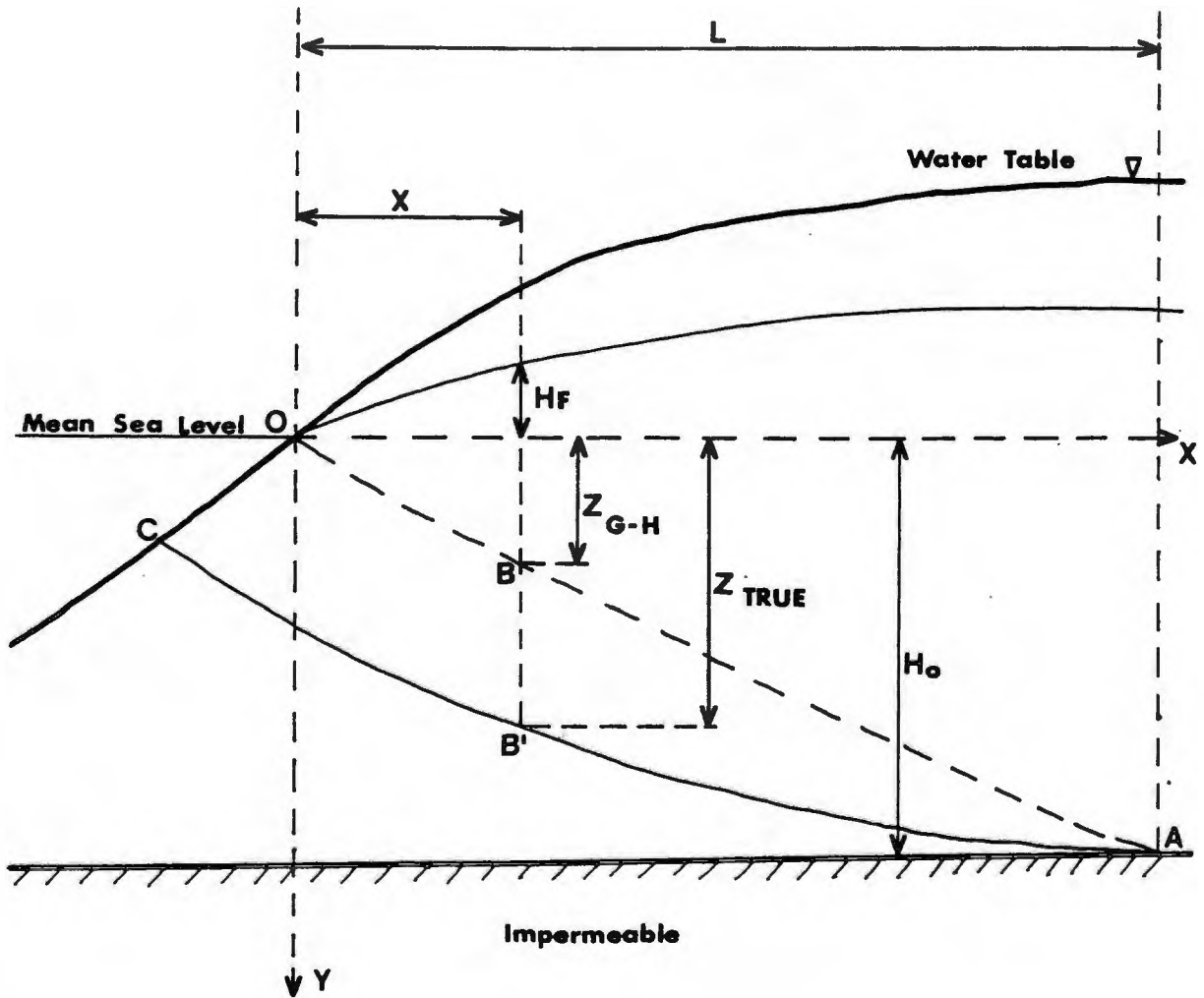


Figure 5. Diagrammatic sketch indicating the Ghyben-Herzberg interface (ABO) and the true interface (AB'C). Differences are exaggerated. After Kashef (1983).

$$z_v/H_o = \sqrt{(H_f/a H_o)^2 + 0.1375 (1-\bar{x}) / (m^2)} \quad (2)$$

$$z_h/H_o = \sqrt{(H_f/a H_o)^2 + .25 m^2} \quad (3)$$

where z_h and z_v are respectively, the depths of the interface below sea level assuming a horizontal and a vertical outflow face and H_o is the vertical distance between sea level and the underlying impervious boundary of an unconfined aquifer. All of the terms on the right side of both equations are either obtained from field measurements or are calculated using the field measurements. The first step taken in applying these equations is the calculation of the theoretical maximum upstream fresh water head at the point of maximum landward extent of the salt water wedge at $x = L$, as pictured in Figure 5. The maximum upstream head is:

$$a H_o / p_f \quad (4)$$

where $a = (p_s - p_f)$ and H_o is the vertical distance between sea level and the underlying impervious boundary of the unconfined aquifer. Using this value the theoretical distance of the intruded salt water wedge from the shoreline (L) is calculated:

$$L = a H_o / 2 i p_f \quad (5)$$

where i is the hydraulic gradient in the aquifer. The next step is the calculation of the ratio between L and H_o . This ratio is designated as m :

$$m = L/H_o \quad (6)$$

The last term which must be calculated, \bar{x} , which is defined

as x/L , is obtained by using the depth below sea level to the salt water wedge (Z) as determined by the basic Ghyben-Herzberg relation. The Ghyben-Herzberg depth, Z , is determined using the field measurement of the height of fresh water above sea level (H_f) in a borehole divided by (a), which was defined previously.

$$Z = H_f p_f/a \quad (7)$$

The term \bar{x} is then obtained by solving for it in the following relation:

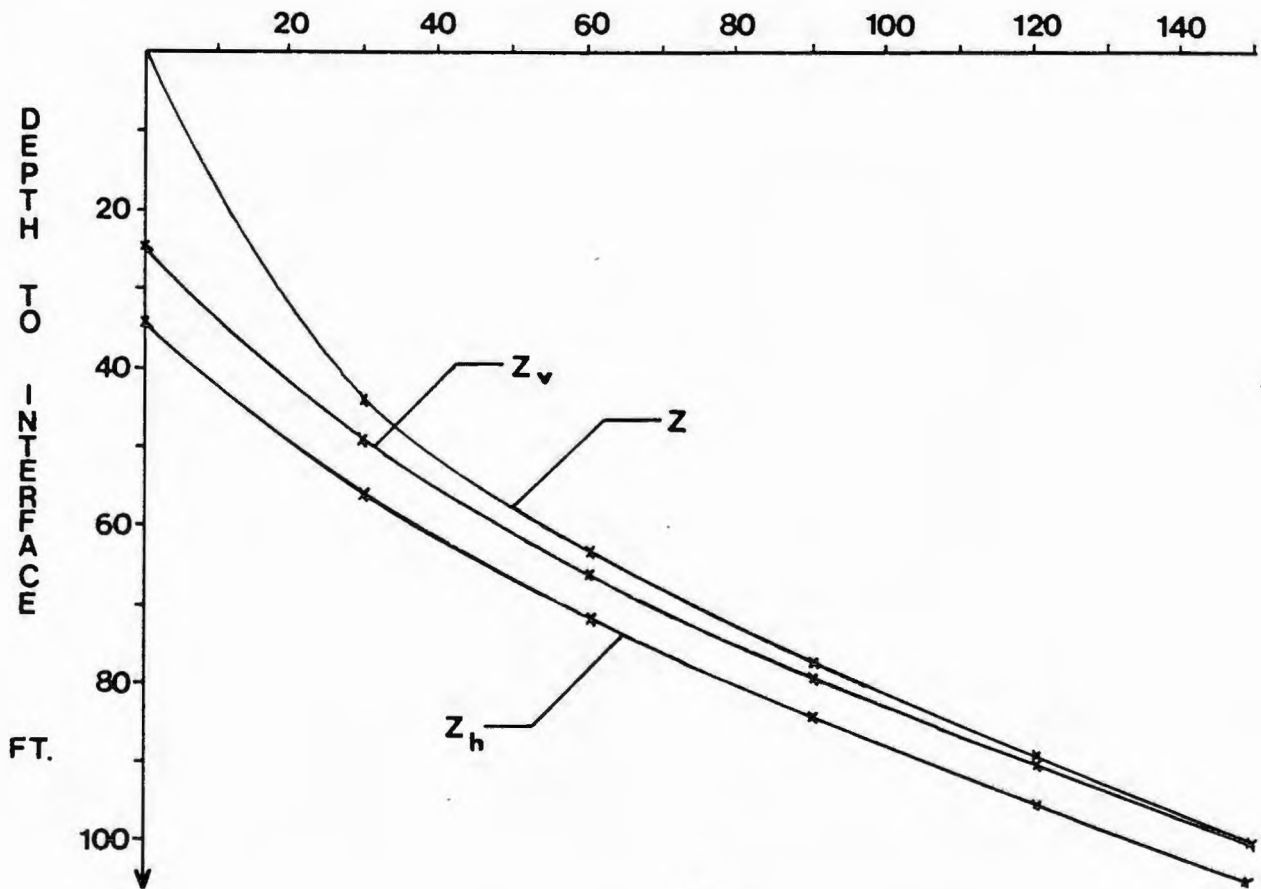
$$Z = H_o \sqrt{(\bar{x})} \quad (8)$$

The application of these terms and of the field measurements in equations 2 and 3 yield values for the depth to the salt/fresh water interface which will always both be larger than the depth as determined by the simple Ghyben-Herzberg relation (Z). The amount of difference between the calculated depth to the salt water interface, using the Ghyben-Herzberg relation versus Kashef's method above depends on where the point of interest is in relation to the shoreline. Figure 6 shows that the closer the point of measurement to the salt water interface is to the shoreline, the greater is the error using the simple Ghyben-Herzberg relation. Part A of this figure also shows that the further inland the salt water wedge extends (L), the less error there is when using the simple Ghyben-Herzberg relation. A sample calculation and the results of the application of this method to the field data is presented in Appendix A and in Section IV.

L \ X	0 30 60 90 120 150 FT						
	150	Z_v	24.7	49.9	66.1	79.0	90.1
Z_h		33.3	55.8	71.5	84.3	95.4	105.4
Z		0.0	44.7	63.2	77.4	89.4	100.0
300 FT	Z_v	12.4	33.7	46.1	55.7	64.0	71.2
	Z_h	16.7	35.7	47.7	57.3	65.4	72.2
	Z	0.0	31.6	44.7	54.7	63.2	70.7

A

DISTANCE FROM SHORELINE (X) FEET



B

Figure 6. Comparison between the depth to a salt/fresh water interface as determined by the Ghyben-Herzberg relation (Z) and the two equations developed by Kashef (Z_v and Z_h). After Kashef (1983).

The second theoretical method used in this investigation was developed by Glover (1959) using a conformal mapping technique. In this method the interface is still assumed to be a sharp boundary between the salt and fresh water. Unlike the Ghyben-Herzberg relation though, this method does take into account that the fresh water outflow occurs over a certain area rather than at a point (Figure 7), and that vertical flow components occur in the aquifer as the fresh water moves up along the fresh/salt water interface to the outflow area. With the assumption that the outflow surface is horizontal, Glover developed the following approximate equation for the depth to the salt/fresh water interface, Z:

$$z^2 = \frac{2 Q x}{a K} - \left[\frac{Q}{a K} \right]^2 \quad (9)$$

where Q = flow in the aquifer per unit width of shoreline
 K = hydraulic conductivity of the aquifer
 x = distance from the shoreline
 a = salt water density minus fresh water density

A plot of the flow net upon which Glover based his solution for the fresh/salt water interface is depicted in Figure 7. A sample calculation and the results of the application of this method to the field data is presented in Appendix B and in Section IV.

Glover also presented an equation for the width of the gap (W) through which the fresh water escapes to the sea. The solution will not be presented here but, the comment Glover made in regard to his flow net analysis of the flow

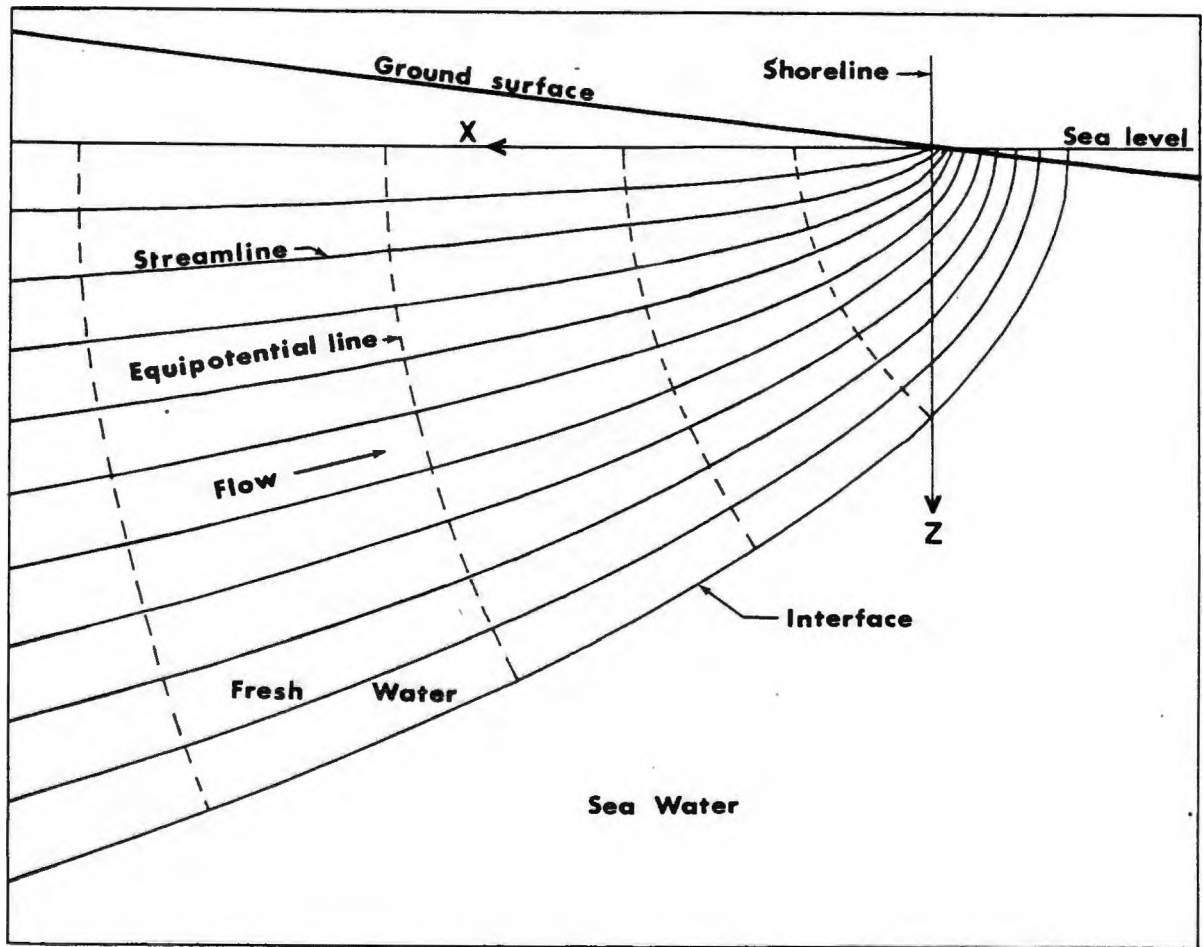


Figure 7. Flow net depicting the flow of fresh water in a coastal aquifer and the resulting salt/fresh water interface. After Glover (1964).

pattern near a beach will be. According to Glover, if the supply of fresh water to the aquifer decreases so that Q decreases, then the width of the gap through which the fresh water can escape also decreases. Also, the seaward flow of fresh water is proportional to the square of the hydraulic potential measured at a selected distance x from the shoreline. Therefore, in times of drought, the fresh water body is conserved because the seaward flow of fresh water is diminished.

The third method used in this investigation to determine the depth to the fresh/salt water interface was developed by Todd (1980) for small oceanic landmasses. The study area meets the requirements of a small oceanic landmass since it is essentially surrounded by saline water on all sides. Because fresh groundwater in this situation is supplied entirely by rainfall, only a limited amount is available. From the Dupuit assumptions (see Appendix C) and the Ghyben-Herzberg relation an approximate fresh water boundary can be determined. Assuming a circular island of radius R , as shown in Figure 8, receiving an effective recharge from rainfall at a rate W , the outward flow of fresh water, Q , at radius r , is:

$$Q = 2(\pi) r K (p_s Z) a \, dz/dr \quad (10)$$

where K is permeability and Z is the depth to the fresh water - salt water interface below sea level. The change in flow through a cylinder of radius r and thickness dr

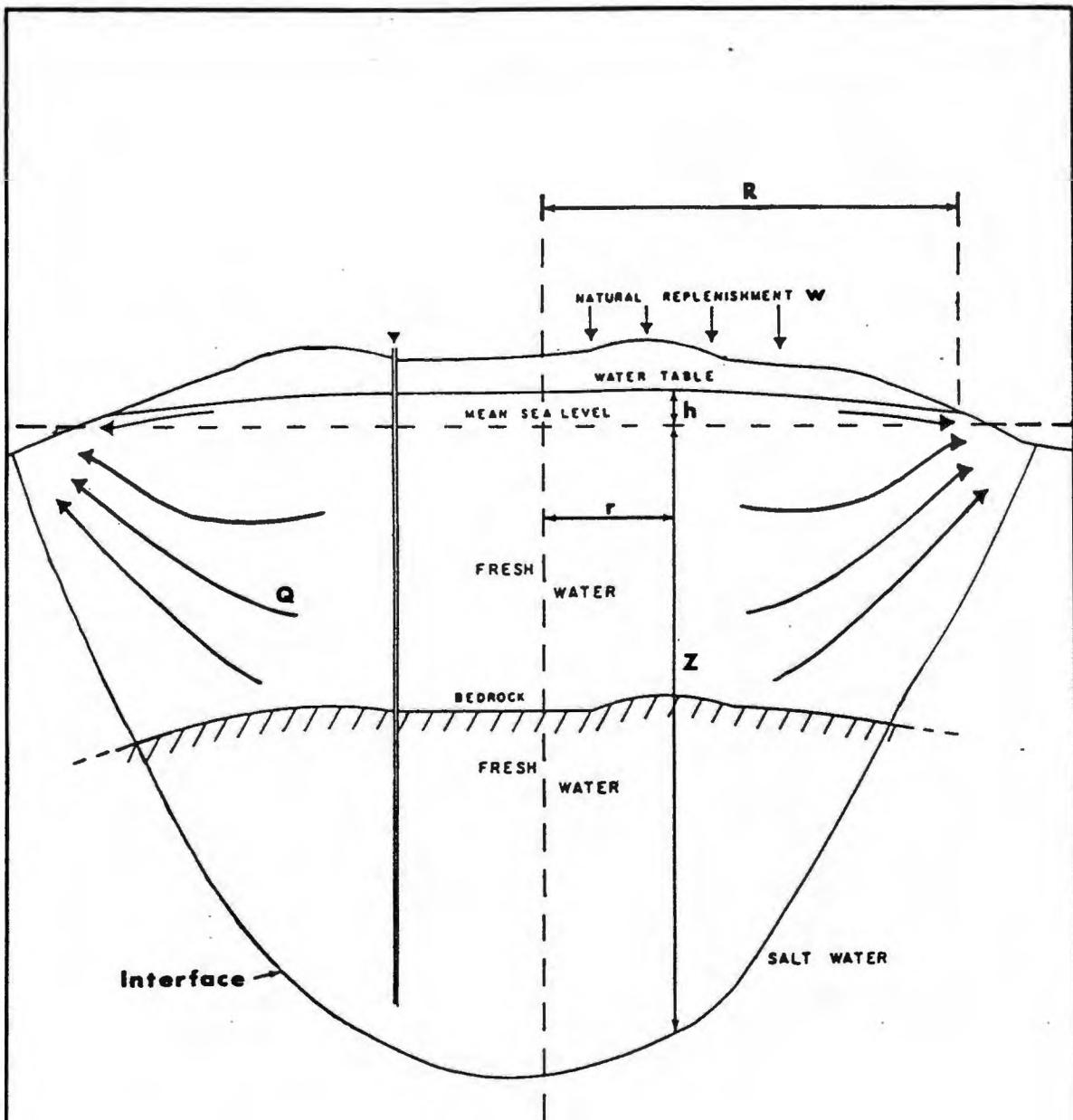


Figure 8. Configuration of a salt/fresh water interface under an oceanic island is dependent upon the size of the island, the effective recharge rate, the aquifer permeability, and the salt-fresh water density contrast. After Todd(1980).

amounts to:

$$dQ = 2 (\pi) r W dr \quad (11)$$

Integrating, and noting that $Q = 0$ when $r = 0$, yields:

$$Q = (\pi) r^2 W \quad (12)$$

Equating equations 10 and 12 gives:

$$\frac{W r dr}{2 K [(1+a/p_f) (a/p_f)]} = h dh \quad (13)$$

Integrating and applying the boundary condition that $h = 0$ when $r = R$;

$$z^2 = \frac{W}{2 K [(1+a/p_f) (a/p_f)]} (R^2 - r^2) \quad (14)$$

where:

a = salt water density minus fresh water density

Therefore, the depth to salt water at any location is a function of the rainfall recharge, size of the island, and permeability of the aquifer. For almost all island conditions, it can be shown that this approximation is indistinguishable from more exact solutions by potential theory (Cooper, et al, 1964). For a sample calculation and the results of the application of this method on the field data see Appendix C and Section IV.

2.4 The Disturbance of a Natural Salt/Fresh Water Interface

In the analyses above the interface is considered to be sharp and well defined. In reality sharp interfaces do not occur under field conditions. Instead the salt water

merges with the fresh water in a zone of diffusion, which is also known as the transition zone. This zone develops from dispersion as a result of the flow of the fresh water. Dispersion is a result of two phenomena: mechanical mixing and molecular diffusion. The magnitude of the dispersion is determined principally by the movements of water in an aquifer produced by tides and seasonal fluctuations in recharge (Henry, 1959).

When a water supply well pumps from a fresh water zone that is underlain by salt water, the interface which separates the two bodies of water rises towards the pumping well. This phenomenon is called interface upconing. The position of the assumed sharp interface is a critical factor in determining the design and safe yield of a well in this type of situation. Using a value for the depth to the sharp interface before pumping begins, it is possible to theoretically calculate the critical pumping rate. Up to this critical pumping rate, an equilibrium with an upconed interface is possible. However, since this pumping rate is determined with the assumption that a sharp interface exists, the presence of a transition zone means that relatively saline water may enter and contaminate a pumping well long before the calculated sharp interface reaches it (Bear, 1979).

Figure 9 shows, qualitatively, a typical situation of a well pumping above the interface in a coastal aquifer.

The phenomenon of upconing is a rate sensitive one. Roman numeral I on Figure 9 marks the initial position of the water table and the interface before pumping commences. At a low pumping rate, part of the fresh water flow which originally discharged to the sea is intercepted by the well. A stagnation point (A) exists seaward of the well, where the specific discharge produced by the well is equal in magnitude and opposite in direction to that of the undisturbed seaward flow. As a result of the pumping the interface upcones a certain distance towards the pumping well until an equilibrium is reached. At the same time, the entire interface rises and its toe advances a certain distance landward to the position marked by II on Figure 9. When the pumping rate is raised to a higher level, yet below the critical pumping rate, a new equilibrium with a higher upconed interface is established. At the critical pumping rate the interface is very unstable and any increase in pumping rate will immediately bring the interface, and sea water, into the pumping well (Bear, 1979).

Although the solution of most upconing problems can be solved using either numerical techniques or simple analytical techniques (Bear and Dagan, 1964), the effects of a transition zone on the determination of safe depths and pumping rates of wells are indeterminate. While numerous investigations have been made into the process of dispersion and the formation of transition zones, the

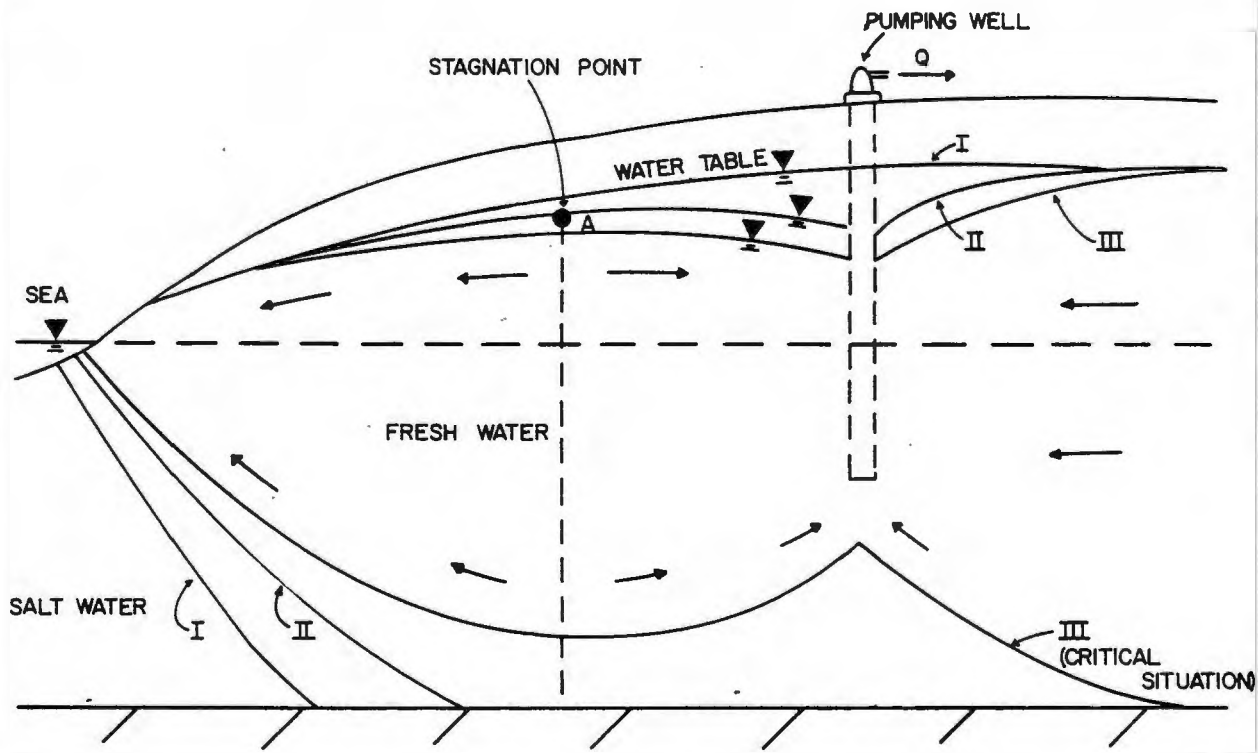


Figure 9. Upconing of a salt water interface beneath a pumping well. I = initial position of water table and interface. II = equilibrium position of water table and interface when pumping below the critical rate, i.e., water table not lowered below point A by pumping. III = upconing of interface induced by pumping above the critical rate. After Bear (1979).

results up to this point have been inconclusive and can not be applied by ground water managers (Kashef, 1976). According to Kashef the occurrence of the transitional zone should be analyzed in order to evaluate its effects and obtain conclusive results to settle the current controversy.

2.5 Previous Applications of the Electrical Resistivity Method to the Problem of Salt Water Intrusion

The direct current resistivity method is a well established tool for groundwater studies. Surface electrical resistivity measurements have been used to study groundwater contamination from sanitary landfills (Kelly, 1976); from connate water (Frohlich, 1974); from industrial waste seepage (Stollar and Roux, 1975); from sewage effluent (Warner, 1969); and from salt piles. (Urish, 1980, and Sanders, 1983).

The electrical resistivity method has also been used to distinguish between fresh and salt water at great depths with a high degree of accuracy (Ginzburg, 1974). Swartz (1937) was probably the first one to locate a salt - fresh water boundary in a coastal area with this method. Electrical resistivity has also been applied to delineate zones of saltwater intrusion in coastal areas by: Ginzburg and Levanon, (1976); Bugg and Lloyd, (1976); and Shipman, (1978). While the method does not appear to have been

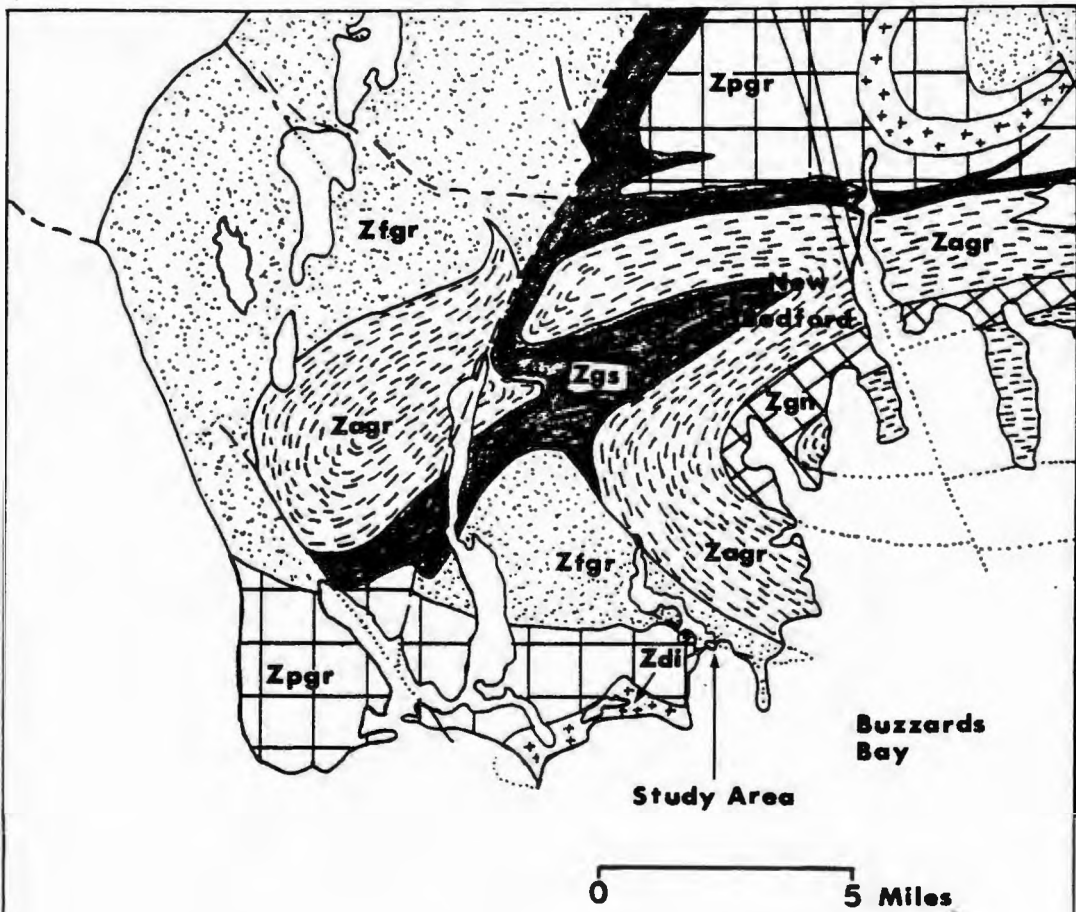
applied in an area with a granite bedrock aquifer to delineate salt water intrusion, previous studies by Kowalski and Sanders (1983) have shown that zones of brackish water in bedrock may be delineated by the electrical resistivity method if the resistivity contrast between the fresh and salt water is great enough. The geoelectric method has also been successfully applied by Sanders (1983) to delineate salt contaminated zones near a salt storage area in a bedrock aquifer with similar hydraulic properties as the rocks found in the proposed study area.

3.0 GEOLOGY AND HYDROGEOLOGY OF THE STUDY AREA

3.1 Surficial and Bedrock Geology

The surficial deposits in the study area are predominately a very poorly sorted glacial till. The till in general consists of 5 to 10% silt and clay, 50 to 60% sand and 30 to 40% gravel, except in areas which have been reworked by waves and in the small kettle holes. The type of deposits along the shorelines vary according to the amount of wave, wind and tidal energy they receive. Along the shores which receive the most energy, the sediments generally consist of coarse sand, gravel and cobbles. The shorelines which receive the least amounts of energy are dominated by salt marsh with thick deposits of silt and clay. The few scattered kettle holes consist of a few feet of silt and clay mantled by sandy till. The kettle holes generally contain fresh water for most of the year and have developed a thin layer of peat where the species *Typha angustifolia* have thrived.

The surficial deposits in the study area are very thin, ranging in thickness from 0 to about 25 feet. These deposits are mantled by a fractured granite with local intrusions of diorite. The granite is a part of the Fall River Pluton, Proterozoic in age, which includes the Bulgarmarsh Granite (Figure 10). The granite is a light grey, medium-grained biotite granite. It is in part mafic-poor and gneissic in the New Bedford area (USGS, 1983).



KEY




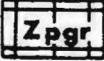
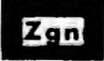
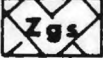
-  **Zfgr** Granite of Fall River pluton
-  **Zagr** Alaskite
-  **Zdi** Diorite
-  **Zpgr** Porphritic granite
-  **Zgn** Biotite gneiss
-  **Zgs** Gneiss and schist

Figure 10. Bedrock geology of study area. After E-an Zen, USGS (1983).

The Fall River Pluton intrudes gneiss and schist near New Bedford, which is also Proterozoic.

In the northern section of the study area, known as Chaypee Hill, there are no bedrock outcrops. Borehole information indicates that bedrock is between 8 and 25 feet beneath the overburden at wells 1 and 2 respectively on Figure 12. In the rest of the study area, the highest points are generally bedrock outcrops. The depth to bedrock in the other wells in the area ranges from 10 to 20 feet.

In an effort to determine the average rock fracture density, field measurements were made of fracture spacings and orientations. This was done in order to make an estimate of the bedrock porosity. The fracture spacings were found to vary widely. In some areas the fracture spacing was very dense where the rock had been fractured or sheared into many parallel sheets. In other areas the fracture pattern was more regular with fracture spacings averaging about 1 to 2 feet apart. The result of the fracture orientation measurements are presented in Figure 11. This Rose diagram shows that the majority (46%) of the bedrock fractures strike between 30 and 45 degrees east of north. The location of the field measurements is indicated on Figure 12. Field measurements of fracture orientations taken outside of the study area about 4 miles north, resulted in a similar pattern. Because of this, the

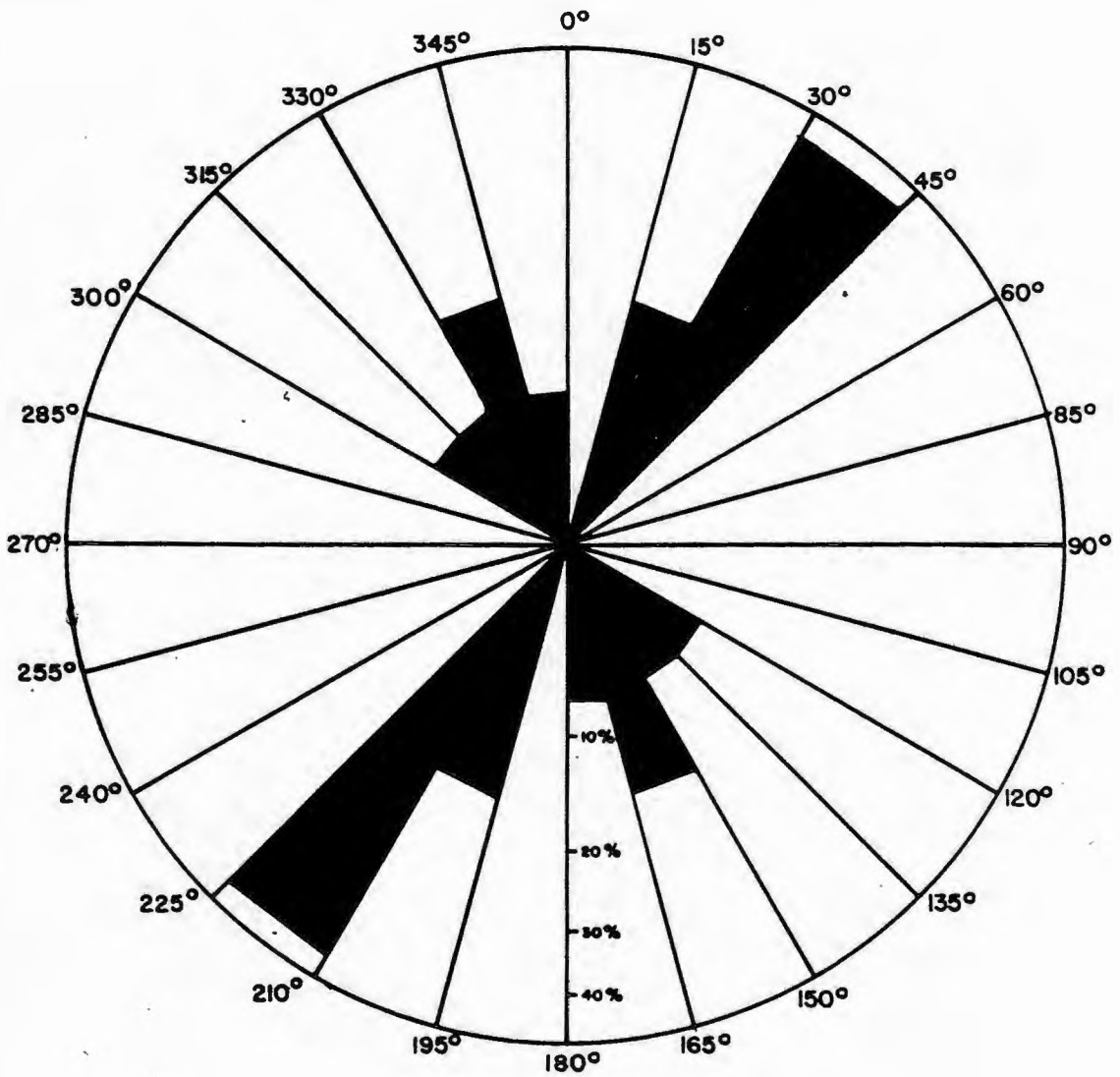
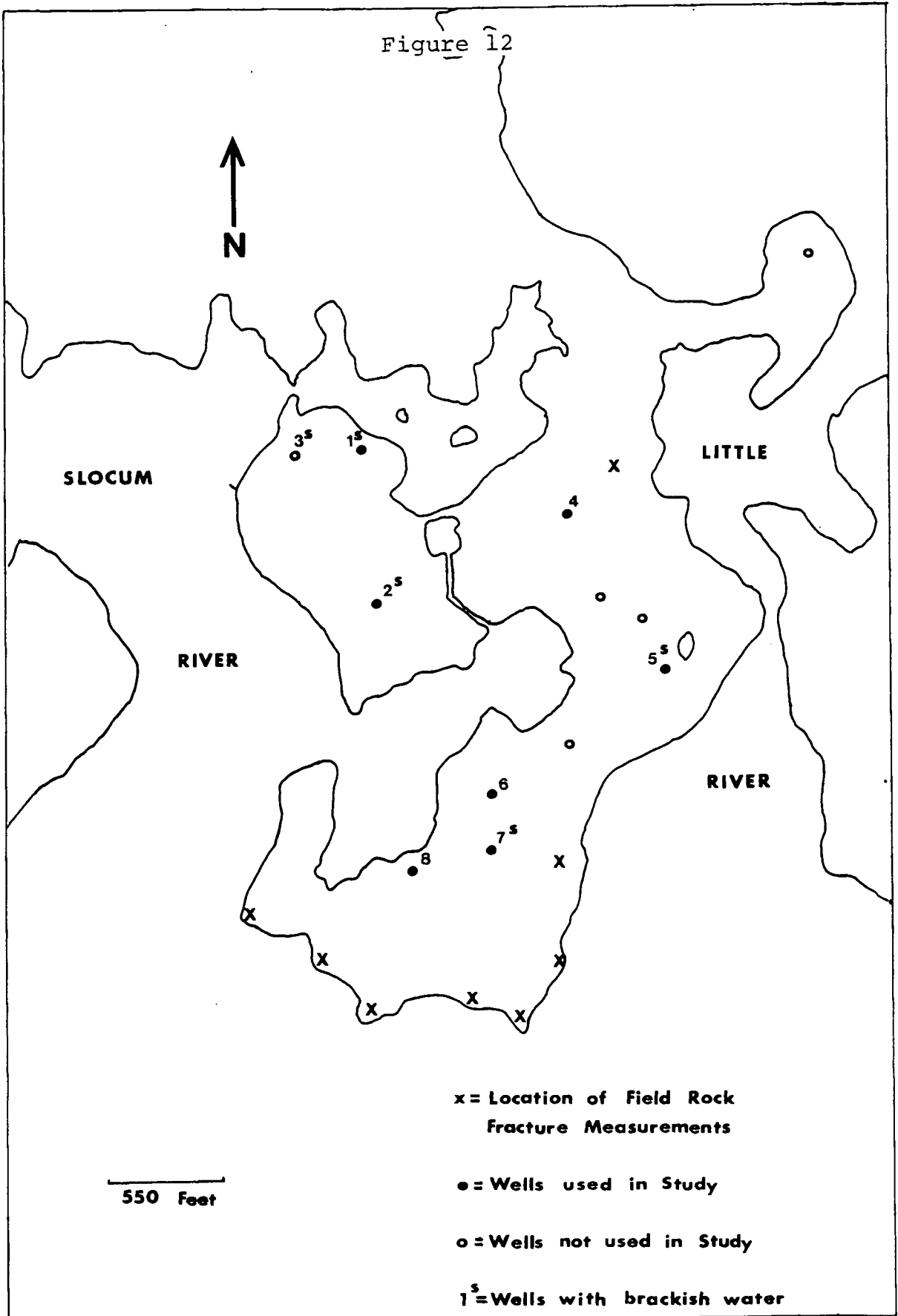


Figure 11. Rose diagram depicting the strike orientations of the surface bedrock fractures in the study area. Forty-six percent of the bedrock fractures measured were oriented between 30 and 45 degrees.

Figure 12



pattern of bedrock fracturing has been assumed to be the same across the entire study area.

3.2 Hydrogeologic Characteristics of the Study Area

The hydrogeologic characteristics of the study area have been evaluated using a combination of field and laboratory investigations. The objective of these investigations was to determine the porosity, hydraulic conductivity, hydraulic gradient and the hydraulic heads in the aquifer. The following is a list of the tasks which were performed:

- communication with local residents to determine what types of wells exist in the area and the history of the water quality (salinity) from these wells.
- installation of a tide gauge for the determination of mean sea level.
- survey to determine the elevation of the wells above mean sea level.
- field measurements of salinity and specific conductivity in the wells and surrounding surface waters.
- installation of a continuous water level recorder in a bedrock well in which the water table fluctuates with the tide to determine the hydraulic conductivity of the fractured bedrock using the Tidal Method.

- field measurements of water table elevations in the wells.
- determination of soil sample in place densities and water content in order to estimate the soil porosity.
- laboratory determinations of soil permeability using the Constant Head Method.

The data from these laboratory and field procedures is presented in Appendices D through J.

The aquifer in the study area was found to be composed of a thin layer of unsorted to fairly sorted sand, silt and gravel. This is mantled by a fractured granitic bedrock aquifer which may be partially confined in some areas. In one bedrock well (well 2) the water level in the well was found to fluctuate with the tides, while in bedrock well 1, no fluctuations were observed.

The results of these investigations indicate that the configuration of the aquifer and the salt/fresh water interface is similar to that which is shown in (Figure 1c). An idealized north-south cross-section through part of the study area in Figure 13 shows a similarity with the situation which is typical for oceanic islands. This figure shows that when an underground fresh water supply is surrounded by salt water on all sides, a Ghyben-Herzberg lens is formed. In this type of situation the depth to the salt/fresh water interface is dependent on more than just

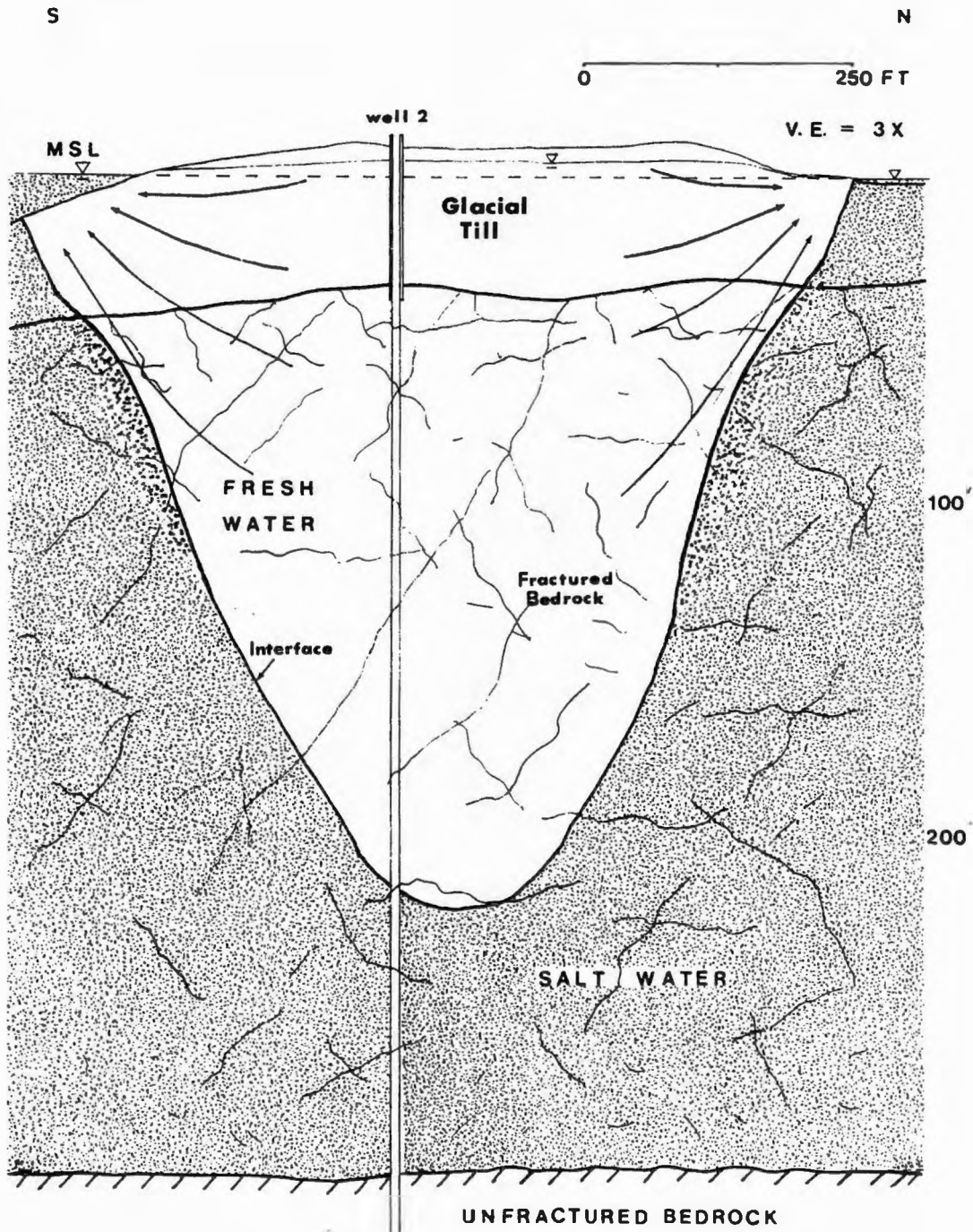


Figure 13. Idealized north-south cross-section through part of the study area illustrating the configuration of a Ghyben-Herzberg lens.

the density contrast between the salt and fresh water. For this reason the theoretical depth to the salt/fresh water interface has been determined by a method (see equation 11) which was developed for oceanic landmasses by Todd (1980). Figure 13 also shows that the majority of the aquifer material is fractured granite bedrock. The total saturated thickness of the aquifer is estimated to be between 200 and 250 feet.

The results of the laboratory and field techniques which were used to determine the hydraulic conductivity of the aquifer are summarized in Table 1. This table shows that the difference in the hydraulic conductivity between the bedrock and the glacial till varies by an order of magnitude. However, in the instances where a value for the hydraulic conductivity of the aquifer was needed, it was found that the higher conductivity of the glacial till did not affect the calculations significantly. Because the bedrock makes up more than 90% of the aquifer material on the average, it was found to be unnecessary to include a separate value for the hydraulic conductivity of the till in the equations which required a representative value for the hydraulic conductivity of the aquifer.

The wells which exist in the study area are identified on Figure 12. The wells to which access was available and were actually used in this study are further identified in Figure 12. Of the thirteen wells identified in this

TABLE 1

MEASUREMENT OF HYDROGEOLOGIC PARAMETERS

SAMPLE LOCATION	DEPTH OF SAMPLE (FT)	POROSITY	HYDRAULIC CONDUCTIVITY (CM/SEC)	METHOD
A	0.5	0.304	0.0135	Constant Head
B	0.5	0.372	0.055	Constant Head
Bedrock Well #2	*	0.05 **	0.008	Tidal Method
Bedrock Well #2	*	0.01 **	0.0016	Tidal Method

- NOTES: 1. * Open borehole test--25 to 380 feet
2. ** These are the estimated porosities which were used in this method to obtain these hydraulic conductivities.
3. Each of these methods are explained in the Appendices
4. Sample/test locations are indicated on Figure 12.

figure, six have drawn in salty water. These wells are also identified in Figure 12. Three of these wells, all which belong to the same family, are deep bedrock wells with depths all exceeding 150 feet. The other three salty wells are all shallow wells which draw their water from the glacial till. Two of these shallow wells have been abandoned.

Two of the bedrock wells have been or will soon be used as a water source. The water from both of these wells have been or are being treated with Reverse Osmosis water purification systems. One of the wells was installed in March of 1983 and was put into use in the summer of 1984. This well is designated well 2 on Figure 12 and has a salinity of approximately 24 parts per thousand when pumped. Approximately 6 months after the well was last pumped, the near surface water salinity in the well was found to be 8 parts per thousand. Well 1 also shows the same type of replenishment of fresh water, only in a more pronounced manner. When well 1 was first sampled in early June of 1983, the well had already been in use for approximately 2 months for short periods of time. The water at that time already contained 2.2 parts per thousand of salt or 1220 parts per million (ppm) of sodium. The owner reported that the water from the well is usually relatively salt free at the beginning of the summer after it has not been pumped all winter. As more water is drawn out of the well, the saltier it becomes. When the well was

sampled on March 16, 1984, after it had not been used all winter, the water was found to have no salt at all to a depth of at least 75 feet (length of cable on probe).

The reason why the fresh water recovered to a much greater extent in well 1 may be due to the position of the well. Well 1 is located a little closer to the shore than well 2 but, the surface elevation at well 1 is 21 feet higher than well 2 above mean sea level. Because the hydraulic head is higher in well 1, which is also closer to the shore than well 2, there is a significantly higher vertical flow component at well 1 than at well 2. This could account for the fast fresh water recovery time at well 1.

4.0 GEOPHYSICAL DEFINITION OF THE SALT/FRESH WATER INTERFACE

4.1 Theory of Direct Current Electrical Resistivity

The use of the electrical resistivity method relies on the ability of subsurface materials to conduct at least small amounts of electric current. Because dissolved ions in groundwater are the main cause for current conduction, the resistivity of a subsurface medium decreases with increasing water content. As a subsurface medium reaches saturation, the resistivity decreases accordingly and, almost all of the electrical current is conducted through the electrolytic solution in the pore spaces. Therefore, the resistivity of the medium is mainly controlled by the porosity, water saturation, and water conductivity and only to a lesser extent by the porous material itself (Zohdy, et al, 1974).

It is expected that the salt water in the aquifer below the study area will have a lower resistivity than the overlying fresh water. This difference in resistivity will enable the interpreter to determine the depth to the salt water at the point of measurement in the study area.

In the resistivity method four electrodes are staked out along a transect at predetermined spacings from a center point. The two outer electrodes are connected to a battery or other power source that produces direct current.

The two inner electrodes are connected to a voltmeter to measure the resulting potential difference from the current in the ground produced by the two outer electrodes. The distance between the outer and inner electrodes controls the depth of penetration of the current below the surface. With a measure of the potential difference (V) in millivolts, the current (I) in milliamperes, and the electrode separation distances in feet, the apparent resistivity (Ra) can be calculated in ohm-feet by the relation:

$$Ra = C V / I \quad (15)$$

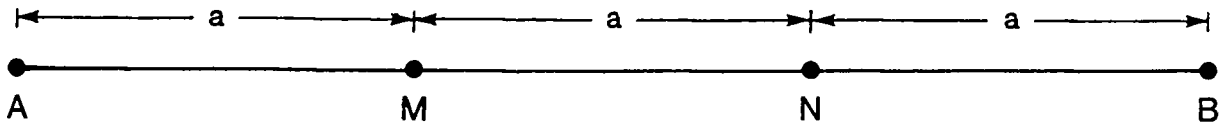
where C is the geometric factor of the electrode configuration (Zohdy, et al, 1974). A Vertical Electrical Sounding can be done using either the Wenner or the Schlumberger electrode configuration (see figure 14).

Unless the subsurface medium being measured by the electrical resistivity method is homogeneous and isotropic, in which case the resistivity is called the true resistivity, the resistivity calculated by the above equation is known as an apparent resistivity. The apparent resistivity measured at any electrode separation depends on the geometry and resistivities of the subsurface materials encountered by the current.

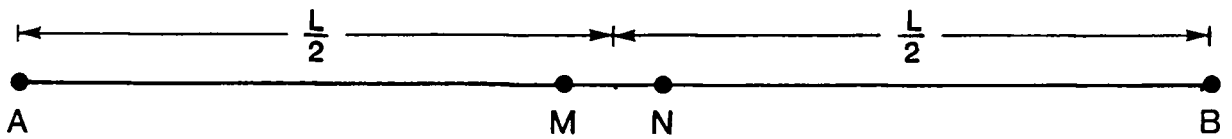
4.2 Methodology

A Vertical Electrical Sounding (VES) is performed in order to determine the vertical changes of resistivity

WENNER ARRAY



SCHLUMBERGER ARRAY



$$(AB \geq 5MN)$$

Figure 14. Two of the most popular electrode configurations for vertical electrical soundings.

below a point on the earth's surface. This is done by first selecting a Center Point. The electrodes are then set at the first predetermined spacing and a measurement is taken. In the Schlumberger configuration, the outer electrodes are moved away from the Center Point along a straight line after each measurement, while the two inner electrodes are only expanded if the resulting voltage is too low. The apparent resistivity is plotted versus half the electrode separation on bilogarithmic paper. This plot presents the change of resistivity with depth below the center point.

4.3 Interpretation of Vertical Electrical Soundings

A depth sounding curve is presented as a graph of the apparent resistivity (R_a) versus $AB/2$ (half the current electrode spacing) as shown in Figure 15. The interpretation of the VES curve is a conversion of the R_a versus $AB/2$ plot into a R_i versus depth plot with R_i true layer resistivities based on horizontal layering. This interpretation results in a Resistivity-Depth Model, or profile (Figure 16).

Resistivity-Depth profiles can only be produced after the VES curve has been interpreted through the use of published Master Curves (Mundry and Homilius, 1979), or a computer curve interpretation program (Zohdy, 1974), or both. In this study a combination of both methods will be used. The VES curves will first be interpreted using the

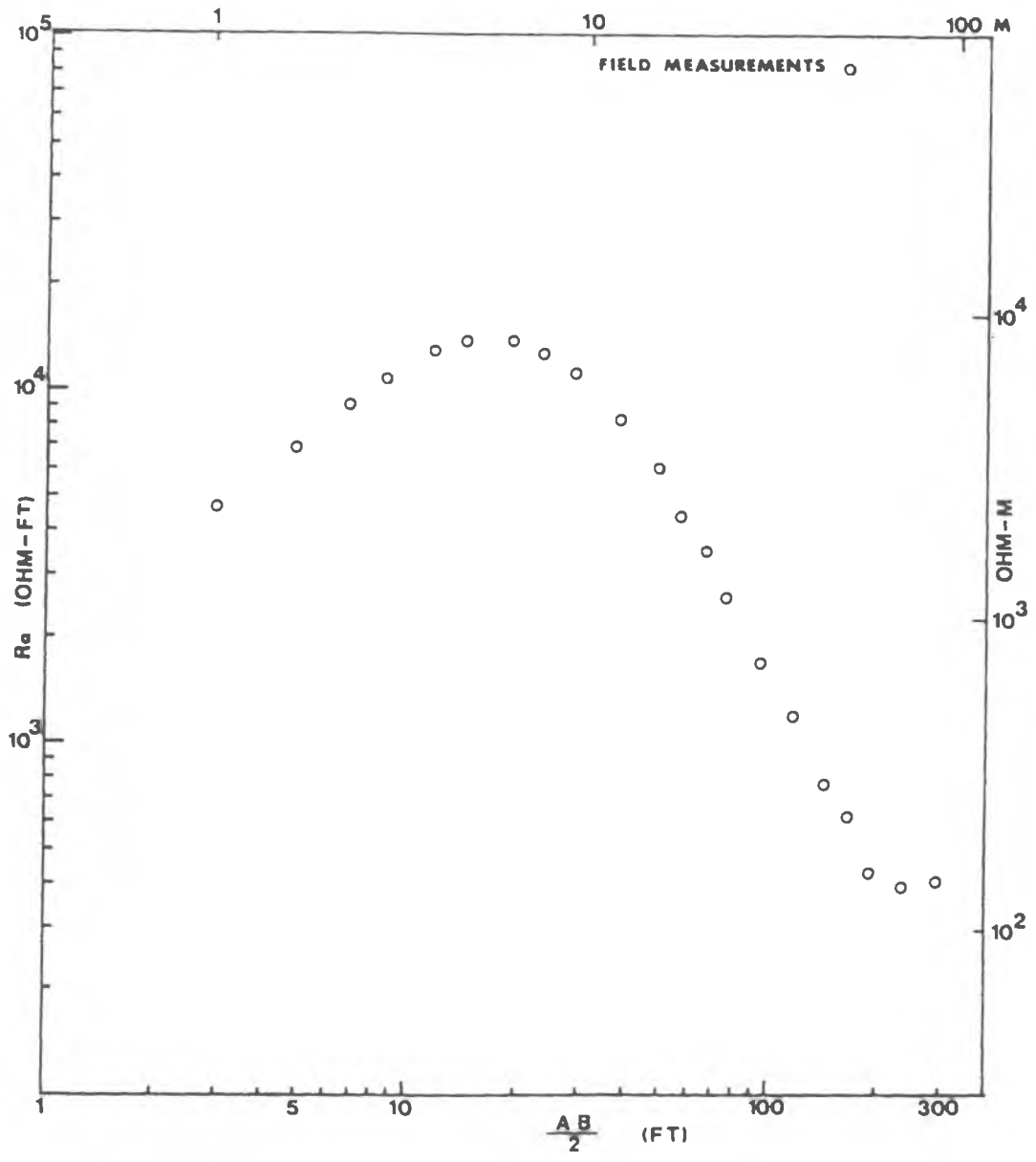


Figure 15. Example plot of field data obtained from a vertical electrical sounding (VES).

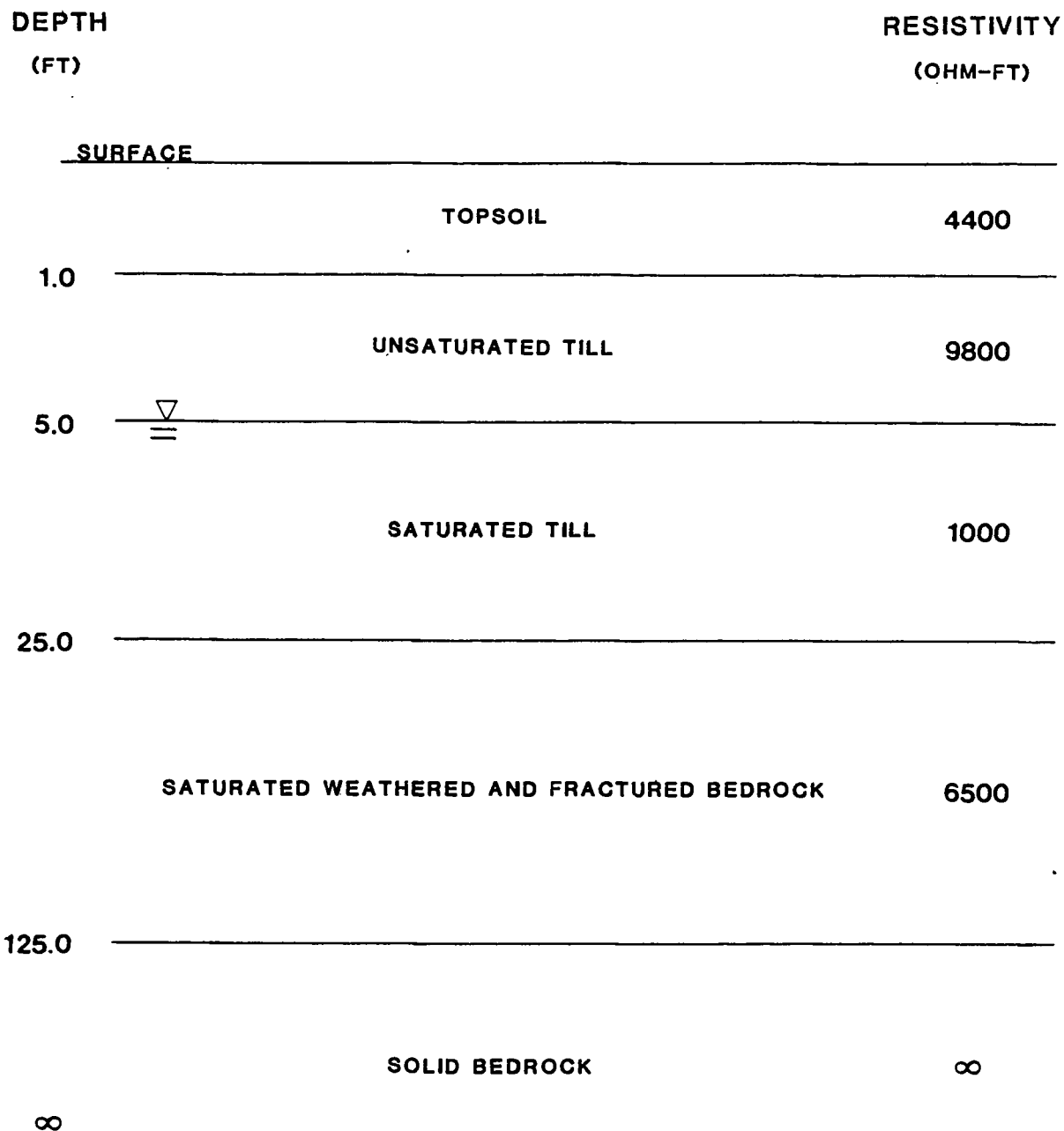


Figure 16. Depth-resistivity model obtained from the interpretation of a VES curve such as shown in Figure 15.

Master Curves cited above followed by checking and refining the depth-resistivity models produced by the curve matching using a computer program. The interpretation of the curves with the use of two-layer master curves, auxiliary point charts and the computer program is summarized briefly below.

In order to interpret the field curve using Master Curves, the field curves must be plotted on transparent bilogarithmic graph paper with a scale which matches the Master Curves. In this case the length of a decade from 1 to 10 is 83.33 mm. The Master curve is placed on a light table and the field curve is superimposed over the Master Curve.

In a two-layer case, the field curve type is first noted (ascending or descending), and the appropriate set of Master Curves is chosen. The field curve is then overlaid on the Master Curves and is shifted in position, keeping the axes parallel to the coordinate system, until a good match is established.

When a match is obtained, the origin of the Master Curves is marked on the field curve. From this match point on the field curve the values of R_1 and D_1 are obtained. From the particular Master Curve with which the field curve was matched is obtained the ratio of R_2 to R_1 (R_2/R_1). Using this ratio and the value of R_1 obtained

above, the value of R_2 is calculated. The results of this procedure are shown in Figure 17.

If the field curve is made up of more than two layers, the first two layers must be combined into an equivalent single layer in order to complete the interpretation using a set of Two-Layer Master Curves. Using the appropriate Auxiliary Point graph, the first and second layers are combined by tracing the curve from the auxiliary graph which corresponds to the R_2/R_1 ratio from above, onto the field curve. This is done after first matching the auxiliary graph origin with the first match point on the field curve. After this is completed the appropriate set of two-layer Master Curves is used by once again overlaying the field curve and attempting to match-up the next portion of the field curve with a Master Curve. In this case the auxiliary curve, which represents the combined effect of the first two layers, (the dashed line traced above the field curve) is moved along the Master Curve origin until a match is found between the next portion of the field curve and an appropriate Master Curve. When a good match is obtained, the Master Curve origin is marked on the curve and the Master Curve with which the field curve matches is noted. This second match point represents the combined effect of the first two layers.

From the second match point the values of $R_{1,2}$ (the combined resistivity of the first and second layer) and D_2

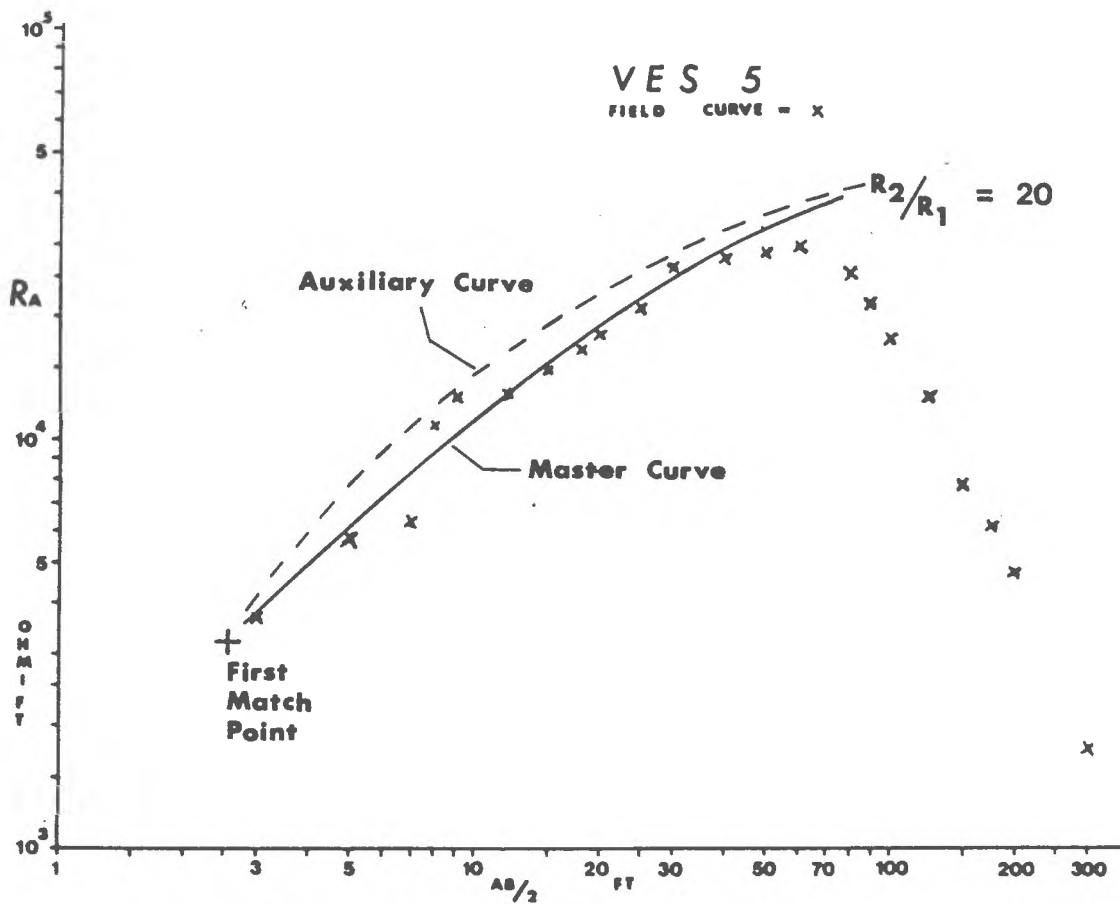


Figure 17. The first step in the interpretation of a VES curve using Master Curves.

are obtained. However, in some cases the value of D_2 can not be obtained directly from the match point; a graph which takes into account the anisotropy of the layers must be used as shown in Figure 18.

In a three layer case the depth and resistivity of the third layer are obtained in the same procedure as above. From the Master Curve which matches the field curve is obtained the ratio between R_3 and $R_{1,2}$ ($R_3 / R_{1,2}$). Using this value and the value of $R_{1,2}$ obtained above, the value of R_3 may be obtained. The results of this procedure is shown in Figure 18. An outline of the Depth-Resistivity model obtained from these procedures for this curve is presented in Figure 19. For any number of successive layers, the same approach outlined above is used.

The Resistivity-Depth model obtained from the Master Curve matching process is used as a starter model to obtain a final curve interpretation through computer analysis. The thickness and resistivity of each layer from the Resistivity-Depth model is used as the input to the computer program. The program generates a theoretical VES curve for the thicknesses and resistivities which are supplied by the curve matching procedure. This theoretical curve is then compared to the field curve. Based on this comparison, the values of the thicknesses and/or the resistivities of the layers of the Resistivity-Depth model are subtly altered by the interpreter until the theoretical

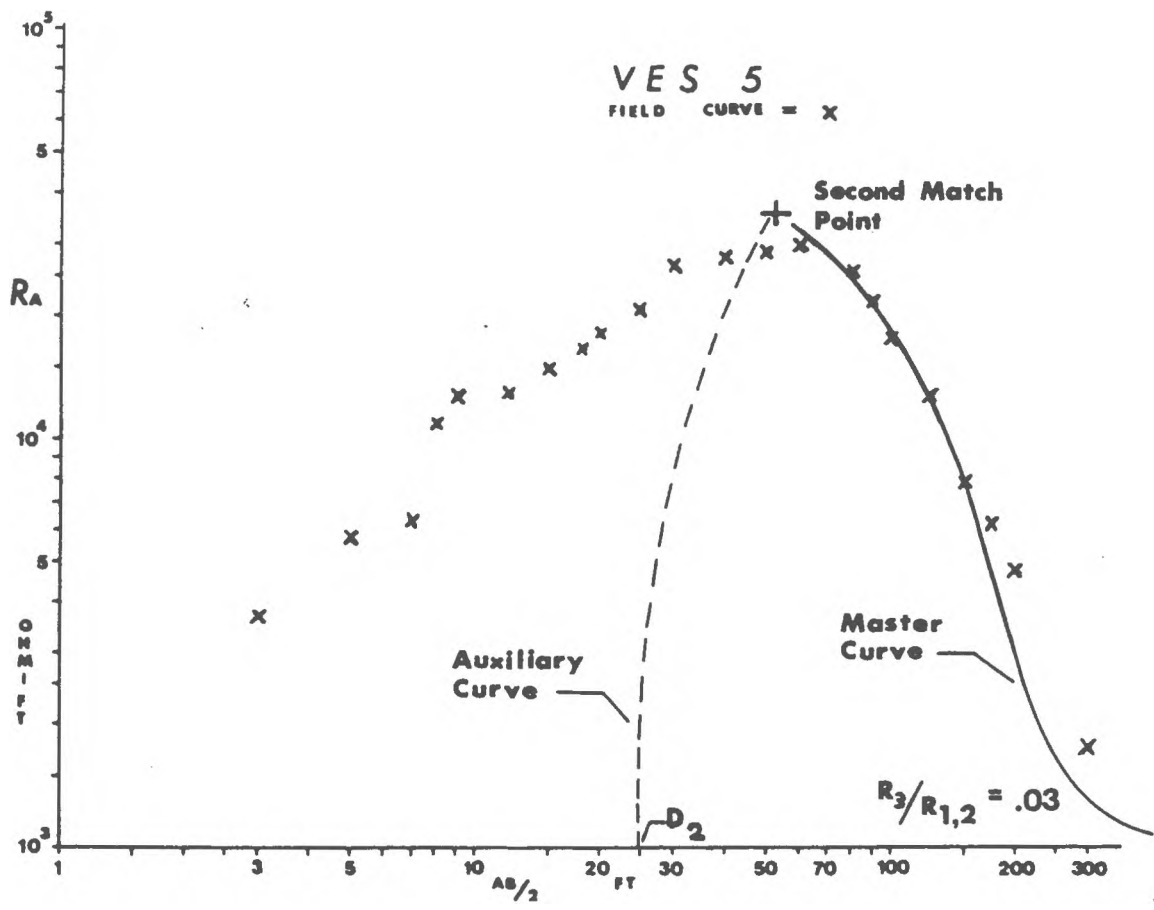


Figure 18. The second step in the interpretation of a VES curve using Master Curves.

STEP 1

$$R_1 = 3200 \text{ OHM-FT}$$

$$D_1 = 2.6 \text{ FT}$$

$$R_2/R_1 = 20$$

$$R_2 = 64000 \text{ OHM-FT}$$

STEP 2

$$D_2 = 25 \text{ FT}$$

$$R_{1,2} = 34000 \text{ OHM-FT}$$

$$R_3/R_{1,2} = .03$$

$$R_3 = 1020 \text{ OHM-FT}$$

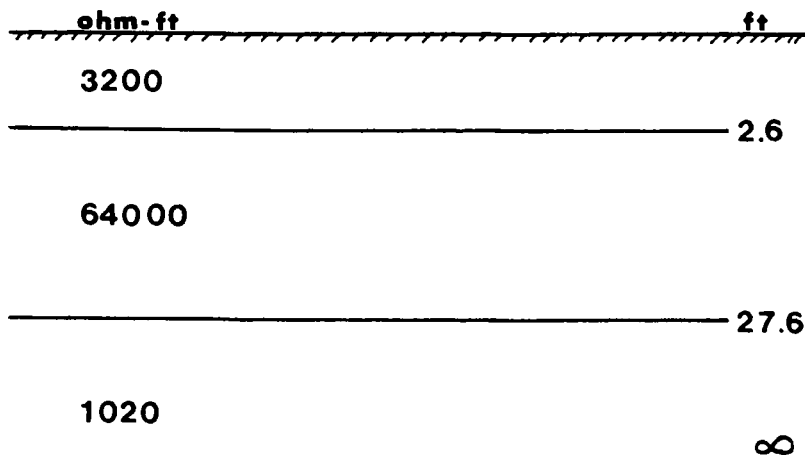
RESULTS

Figure 19. Summary of the two step Master curve interpretation of the VES data shown in figures 17 and 18 and the resulting depth-resistivity model.

curve generated by the model best matches the field curve.

The computer program for calculating the final Resistivity-Depth model is the same used for calculating the Master Curves employed in the curve matching procedure. The program is based on the theory developed by Stephanesau (1930) which was developed for computer computation by Ghosh (1972).

4.31 Archie's Law and the Formation Factor

As stated before, the final product of a VES curve interpretation is a model which delineates layers of the earth below the test site according to their affinity to conduct electrical current. In this case most of the electrical current passed through the ground is conducted by the porewater and not by the soil or rock matrix. Therefore, the two most important factors are the porosity and the porewater resistivity. Once this model is obtained, the bulk resistivities of the layers are analyzed to determine whether or not these values are indicating the presence of higher than normal levels of dissolved ions in the porewater. The most common way this is done is to employ an equation which relates the bulk resistivity, $R(\text{bulk})$ obtained from the curve interpretation, to the ion content of the porewater, $R(\text{water})$, and to a term known as the formation factor (FF) (Archie, 1942):

$$R(\text{bulk}) = R(\text{water}) * FF \quad (16)$$

The formation factor is related to a material's porosity, n , in the following empirical equation (Winsauer, et al, 1952):

$$FF = t * n^{-m} \quad (17)$$

where: n = porosity,

t = a constant ranging from .47 to 2.2 and

m = a cementation constant ranging from 1.3 to 2.6

The use of the Formation Factor in groundwater investigations is very useful but, it does have some limitations. The formation factor was initially used in the petroleum industry where the formations studied were commonly saturated with brine, not fresh water. Archie defined the formation factor as the ratio of the resistivity of the formation 100% saturated with brine to the resistivity of the brine, (Patnode and Wyllie, 1950):

$$FF = R(\text{bulk})/R(\text{water}) \quad (18)$$

It later became apparent that the rock resistivity was not independent of the fluid resistivity, and the Formation Factor (here designated the true formation factor) was distinguished from the apparent formation factor. The True Formation Factor is the formation factor that the rock would have if none of the solid material contributed to conduction. The True Formation Factor is a constant. However, some of the electrical current can be conducted by ions on the surface of the matrix. Therefore, the overall

conduction is controlled by the porewater and the total matrix surface area available for surface conduction.

The apparent formation factor is the measured resistivity of the rock divided by the measured resistivity of the fluid with which it is saturated. If the porewater has a very low resistivity (salty) the apparent formation factor is approximately equal to the true formation factor. As the resistivity of the porewater increases, the apparent formation factor decreases. Therefore, the apparent formation factor of a given material is not constant (Patnode and Wyllie, 1950). Using equation 18, the formation factor can exhibit major variations as a result of small changes in porewater resistivity. Since the porewater resistivity of most of the fluid in the aquifer in this study area does not exceed 10 ohm-meters (33 ohm-ft), the apparent formation factors used will be approximately equivalent to the true formation factors (Keller and Frischknecht, 1966).

In this investigation equation 17 was only used in conjunction with equation 18 in order to check the values of bulk resistivity for the saturated till over the bedrock. Equation 17 was not used for the bedrock since a value for the porosity of the bedrock could only be estimated. Instead, a value for the formation factor was determined using the data obtained from VES #1 and from the adjacent well, Well 2. The value for the bedrock bulk

resistivity was determined from the curve interpretation while the porewater resistivity was measured in the well with a probe. The formation factor was calculated using equation 18.

Once a value for the formation factor had been determined using equation 18, equation 16 was then applied in those areas where deep boreholes were not available for the measurement of the porewater resistivity. In this way it was possible to determine whether or not the bulk resistivity of a layer of saturated bedrock was indicative of salt water intrusion. To facilitate this determination, the calculated values of porewater resistivity were converted to specific conductance units

(Alger, 1966):

$$S.C.(umhos/cm) = 10000/R(\text{water}) \text{ ohm-meters} \quad (19)$$

where: 10000 is a unit conversion factor and

$$R(\text{water}) \text{ ohm-meters} = R(\text{water}) \text{ ohm-feet}/3.28 \quad (20)$$

also:

$$10^6 \text{ umhos/cm} = 1 \text{ S/cm (Siemens/cm)} \quad (21)$$

4.4 Limitations on the Interpretation of VES Curves

The most severe problem encountered by the interpreter of VES curves is the nonuniqueness of resistivity curves. This problem is of concern when a layer has a resistivity which is either greater than, or

less than, both of the resistivities of the layers above and below ($R_1 < R_2 > R_3$ or $R_1 > R_2 < R_3$).

In the first case, when the middle layer resistivity is the greatest, it has been found that this resistant bed manifests itself mostly by its transverse resistance (T), such that:

$$T = H * R \quad (22)$$

where: H = thicknesses of the bed

R = resistivity of the bed

In other words, the current tends to flow nearly perpendicular through the most resistant layer or layers. The problem of nonuniqueness enters at this point since any value of T may be obtained by a range of combinations of layer thicknesses and resistivities. This means that a sequence of layers which is characterized by a specific value of T can produce the same curve as a slightly different sequence of layers which has the same value of T. This phenomenon is known as the Principle of Equivalence in T. The possible range of layer thicknesses and resistivities is limited in most cases by the configuration of the curve and any available borehole data.

In the second case, where the middle layer has the lowest resistivity, the conductive layer between two resistive layers is defined by its longitudinal conductance, S.

$$S = H/R \quad (23)$$

This is due to the tendency of the current to flow parallel to the least resistive bed. By analogy with the case above it can be seen that the Principle of Equivalence applies in this case as well (Bhattacharya, 1968).

Another factor of concern is the principle of suppression. This relates to those layers whose resistivities are intermediate between the resistivities of the enclosing layers. Such layers, as long as they do not have a great thickness, have practically no effect on the resistivity curve. When the thickness of such an intermediate layer increases, this layer will eventually affect the resistivity curve. However, before the layer reaches a thickness at which it can be positively identified, its effect at first remains indistinguishable from that due to a change in thickness or resistivity of one or both of the enclosing layers (Kunetz, 1966).

4.5 Instrumentation

The instrumentation used is somewhat more sophisticated than what is normally employed. Figure 20 shows the schematic of the unit, which is capable of a maximum electrode separation of $AB = 800$ meters. The current for this unit is provided by a 12 volt battery (15 amperes) which is converted to a maximum of 400 volts direct current at 0.25 amperes. A number of variable and constant resistors can be used to regulate the current which is fed into the ground via two steel stake

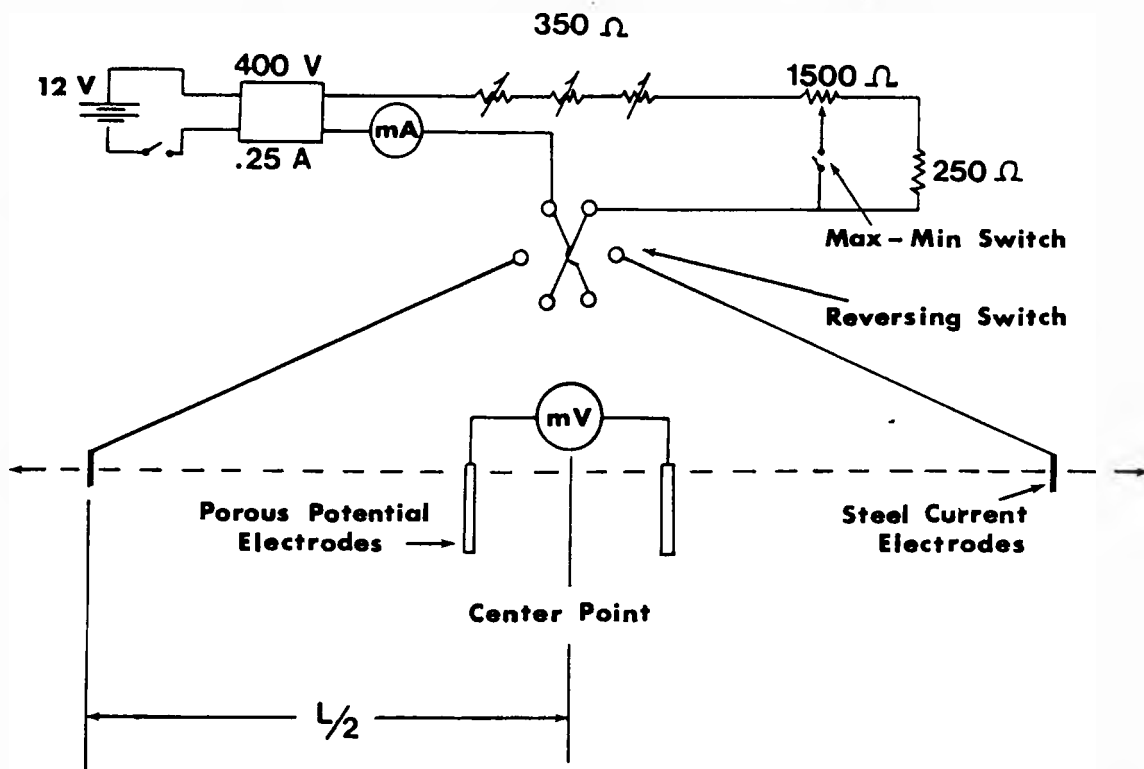


Figure 20. Schematic of equipment for vertical electrical depth sounding. After Frohlich (1973).

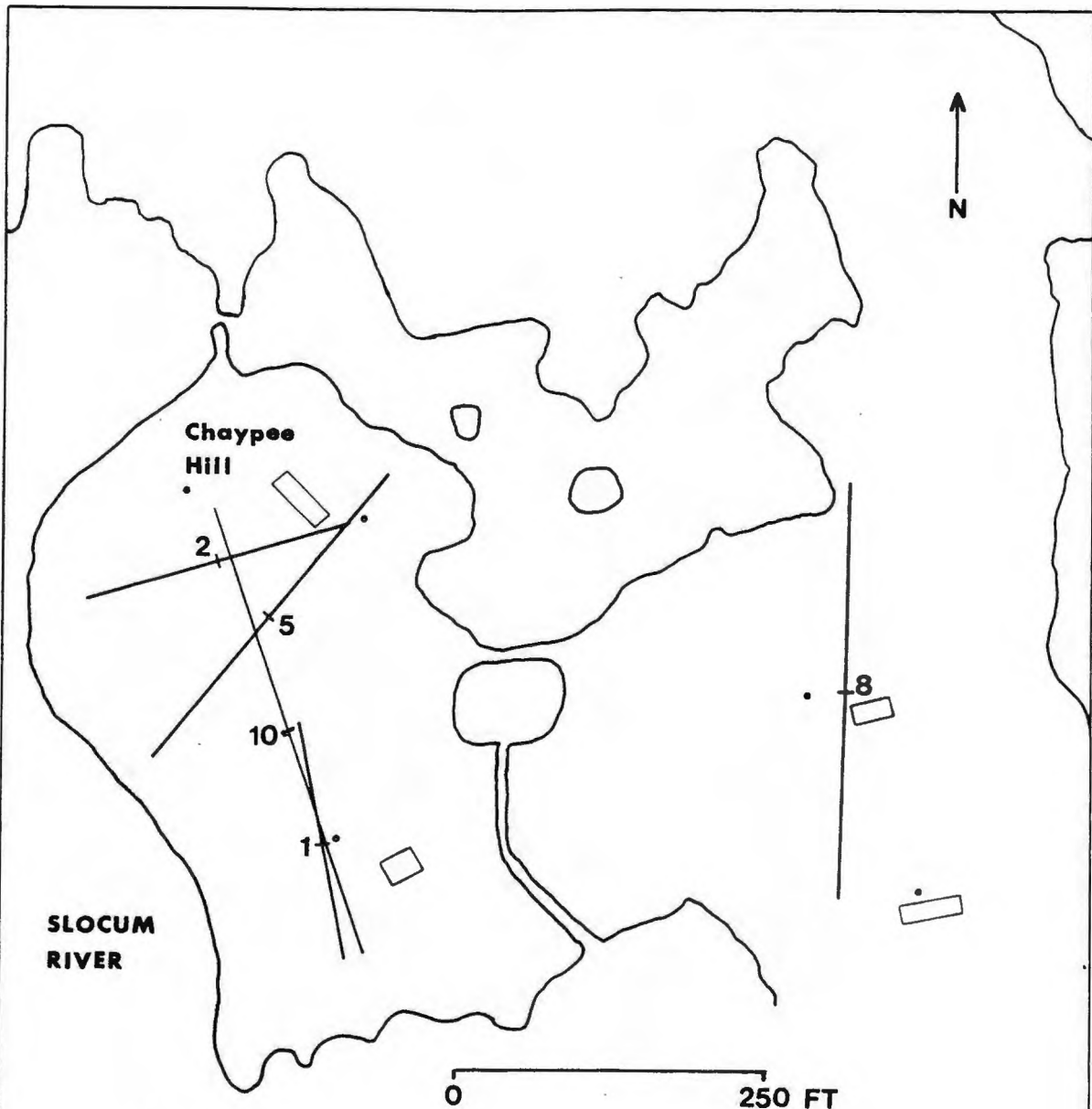
electrodes. The amount of current is measured with an in-line amperemeter. The current may be reversed so that polarization effects at the current electrodes can be kept to a minimum and so that each reading may be checked twice.

The resulting potential between points M and N due to the current flowing from A to B, is measured with a DC Millivoltmeter, Hewlett Packard Model 4304 B. The millivoltmeter is coupled to the earth at points M and N via two nonpolarizable copper-copper sulfate electrodes. This type of electrode minimizes the contact effects with the soil which might occur with metal electrodes and cause unwanted potentials. In some situations it may not be possible to zero the millivoltmeter. This usually occurs when the most sensitive ranges of the millivoltmeter must be used. To overcome this problem a separate source of voltage is necessary. For this investigation a simple apparatus which consists of a 1.5 volt battery, a reversing switch and two variable high precision resistors were used. This instrument was put in line between one of the potential electrodes and the positive input jack of the millivoltmeter. Insulated copper cables for the connections from the power source to the current electrodes and fiberglass tapes for measuring the electrode separations complete the field equipment.

4.6 Location of the Test Sites

A total of eleven Vertical Electrical Soundings were performed at ten different locations as indicated on Figures 21 and 22. An attempt was made to perform the soundings at right angles to one another in order to determine if anisotropy of the soil and or bedrock was a significant factor. In most areas it was not possible to perform two soundings perpendicular to each other using the same Center point due to either topography or space limitations.

The soundings were located and orientated in order to best take advantage of the limited boreholes which were available. The depth to the salt water could only be determined in two wells in the area; Wells 1 and 2. However, only one of these wells, Well 2, is located in an area in which a Vertical Electrical Sounding could be performed right next to it. Two Vertical Electrical Soundings were performed next to Well 2, namely, VES 1 and Ves 11. The depth to bedrock in this well was reported to be 25 feet. The water table was found to fluctuate with the tide in Well 2. This made it possible to determine the permeability of the bedrock in this area using the Tidal Method (Carr and Van Der Kamp, 1969). The results of this test can be found in Appendix G. A record of the water table elevations and other well data is listed in Appendix F.



KEY
 • WELL
 + VES CENTER POINT

Figure 21. Vertical electrical sounding (VES) locations.

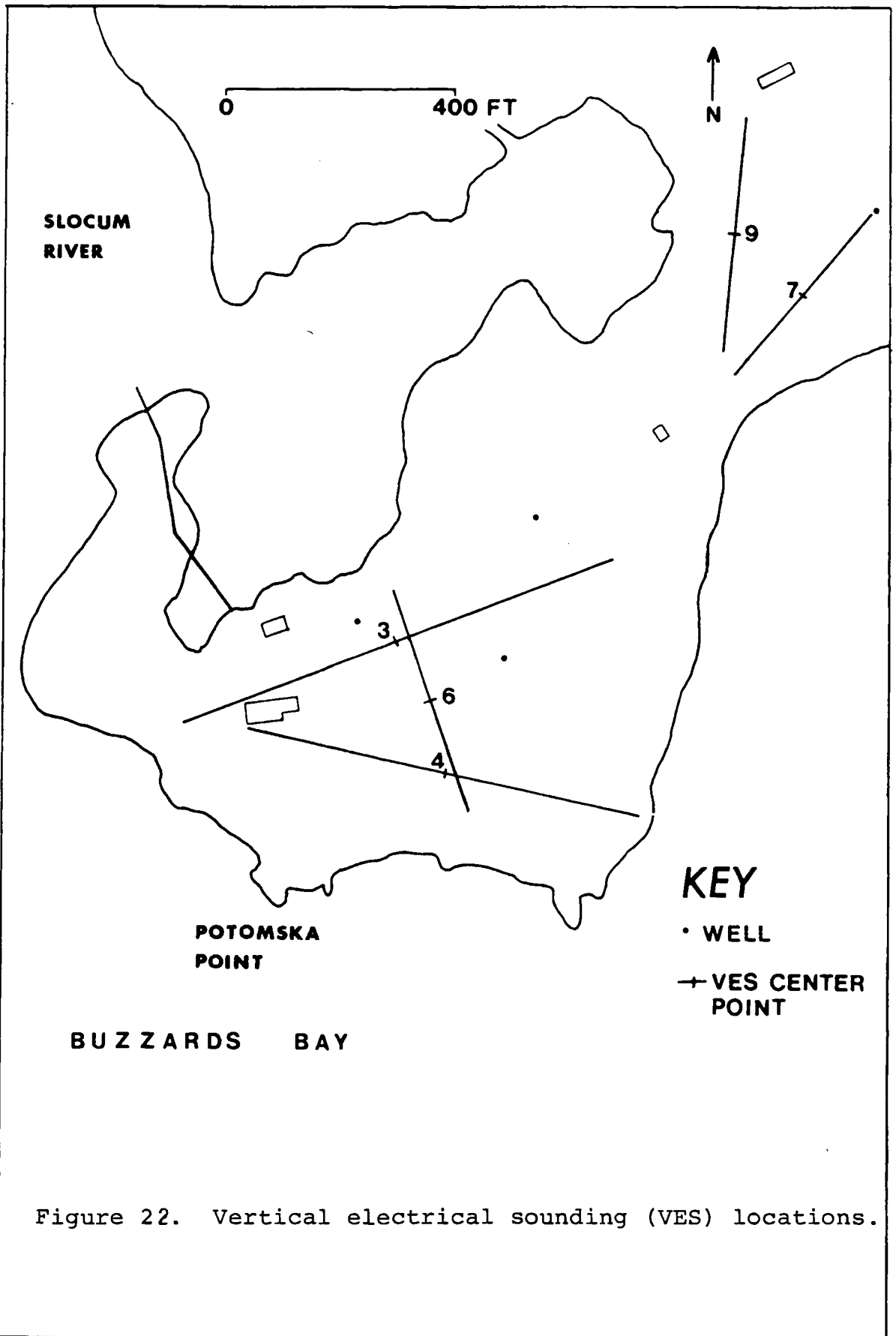


Figure 22. Vertical electrical sounding (VES) locations.

4.7 Data Interpretations

The plots of the field data along with the computer generated match for each of the field curves are shown in Figures 23a - 33 of this section. Along with each curve is presented a diagram which illustrates the interpretation of the field curve. On each of these diagrams there is also a comparison of the depth to the salt/fresh water interface, as determined from the VES interpretation, with the depth to the interface obtained from the theoretical calculations presented in Appendix A. These diagrams are presented as Figures 23b -31b. Following these two figures for each curve is a short discussion of the results.

Some of the computer generated curves may not appear to fit the field data too well. This is due to the effect of subsurface lateral inhomogenities on the field curve. None of the field curves were smoothed to any great extent.

5.0 DISCUSSION OF RESULTS

5.1 Vertical Electrical Sounding # 1

Vertical Electrical Sounding Potter-1 is located in a low-lying area approximately 200 feet from the nearest shoreline at an elevation of approximately 7.5 feet above mean sea level (see Figure 21). This sounding was performed adjacent to the only well in the area in which the depth to salt water could be determined under static conditions. The well (Well 2) was drilled in March of 1983 to provide fresh water to a family which was building a new home. The 386 foot deep well encountered bedrock at 25 feet. The well, which is cased 5 feet into bedrock, immediately drew in salt water when it was first pumped for testing. The results of a water quality analysis of the pumped sample revealed that the water had a salinity of 24 parts per thousand. When the water was tested with a salinity meter, shortly after the Vertical Electrical Sounding was performed at this site, the salinity was found to be 21 parts per thousand at a depth of 4 feet below the water level surface, and the specific conductivity was 24,900 micromhos per centimeter. These readings indicate that the bedrock at 25 feet is contaminated with highly conductive porewater. Because the well is cased down into the bedrock, when the well is pumped no water is drawn into the well through the overlying sediments. Therefore, the

soil above the bedrock was not found to contain salty porewater.

The Vertical Electrical Sounding curve and the computer generated curve which best matches the field data is shown in Figure 23 a. The interpretation of this VES shows that the depth to a salt/fresh water interface in fractured bedrock may be determined with this method. With the aid of the borehole information (depth to water and bedrock) the range of depths possible to the salt water from the VES interpretation is from 24.3 to 24.8 feet. Since it is known that salt water was pumped up into the bedrock in the vicinity of this well, it can be seen that these values are in very good agreement with the known depth to bedrock. The depth to bedrock value is probably accurate to within plus or minus .5 feet.

While the depth to the salt water in the bedrock is known from the borehole information, the bulk resistivity of the salt water saturated fractured bedrock can only be obtained from the interpretation of the VES curve. Figure 23a shows that there are more than one field data points for each $L/2$ greater than 80 feet. Because of this the bulk resistivity of the fractured bedrock is given as a range. This range of values was obtained from two theoretical curves, one which matched the top set of points (curve 1) and the other which matched the bottom set of points (curve 3) on the bottom right hand side of the field

VES 1

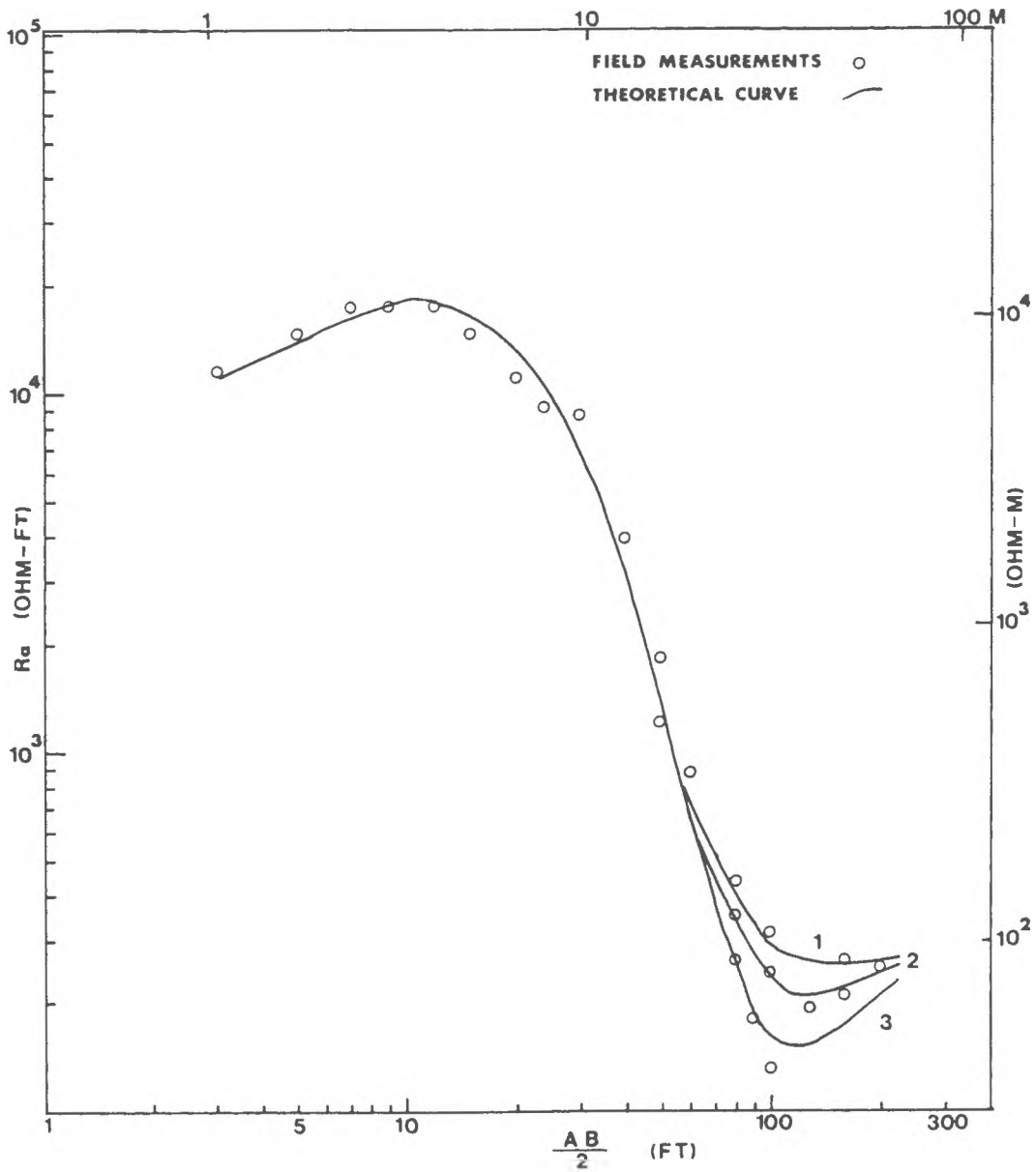


Figure 23a. Sounding 1 field data shown with best match theoretical curves.

data. A curve which falls in between these two curves, as shown in Figure 23a, was chosen as the best fit curve. The Resistivity-Depth models used to produce these three curves are shown in Table 2.

The depth-resistivity model used to produce the best match curve (curve 2) is shown in Figure 23b. The left hand column in Figure 23 b shows that the bulk resistivity of the fractured bedrock from a depth of 24 to about 62 feet is 125 ohm-ft. From the other two curves the range on this value is from 55 to 200 ohm-ft. The increase in the bulk resistivity of the fractured bedrock below this layer, up to 375 ohm-ft, is probably due to the decrease in both the size and spacing of the fractures at this depth in the bedrock. The range on the resistivity of this bottom layer is from 300 to 750 ohm-ft.

The top four layers shown for the interpretation of VES 1 in Figure 23 b are interpreted to represent in descending order: moist top soil with some clay (9000 ohm-ft), dry till with many large cobbles (145,000 ohm-ft), saturated till (8000 ohm-ft), and saturated compacted till above the bedrock (1000 ohm-ft). All of these layers were verified in the field with the exception of the compacted till layer. This layer is inferred to exist from observation of the confined aquifer type response of Well 2 to the tidal fluctuations.

TABLE 2

VES 1 Depth-Resistivity Models

	Curve 1	Curve 2	Curve 3
0.0	-----	-----	-----
	9000	9000	9000 ohm-ft
2.5	-----	2.5 -----	2.5 ft -----
	145000	145000	145000
3.8	-----	3.8 -----	3.8 ft -----
	8000	8000	8000
5.8	-----	5.8 -----	5.8 ft -----
	1000	1000	1000 ohm-ft
24.3	-----	24.3 -----	24.3 ft -----
	200	125	55 ohm-ft
			62.3 ft -----
		71.3 -----	
74.3	-----		
	300	375	750 ohm-ft

VES 1

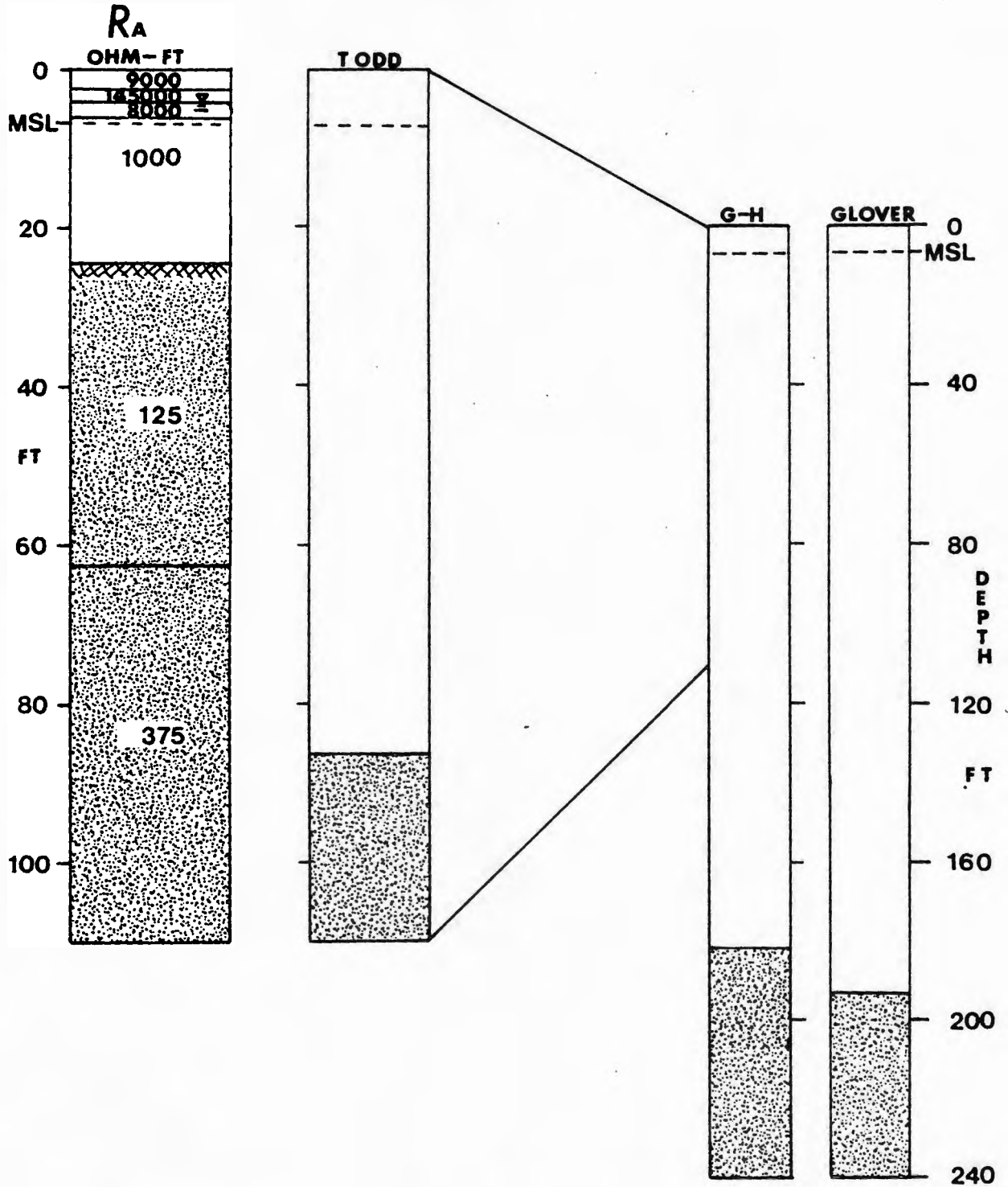


Figure 23b. The column on the left shows the true depth to the salt/fresh water interface as measured by the VES and verified in well 2. The other three columns indicate the theoretical steady-state depth to the interface in this location (i.e., if well 2 had not pumped salt water).

Figure 23b not only shows the VES interpretation, it also illustrates the calculated depth to the salt/fresh water interface from the three theoretical methods applied. Because it has been verified that salt water intrusion has occurred in this location the depth to the interface as determined by these three methods will serve to indicate at what depth the interface was located before it was disturbed by the pumping of Well 2.

By subtracting the depth to the interface as determined by the theoretical methods from the depth to the interface as measured by the VES, the amount of salt water intrusion that has occurred may be determined. By performing this calculation, the method of Todd indicates that the salt/fresh water interface advanced upward a distance of 62 feet. The other two methods, Glover's and Kashef's modification of the Ghyben-Herzberg equation, indicate that the interface intruded vertical distances of 170 and 157 feet respectively.

In order to check the values of the bulk resistivity of the saturated till which covers the bedrock in this location equations 17 and 18 were employed. Using the value of the bulk resistivity of the saturated till from the VES interpretation and the measured resistivity of the water in a nearby shallow dug well, the formation factor was calculated with equation 18:

$$FF = 1000 \text{ ohm-ft} / 328 \text{ ohm-ft}$$

$$FF = 3.05$$

This measured value for the formation factor was then compared with the theoretical value of the formation factor for this soil calculated with equation 17. In order to use this equation the porosity of the soil had to be measured in the laboratory. This information is presented in Appendix J. The theoretical formation factor was calculated as follows:

$$FF = 1.0 * .34^{-1.3}$$

$$FF = 4.06$$

Comparing this theoretical formation factor with the measured formation factor presented above shows that they are in fairly close agreement with each other. In order for them to be in perfect agreement the interpreted value for the bulk resistivity of the saturated till would only have to be increased by 331 ohm-ft or the water resistivity decreased by 82 ohm-ft.

The successful employment of the electrical resistivity method at this site now allows the use of equation 18 in order to determine the formation factor of the bedrock. The formation factor obtained in this case will allow for more accurate interpretations at the other sites which do not have deep boreholes. Using the average value for the bulk resistivity of the bedrock from the curve interpretation, 125 ohm-ft (38.1 ohm-m), and the

value of the porewater resistivity as measured in the borehole, 1.3 ohm-ft (0.4 ohm-m) or 24900 micromhos/cm, the formation factor is:

$$FF = 125 \text{ ohm-ft} / 1.3 \text{ ohm-ft}$$

$$FF = 96$$

Given the range in bulk resistivity of the bedrock as 55 to 200 ohm-ft the range in the value of the formation factor is:

$$FF \text{ (range)} = 42 - 154$$

This range of values is comparable to the formation factor obtained by Sanders (1983) in his study of salt contamination in bedrock in Little Compton, Rhode Island. Sanders obtained a formation factor of 77 for the salt water saturated schist bedrock in his study area. The bulk resistivity of his bedrock and the resistivity of his porewater in the bedrock were 1325 ohm-ft (404 ohm-m) and 17.3 ohm-ft (5.3 ohm-m), respectively. This means that the salinity of the porewater was only about 1 part per thousand (ppt).

Sanders (1983) compared his formation factor with formation factors of bedrock samples measured in the laboratory by previous investigations. Although his formation factor was much lower than the laboratory formation factors, Sanders felt that his formation factor was reasonable since the porosities of the bedrock samples

used in the laboratory experiments were very low. The porosity of one bedrock sample used by Brace et al (1965) was only 0.9%, or 0.009. For comparison purposes the average formation factor obtained in this investigation along with the values obtained by Sanders and Brace are presented below:

TABLE 3

COMPARISON OF BEDROCK FORMATION FACTORS

Researcher	R(bulk)		R(water)		FF
	ohm-ft	ohm-m	ohm-ft	ohm-m	
Kowalski	125	38	1.3	0.4	96
Sanders (1983)	1325	404	17.3	5.3	77
Brace et al (1965)	1017	310	1.0	0.3	1017
Brace and Orange 1968	623	190	0.8	0.25	760

5.2 Vertical Electrical Sounding #2

This sounding was performed at the top of Chaypee Hill at an elevation of approximately 27 feet above mean sea level. Figure 21 shows that this sounding was done close to Well 3. Unfortunately, this well has not been used for over twenty years. Attempts to remove the pump housing to gain access to the well were unsuccessful. No records for the well are known to exist other than that it is a bedrock well of more than 150 feet in depth. Therefore, the lack of information as to the depth to water and bedrock in this area made the interpretation of this sounding difficult. An attempt to dig a shallow observation well ended with a dry 5 foot hole. However, a water level measurement in March in Well 1 indicated that the depth to the water table under Chaypee Hill probably exceeds 12 feet in the summer months. Also, the depth to bedrock at Well 1 is 8 feet.

Using this limited information the original Master Curve interpretation was refined to give the model presented in Figure 24 b. Upon comparison of Figure 24 a with Figure 23 a the reason why the interpretations for these two curves is so different becomes apparent. In VES 1 the curve falls across two decades towards the right and then starts to rise again. This is a good indication that salt water has been encountered. However, in VES 2 the right hand side of the curve has not bottomed out yet. This indicates that the salt water is at a deeper depth, if

VES 2

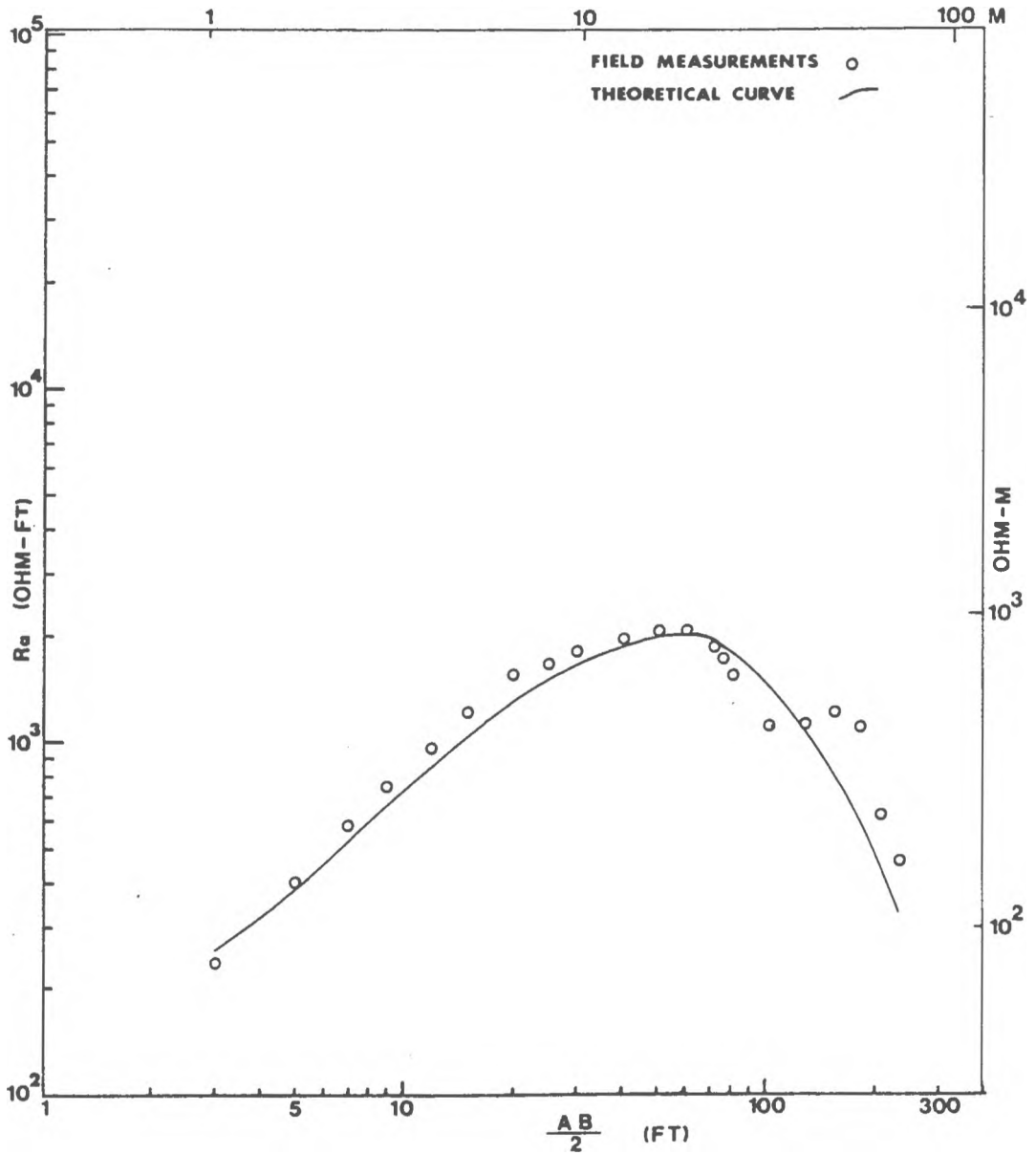


Figure 24a. Sounding 2 field data shown with the best match theoretical curve.

VES 2

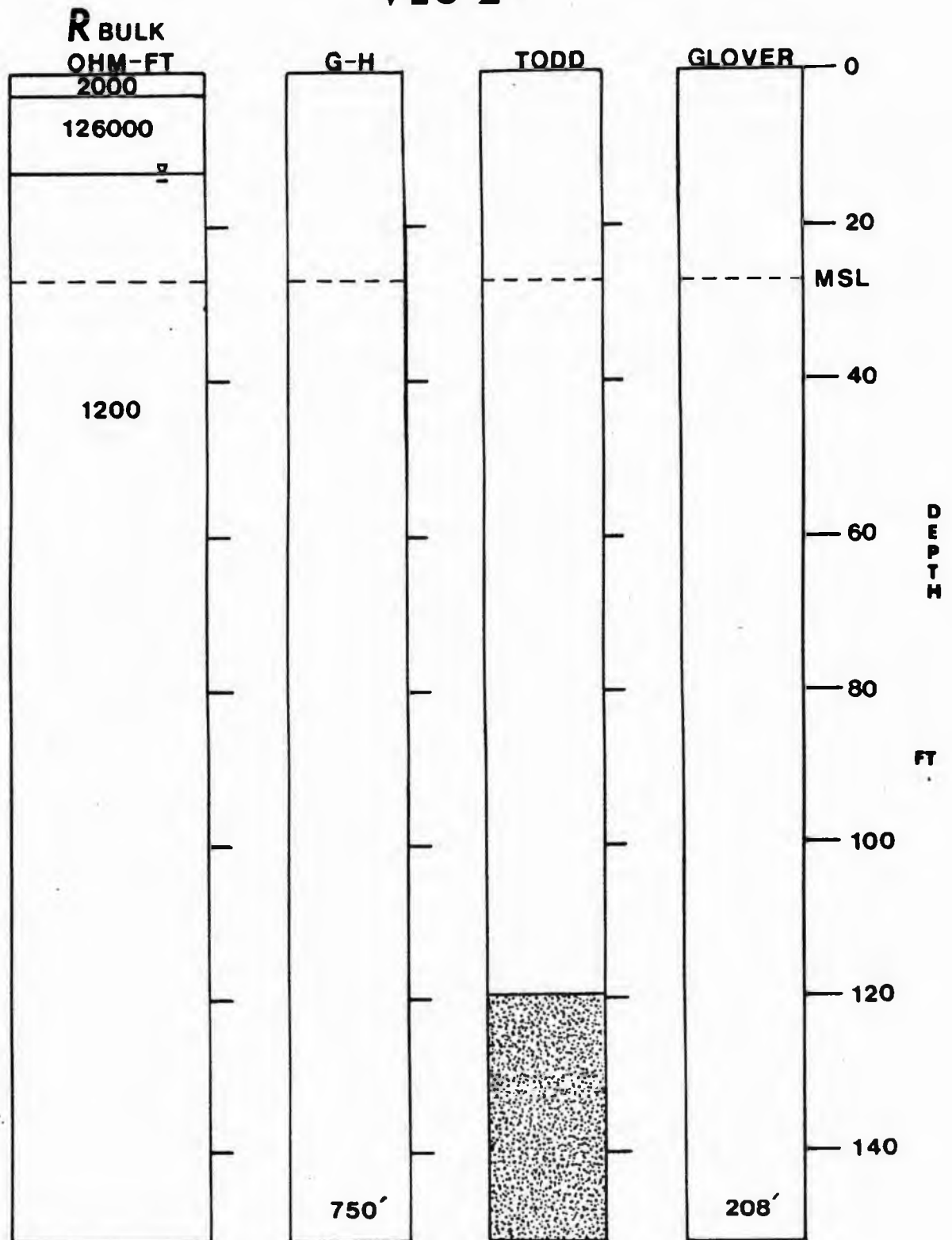


Figure 24b. The column on the left shows that the depth to the salt/fresh water interface could not be determined by the VES. The theoretical depth to the interface is indicated in the other three columns.

it is there at all. However, the bottom layer of the interpretation does indicate that the porewater is slightly salty. This determination was made using the value of the bulk resistivity from the curve interpretation and the value of the formation factor determined from VES 1 with equation 18:

$$R(\text{water}) = R(\text{bulk}) / FF$$

$$R(\text{water}) = 1200 \text{ ohm-ft} / 96 = 12.5 \text{ ohm-ft}$$

$$R(\text{water}) = 12.5 \text{ ohm-ft} / 3.28 = 3.8 \text{ ohm-meters}$$

Converting this to specific conductivity units:

$$S.C. = 10000 / 3.8 = 2632 \text{ micromhos/cm}$$

This value for the porewater specific conductivity indicates that the water in the bedrock at the depth of 62.5 feet is slightly salty (salinity about 1 ppt). This slightly salty layer is interpreted as the top of the Transition Zone. Due to the space limitations at this site the electrodes could not be separated any further to penetrate down to the salt/fresh water interface.

Although the depth to the actual salt/fresh water could not be determined with this sounding, for practical purposes the depth to the transition is probably more useful. Comparison of the depth to the transition zone with the depth to the theoretical salt/fresh water interface is of interest in this case. This comparison shows that the depth to the interface determined by the Ghyben-Herzberg method is unrealistic, even with Kashef's modifications. The depth obtained with Todd's method is

the closest with a value of 120 feet below the datum point. The depth calculated with the method of Glover is higher at 208 feet below the datum point.

5.3 Vertical Electrical Sounding #3

Sounding 3 was performed along a driveway on Potomska Point in the southern section of the study area at an elevation of approximately 22 feet above mean sea level. Figure 22 shows that this sounding is located near shallow Well 8. The depth to the water table in this well was 10.4 feet. Subtracting this from the surface elevation of the measuring point gives a value for the height of fresh water above mean sea level of 11.5 feet. Due to the extensive bedrock outcrops nearby, the depth to bedrock was estimated to be about six feet.

The interpretation of the curve from this sounding, shown in Figure 25a was complicated by the possibility that the top of the water table started below the bedrock surface in this location. The high resistivity of the bedrock with its fractures filled with porewater of relatively high resistivity makes detection of the water table surface difficult. This curve looks similar in shape to VES 2, but it is apparent from the sharply dipping right hand side of the curve that the sounding has penetrated the salt water zone.

The interpretation of this curve produced many different depth-resistivity models which all produced a very similar curve. The range of values from these models for the depth to the salt/fresh water interface went from 37 to 183 feet. To eliminate some of the possibilities,

VES 3

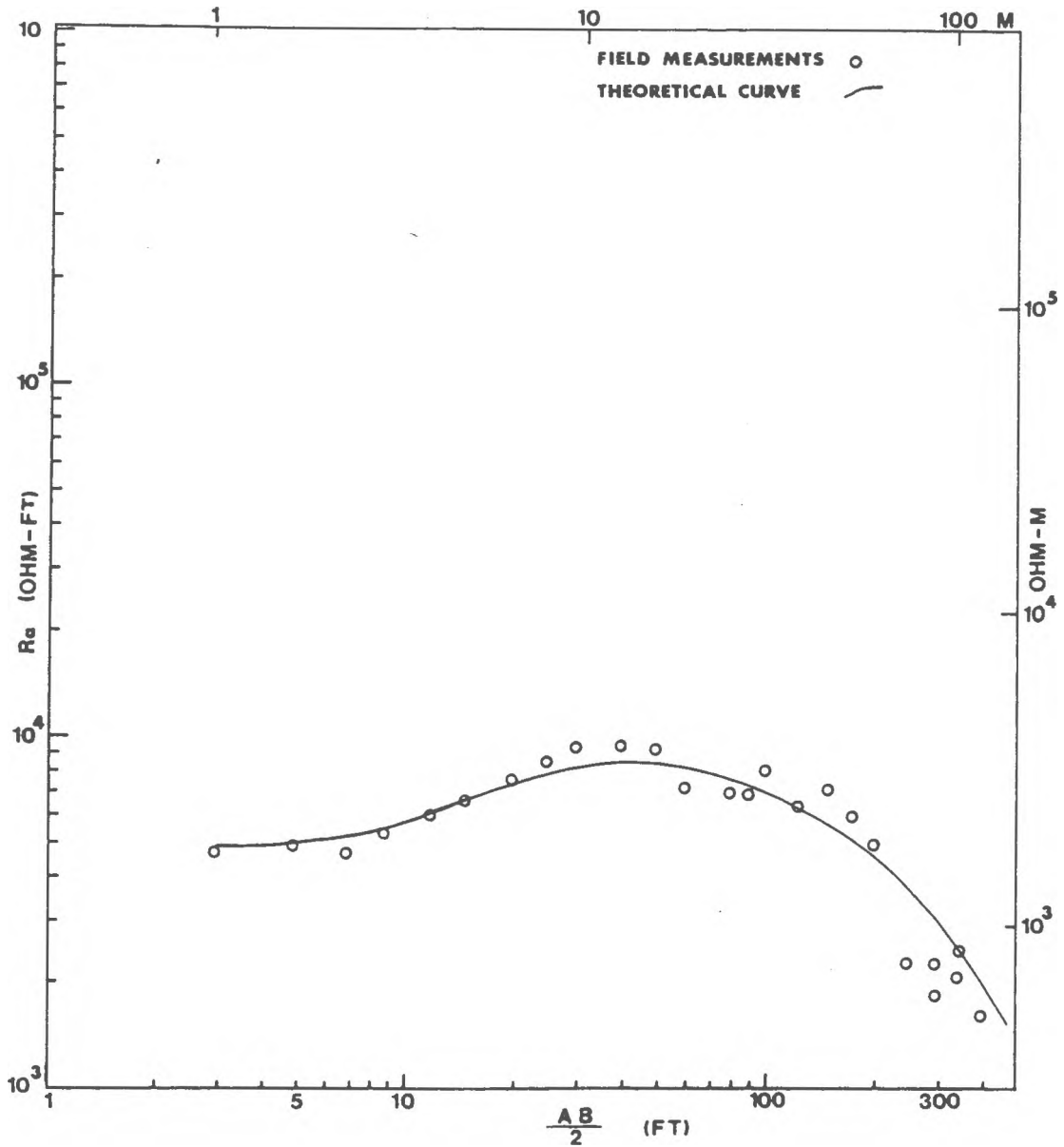


Figure 25a. Sounding 3 field data with the best match theoretical curve.

the interpretation of VES 4 was used. The interpretation of this curve, which was relatively simple, showed that the depth to the interface at a point closer to the shoreline was at least 75.5 feet. This automatically eliminated many of the interpretations for VES 3. Some of the other interpretations for VES 3 were eliminated because the layering sequences they produced disagreed greatly with the known approximate depth to the water table and bedrock surface. This left only two possible interpretations for this curve. The depths to the top of the transition zone from these two interpretations are 145 and 183 feet. The interpretation with the most plausible layering sequence and best fit to the curve is the former of these two. The matching curve and the depth-resistivity model which produced it are shown in Figures 25 a and 25 b, respectively.

The layers in this four layer sequence are interpreted as follows: the top layer represents the moist topsoil (4600 ohm-ft, 1402 ohm-m); the second layer is saturated fractured bedrock (11500 ohm-ft, 3500 ohm-m); the third layer is fractured bedrock saturated with porewater of slightly higher conductivity (5800 ohm-ft, 1770 ohm-m); and the fourth layer is the top of the transition zone with porewater that is slightly salty (750 ohm-ft, 230 ohm-m). The porewater resistivity in this bottom layer is 7.8 ohm-ft (2.4 ohm-m) with a salinity of about 3 ppt.

VES 3

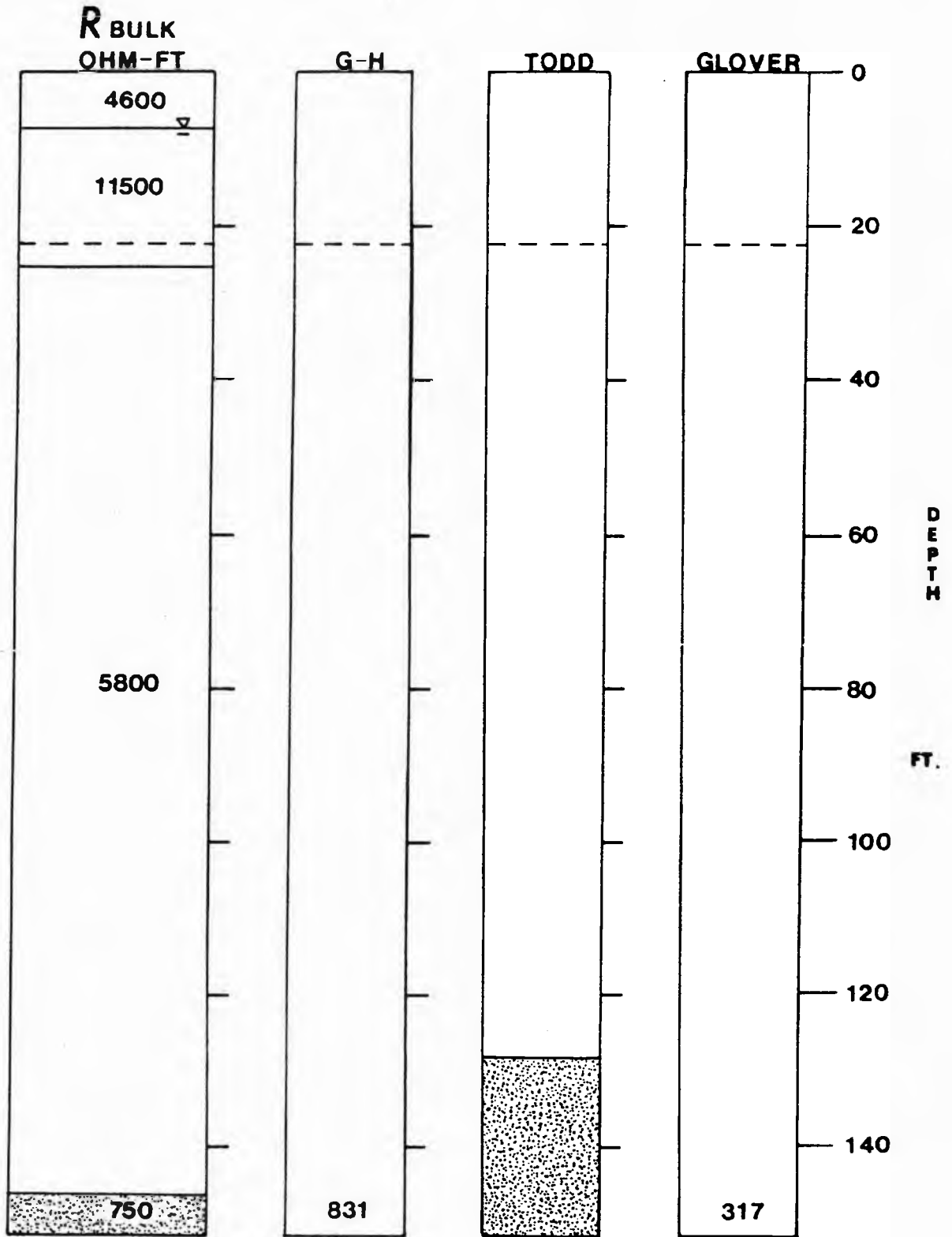


Figure 25b. The depth to the salt/fresh water interface determined from the VES is shown to be at least 145 feet in the left column. The theoretical depth to the interface is indicated in the other three columns.

By analogy with the calculation of the specific conductivity of the porewater in VES 2 in the bottom layer, it can be deduced that the porewater in the bottom layer of this curve interpretation is only slightly saltier. However, in this case the bottom layer with a bulk resistivity of 750 ohm-ft at a depth of 145 feet does indicate that the salt water has definitely been detected in this location.

The depth to the interface using Todd's method was determined by taking the average of the values obtained for Wells # 7 and 8 since the location of this sounding was midway between these two wells. The resulting depth to the interface from Todd was 128 feet (39 m). This value agrees very well with the depth to the interface as determined above.

In this location Kashef's method could not be applied due to the steep hydraulic gradients in this area. The value of 800 feet in the column labeled G-H is the result of applying the Ghyben-Herzberg relation without Kashef's modifications. The depth to the interface according to Glover's solution was 317.1 feet or 96.8 meters.

5.4 Vertical Electrical Sounding #4

Vertical Electrical Sounding 4 was run parallel to the shoreline about 300 feet south of VES 3 on Potomska Point. The center point was located 100 feet from the shore at an elevation of approximately 10 feet above mean sea level. Bedrock in the vicinity is very shallow, with outcrops less than 20 feet away. No nearby wells were available, but the depth to the water table is estimated to be about 6 feet in this area.

The curve which was produced by this sounding was relatively easy to interpret. The curve shown in Figure 26a appears very similar to VES 3, but it lacks the steep ascending and descending portions that VES 3 has. The flat sections of a VES curve such as the ones in VES 4, indicate that the apparent resistivity as read directly from the curve is very close to the actual combined resistivity of the layers below the center point.

The resulting five layer interpretation for this curve shown in Figure 26b indicates that the depth to the top of the transition zone in this location is at least 75.5 feet. Employing equation 16 and a formation factor of 96 from VES 1, the specific conductivity of the porewater at this depth can be calculated:

$$R(\text{water}) = R(\text{bulk}) / FF$$

$$R(\text{water}) = 5000 \text{ ohm-ft} / 96 = 52 \text{ ohm-ft}$$

$$R(\text{water}) = 52 \text{ ohm-ft} / 3.28 = 15.9 \text{ ohm-meters}$$

VES 4

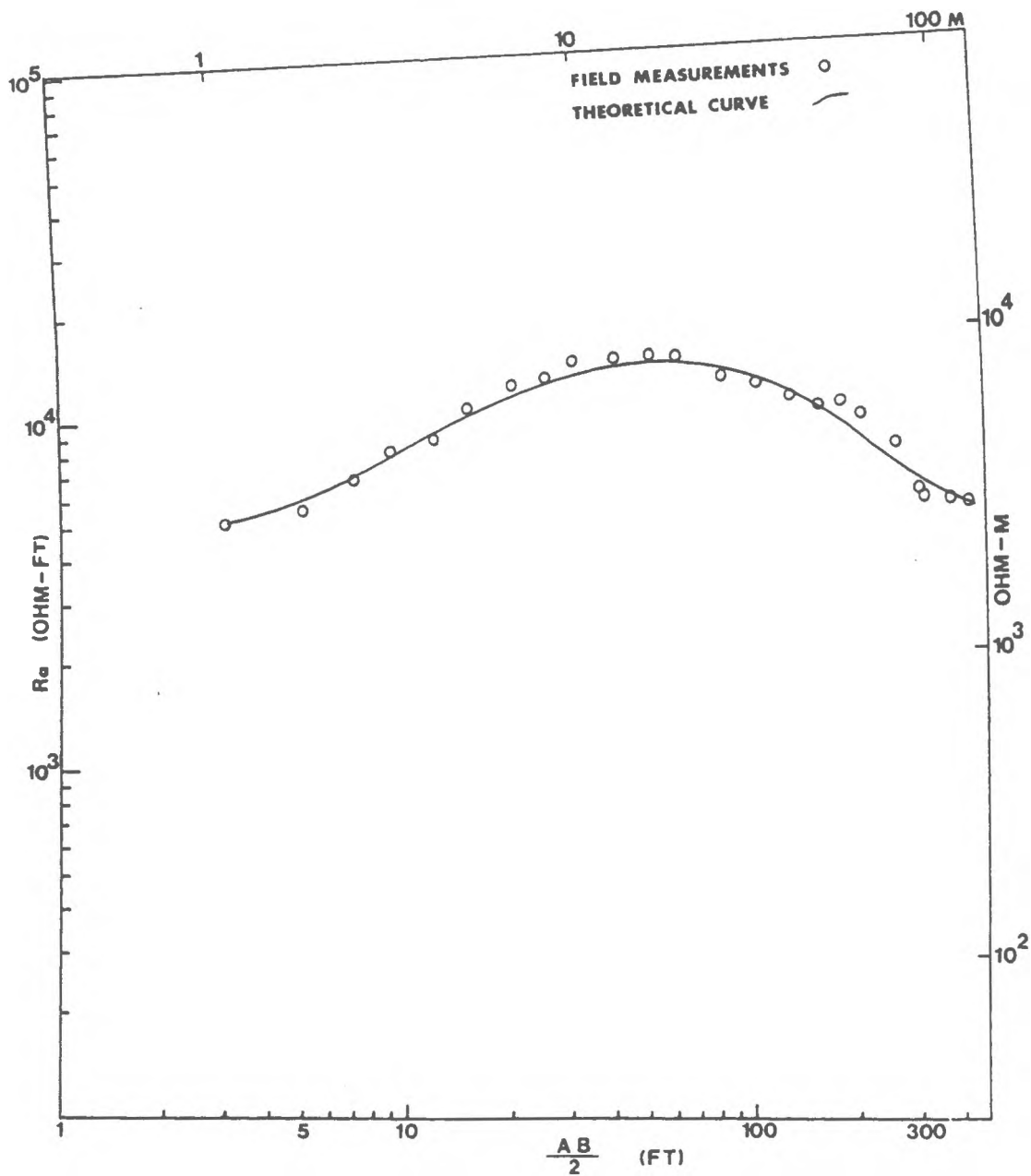


Figure 26a. Sounding 4 field data shown with the best match theoretical curve.

VES 4

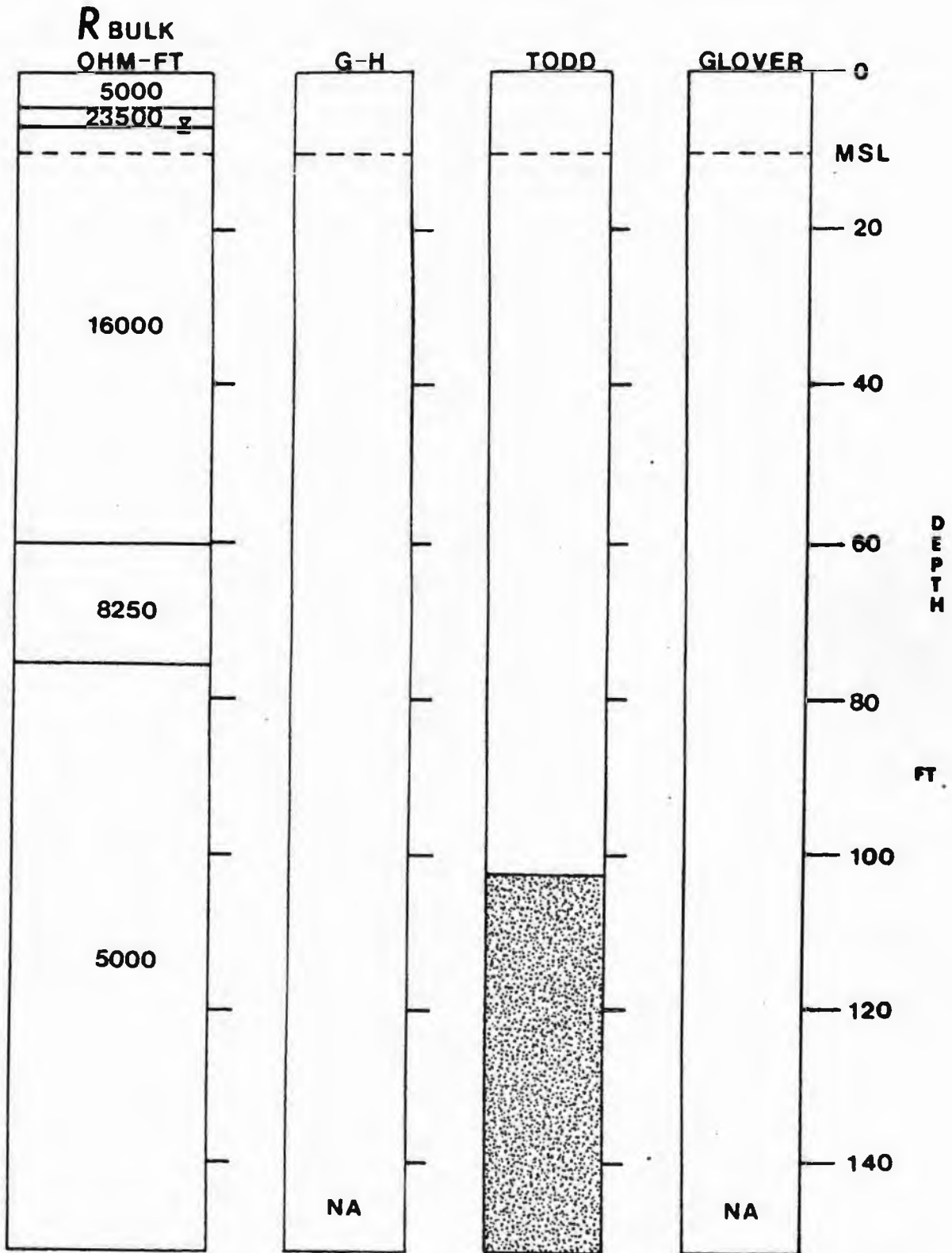


Figure 26b. The VES interpretation in the left column shows that the depth to the salt/fresh water interface is at least 75 ft in this location. The only theoretical calculation which could be used gave a depth of 103 ft to the interface.

Converting this to specific conductivity units:

$$\text{S.C.} = 10000 / 15.9 \text{ ohm-meters} = 630 \text{ micromhos/cm}$$

This value for the porewater specific conductivity is not much higher than the average specific conductivity of the fresh water drawn from the wells in this area which is about 100 micromhos/cm. Therefore the depth of 75.5 feet must be considered to be a minimum depth to the top of the transition zone.

Due to the lack of wells in the immediate area of VES 4 neither the Ghyben-Herzberg method nor Glover's method could be applied at this site. Figure 26b does show that the theoretical depth to the interface using Todd's method is 103 feet in this location. If this is considered to be the depth to the middle of the transition zone the agreement between this value and the value of 75.5 feet to the top of the transition zone is good. These calculations indicate that the thickness of the transition zone in this area is 55 feet.

5.5 Vertical Electrical Sounding #5

This electrical sounding was performed on Chaypee Hill at an angle to VES 2 as shown in Figure 21. The center point was located about 324 feet from the shoreline at an elevation of about 20 feet above mean sea level. Again, as in the interpretation of VES 2, this interpretation was hampered by a lack of borehole information. However, unlike the interpretation of VES 2, the interpretation of this curve presented many problems.

Due to the shape of the sounding curve, shown in Figure 27a, the interpretation of VES 5 did not lead to a unique answer for the depth to the salt/fresh water interface. As discussed in Section 4 D, the interpretation of all VES curves is limited by a number of factors. In this case the interpretation is limited due to the principle of equivalence. Because curve 5 has a steeply downward dipping terminal end with no minimum, the curve may be interpreted with a range of values. Figure 27b shows two different models which both produce very similar curves. These two models show that the depth to the top of the transition zone could be any where between 53.5 and 173.5 feet below the surface. Considering that both nearby wells (Well 1 and Well 3) have produced salty water, the interface is probably closer to 53.5 feet, obtained by depth-resistivity model 5-13.

VES 5

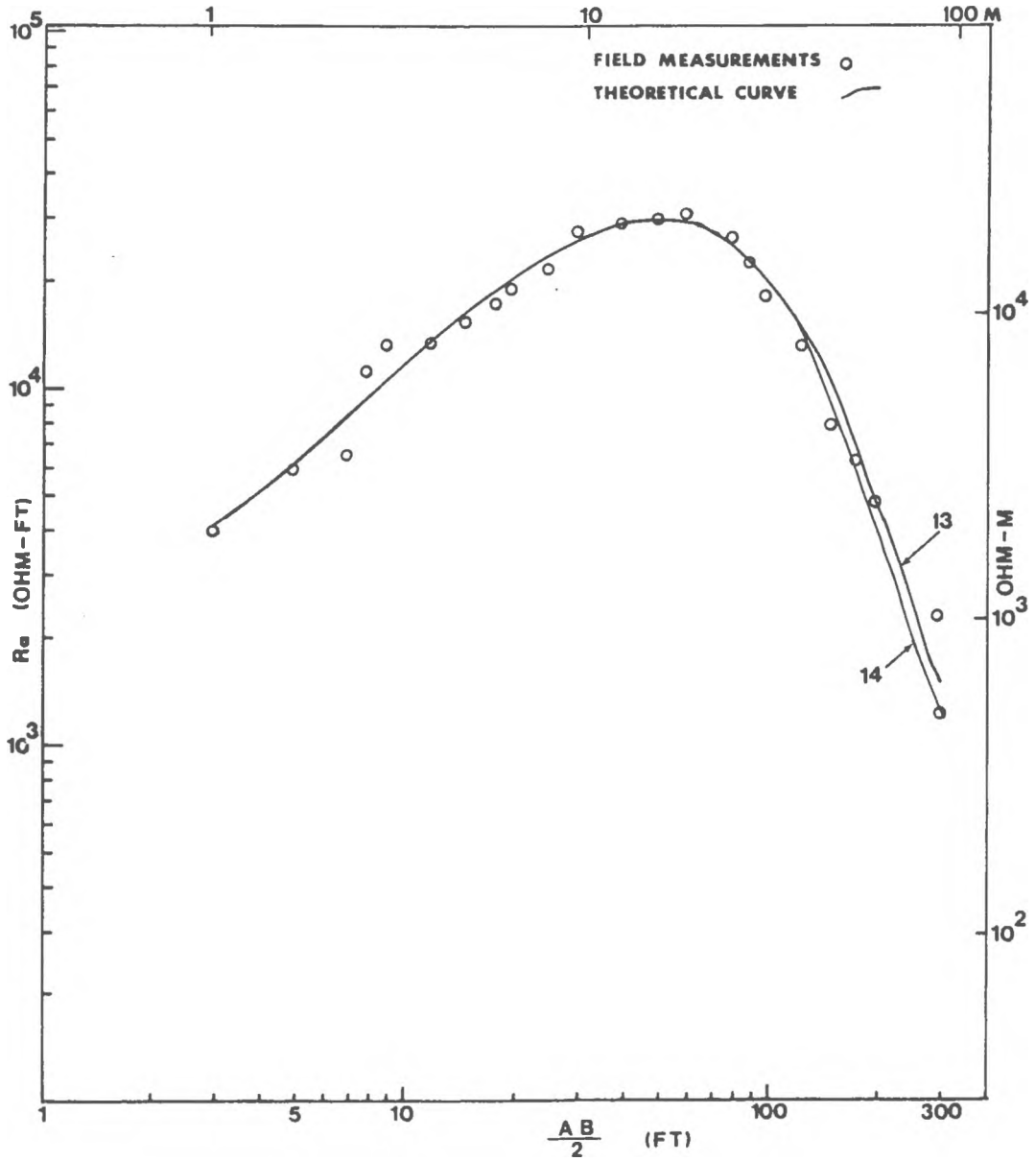


Figure 27a. Sounding 5 field data shown with the two matching curves produced by the theoretical depth-resistivity models shown in Figure 27b.

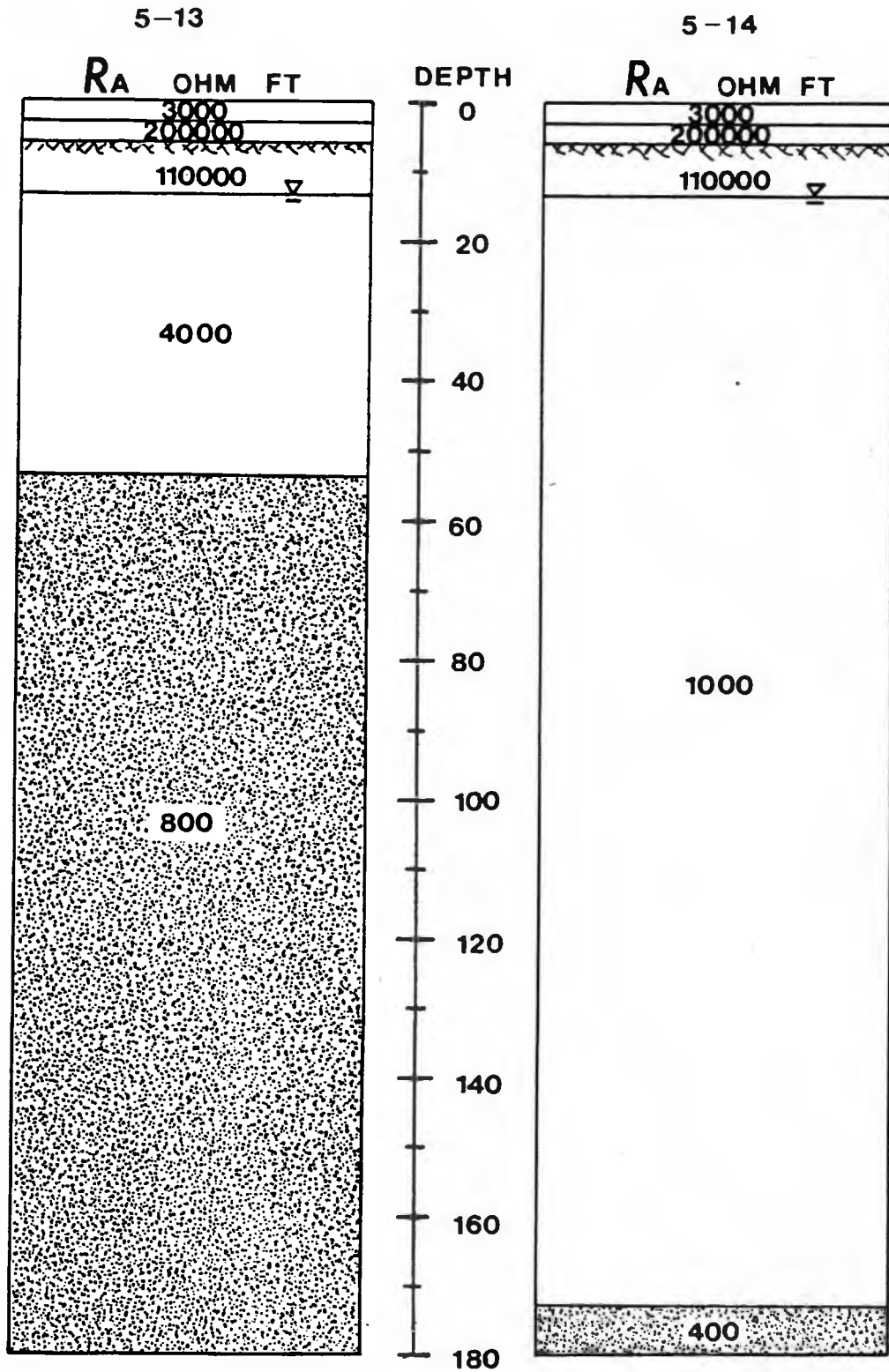


Figure 27b. Two possible depth-resistivity models for the interpretation of VES 5 which produce very similar curves and match the field data, as shown in figure 27a.

Figure 27c compares the depth to the interface as determined by curve model 5-13 with the values determined by the empirical methods. In this case the Ghyben-Herzberg relation could not be applied due to the lack of a nearby well. Figure 27c shows that the method of Todd once again is in fairly close agreement with the VES interpretation with a calculated depth to the middle of the transition zone of 125 feet. Applying Glover's method yielded a value of 282 feet for the depth to the interface.

VES 5

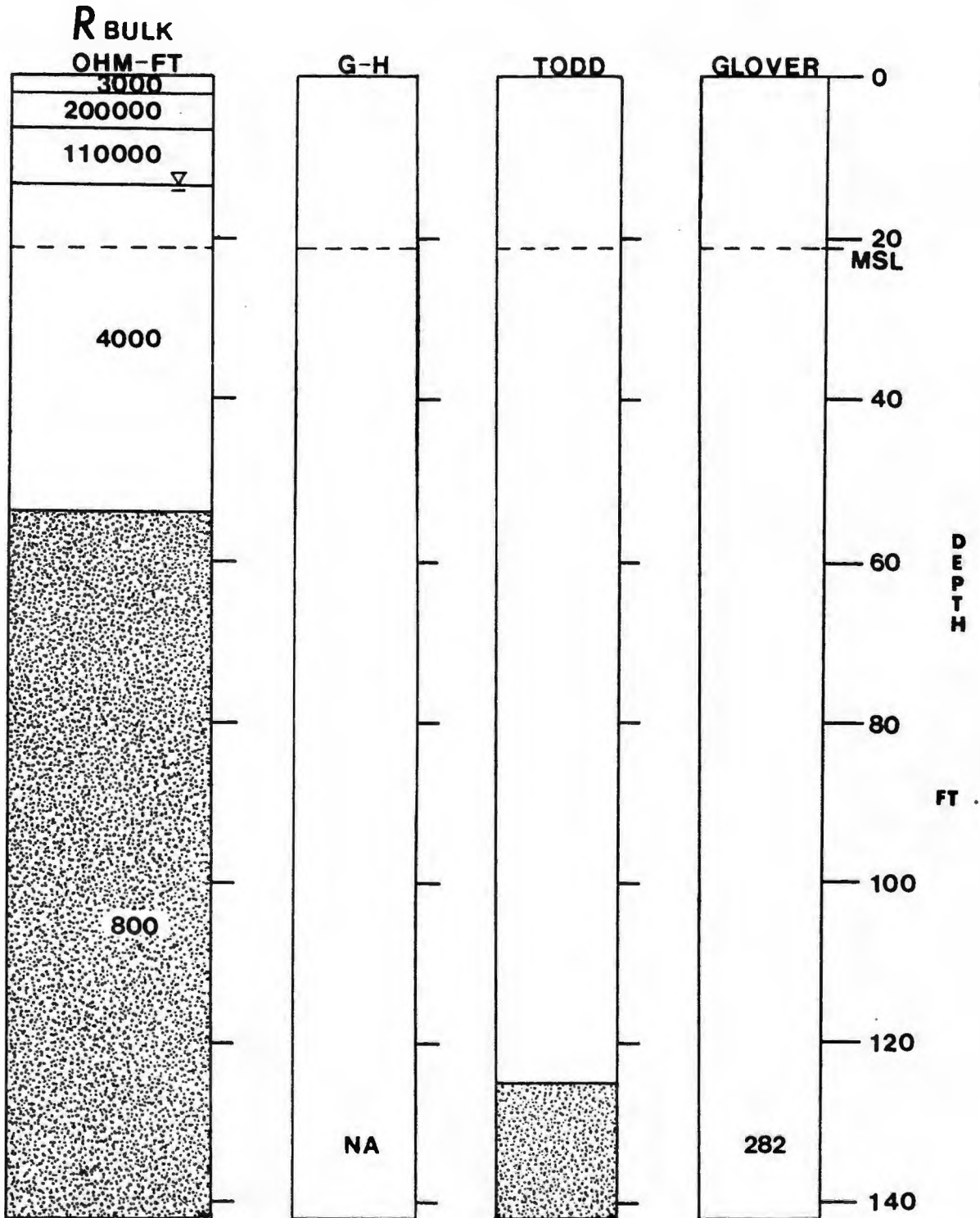


Figure 27c. The VES interpretation shown in the left column indicates the depth to the interface is 53 ft in this location. The two theoretical methods indicate the depth to the interface should be at least twice this amount under nonpumping conditions.

5.6 Vertical Electrical Sounding #6

The center point of this sounding was located about midway between VES 3 and VES 4 but was run perpendicularly to them. The sounding was done at a distance of 300 feet from the shore at an elevation of approximately 20 feet above mean sea level. Depths to bedrock and the water table were estimated to be 3 and 8 feet respectively.

Figure 28a shows that VES 6 is similar in shape to VES 3 with the exception that the right hand side of VES 6 does not drop off like VES 3. Figure 28b indicates that a depth to the interface could not be determined with this sounding. The layer sequence was interpreted as follows: topsoil, 2750 ohm-ft (840 ohm-m); unsaturated bedrock, 45000 ohm-ft (13720 ohm-m); partially saturated bedrock, 31500 ohm-ft (9600 ohm-m); saturated bedrock, 18000 ohm-ft (5488 ohm-m); bedrock saturated with porewater of a slightly higher conductivity, 5750 ohm-ft (1753 ohm-m).

The resistivity of the porewater in the bottom layer of the depth-resistivity model for this curve has been calculated as:

$$R(\text{water}) = R(\text{bulk}) / FF$$

$$R(\text{water}) = 5750 \text{ ohm-ft} / 96 = 59.9 \text{ ohm-ft}$$

$$R(\text{water}) = 59.9 \text{ ohm-ft} / 3.28 = 18.2 \text{ ohm-meters}$$

Converting this to specific conductivity units:

$$S.C. = 10000 / 18.2 \text{ ohm-m} = 549 \text{ micromhos/cm}$$

VES 6

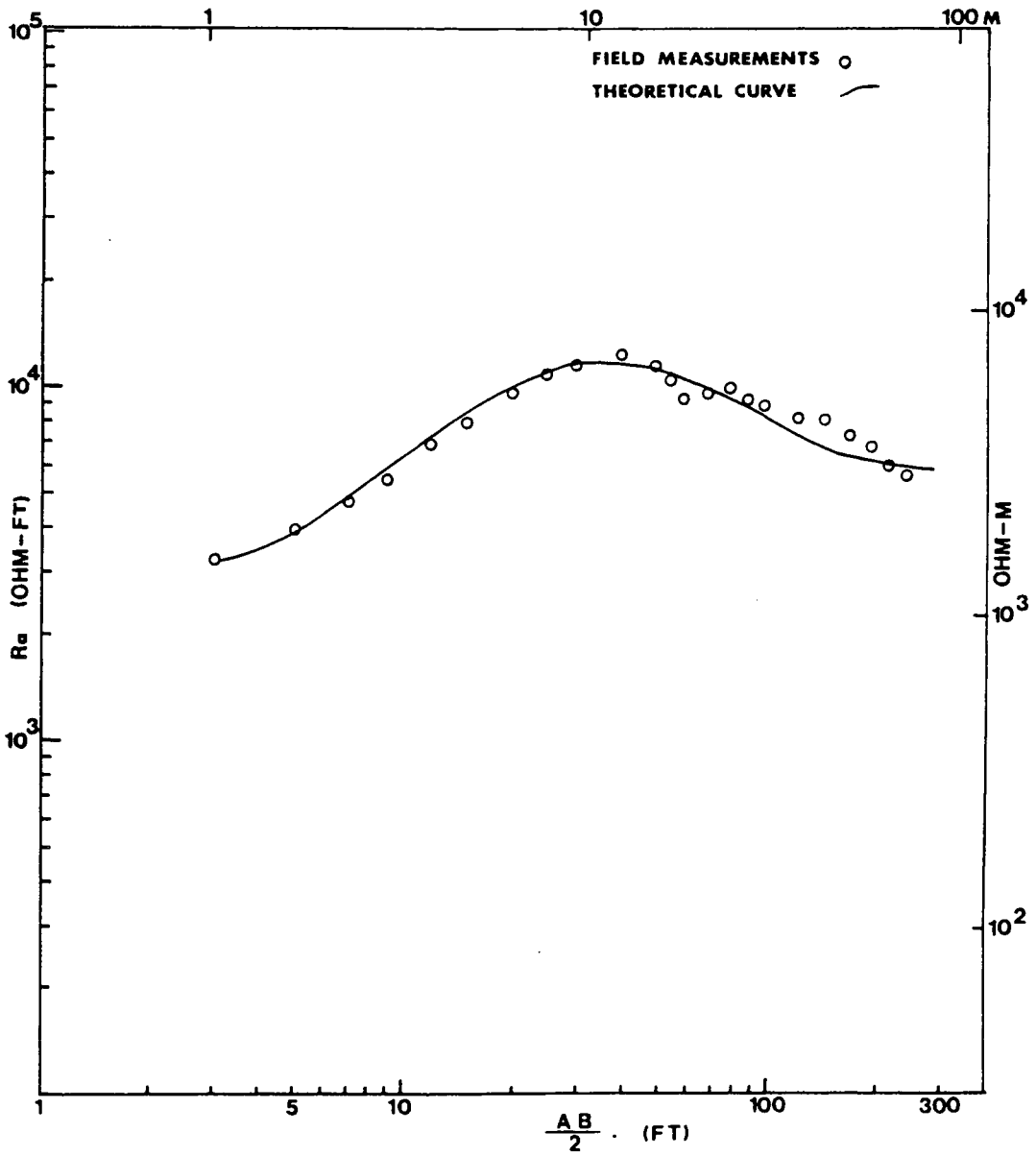


Figure 28a. Sounding 6 field data shown with the best match theoretical curve.

VES 6

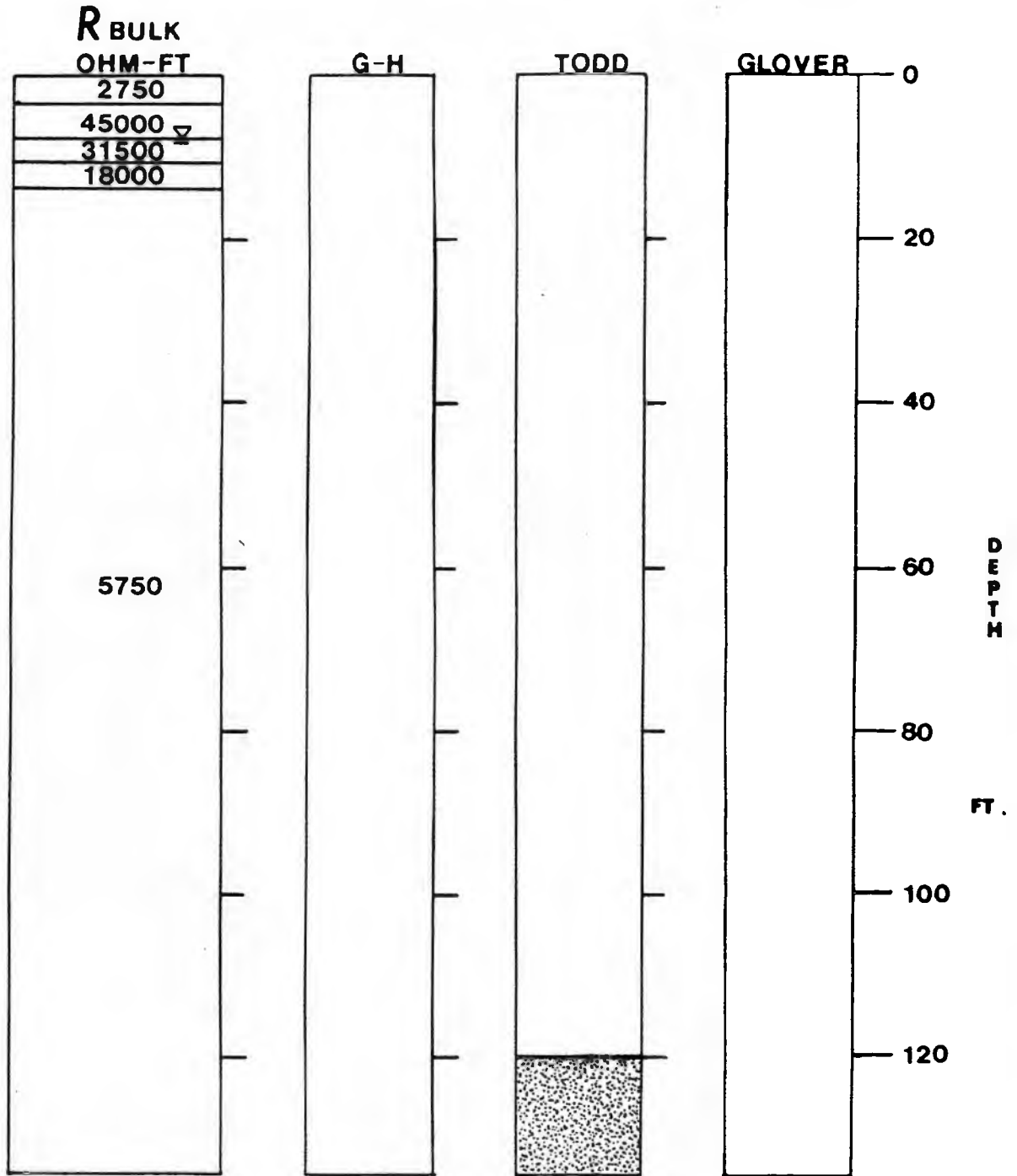


Figure 28b. The interpretation of this VES, shown in the left column, indicates that the depth to the salt/fresh water interface could not be determined in this location. The two theoretical depths to the interface were estimated using data from VES 3 and VES 4.

Again, as in VES 4, the porewater specific conductivity in the bottom layer of this VES curve interpretation is not much higher than the specific conductivity of the fresh water in the area.

5.7 Vertical Electrical Sounding #7

Sounding number 7 was run about 150 feet from the shore at an elevation of approximately 5 feet above mean sea level. The sounding location is indicated in Figure 22. Nearby bedrock outcrops indicate that the depth to bedrock is probably less than 10 feet in this area. The depth to the water table is estimated to be about 3 feet. Permission to dig a test pit to determine the subsurface material and the depth to the water table could not be obtained in this location. However, the material at the surface appeared to be a very thin layer of soil covering coarse sand, gravel and cobbles, similar to the high energy shorelines in other areas. The driveway between the center point of this sounding and the water was built on top of fill materials in order to raise it above the high tide shoreline which used to lie behind the driveway.

The long, steeply descending portion of the curve for VES 7, shown in Figure 29a, is indicative of the fact that the salt water layer has been detected. The ascending far right hand side of this curve has been interpreted as the underlying massive bedrock. Due to the scatter in the field data on the bottom portion of this curve, it was impossible to generate one single theoretical curve to best match all of the data points. For this reason three different resistivity-depth models were created. In all three of these six layer models the first three layers are

VES 7

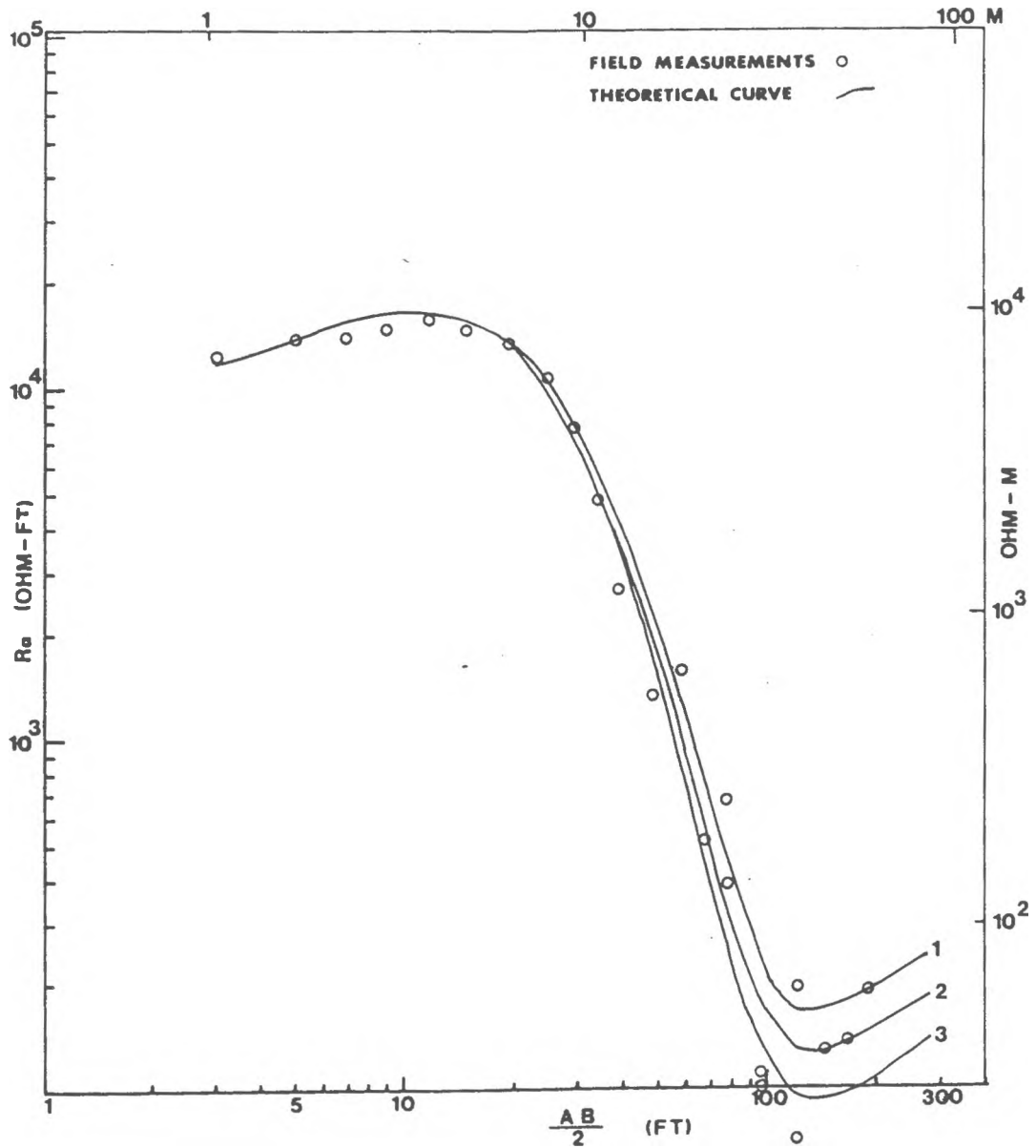


Figure 29a. Sounding 7 field data shown with the best fit theoretical curve (curve 2) and the two other curves which represent the range in the possible interpretation of the field data.

common, only the last three layers are different in each model, as shown in Table 4.

The depth-resistivity model shown in figure 29b produced the best fit curve (curve 2) to the field data. The other two models which produced the other two curves can be assumed to represent the range in the interpretation of the final three layers.

As shown by the calculations for VES 2, the fourth layer with a bulk resistivity of 1450 ohm-ft is interpreted to be the top of the transition zone. The specific conductivity of the porewater in this layer was calculated as 2171 micromhos/cm (salinity of 1.5 ppt). In order to determine the depth to the theoretical sharp interface, the porewater specific conductivities of the second to last layer was determined:

$$R(\text{water}) = R(\text{bulk})/FF$$

$$R(\text{water}) = 80 \text{ ohm-ft} / 96 = 0.83 \text{ ohm-ft}$$

$$R(\text{water}) = 0.83 \text{ ohm-ft} / 3.28 = 0.254 \text{ ohm-meters}$$

Converting this to specific conductivity units:

$$S.C. = 10000 / 0.254 = 39360 \text{ micromhos/cm}$$

The range in this value is 31488 to 57250 micromhos/cm. From these calculations it is apparent that the porewater in the layer with a bulk resistivity of 80 ohm-ft is as salty as the water in the ocean. Therefore, the depth to the salt water in this location is interpreted to be approximately 30 feet.

TABLE 4

VES 7 Resistivity - Depth Models

	Curve 1	Curve 2	Curve 3	
0.0	-----	-----	-----	
	10200	10200	10200	ohm-ft
2.5	-----	2.5 -----	2.5 ft -----	
	43000	43000	43000	
2.8	-----	2.8 -----	2.8 ft -----	
	25000	25000	25000	
9.9	-----	9.9 -----	9.9 ft -----	
	2000	2000	2000	ohm-ft
27.9	-----	27.9 -----		
			29.9 ft -----	
	100	80	55	ohm-ft
97.9	-----	97.9 -----		
			99.9 ft -----	
	500	350	300	ohm-ft

VES 7

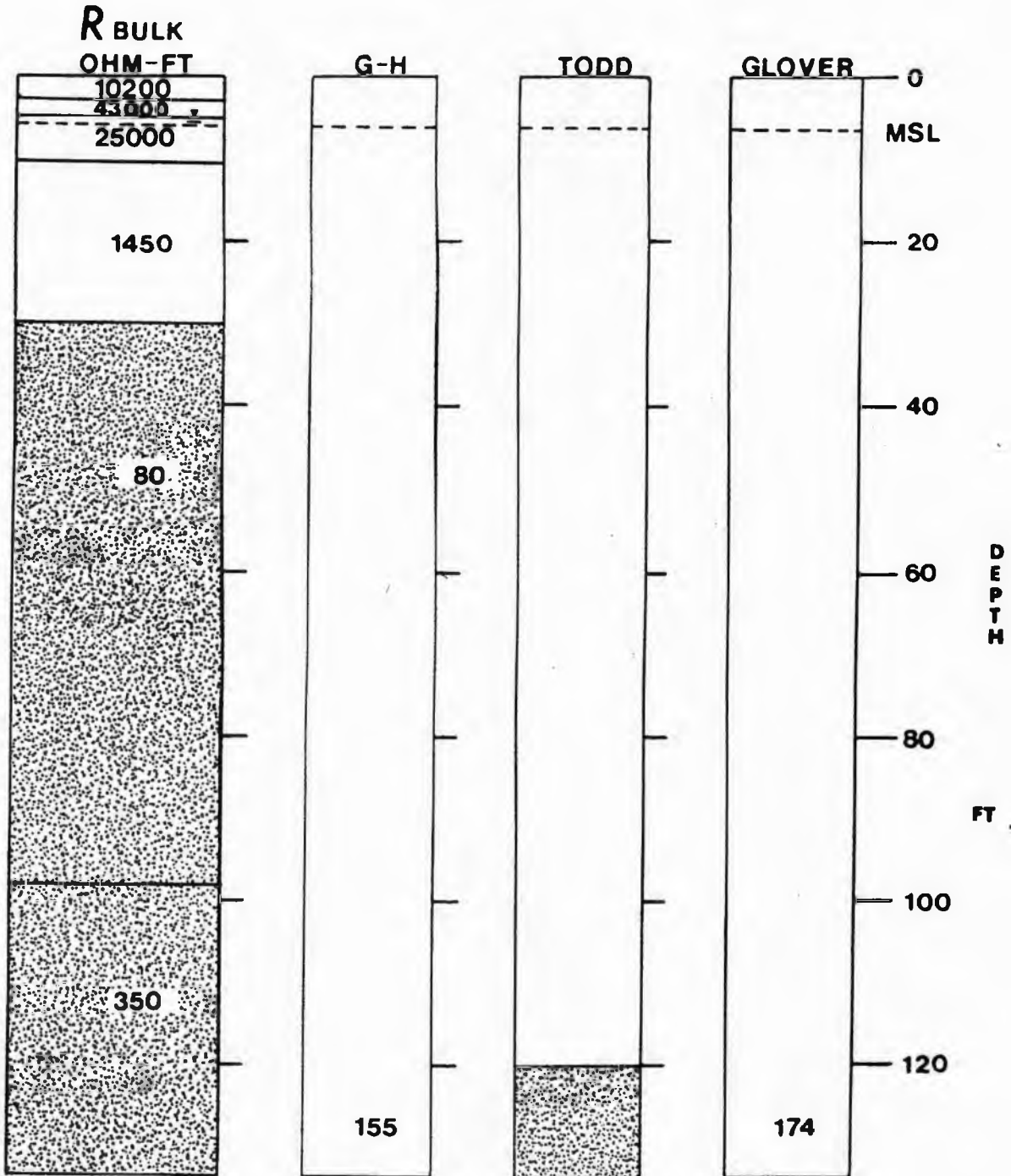


Figure 29b. The depth to the interface interpreted from the VES curve is 29 ft, as shown in the left column. The three theoretical methods applied indicate a minimum depth of 115 feet to the interface under nonpumping conditions.

As shown in Figure 29b the top of the transition zone lies at about 10 feet according to this interpretation. While this may seem unlikely, it must be pointed out that the porewater specific conductivity of this first layer in the transition zone is only 2171 micromhos/cm, or only slightly salty. Also, the well closest to this sounding was just abandoned in 1982 because it was drawing in brackish water. This is a good indication that the depth to salt water has been affected by the pumping of this well, and should be expected to be at a shallow depth.

Since the position of the salt/fresh water interface has probably been affected by the pumping of fresh water from a nearby well in this area, the depth to the interface as predicted by the three theoretical methods is greater than that as predicted by the VES interpretation. However, in this case the three methods yield similar values for the depth to the midpoint of the transition zone: Glover = 174 ft, G-H = 155 ft, Todd = 120 ft. These values were calculated for the point at which well 5 is located. The depth to the interface at the center point of sounding 7 would probably be less. With this in mind, the amount of salt water intrusion which may have occurred in this area has been calculated to be approximately 85 vertical feet.

5.8 Vertical Electrical Sounding #8

The Center Point of Vertical Electrical Sounding number 8 was located 400 feet from the shoreline at an elevation of approximately 16 feet above mean sea level. Extensive bedrock outcrops 100 feet to the east and a 20 foot deep dug well 40 feet to the west indicate that the depth to bedrock in the area is greater than 20 feet but probably no more than 40 feet. The nearby shallow well supplies high quality water to the property owners. This well has never had any salt problems in the last thirty years. The depth to water in the well under steady state pumping conditions was measured to be 12.5 feet below the ground surface in the month of June. The elevation of this well was only partially surveyed due to logistical problems but, the elevation of the well above mean sea level was estimated to be 14.4 feet.

Figure 30a shows the field curve and best match curve for VES 8. Note the similarity of this curve with VES 7. The resistivity-depth model used to produce the matching curve is presented in Figure 30b. This figure shows that the top of the transition zone is at a depth of 44.5 feet in this location. Due to the suppression of the fresh water layer in this VES, the bulk resistivity and thickness of the third layer was found to range from 7000 to 10000 ohm-ft (2134 to 3049 ohm-m) and from 36 to 51.4 feet thick (11 to 15.7 meters). Therefore, the depth to the interface

VES 8

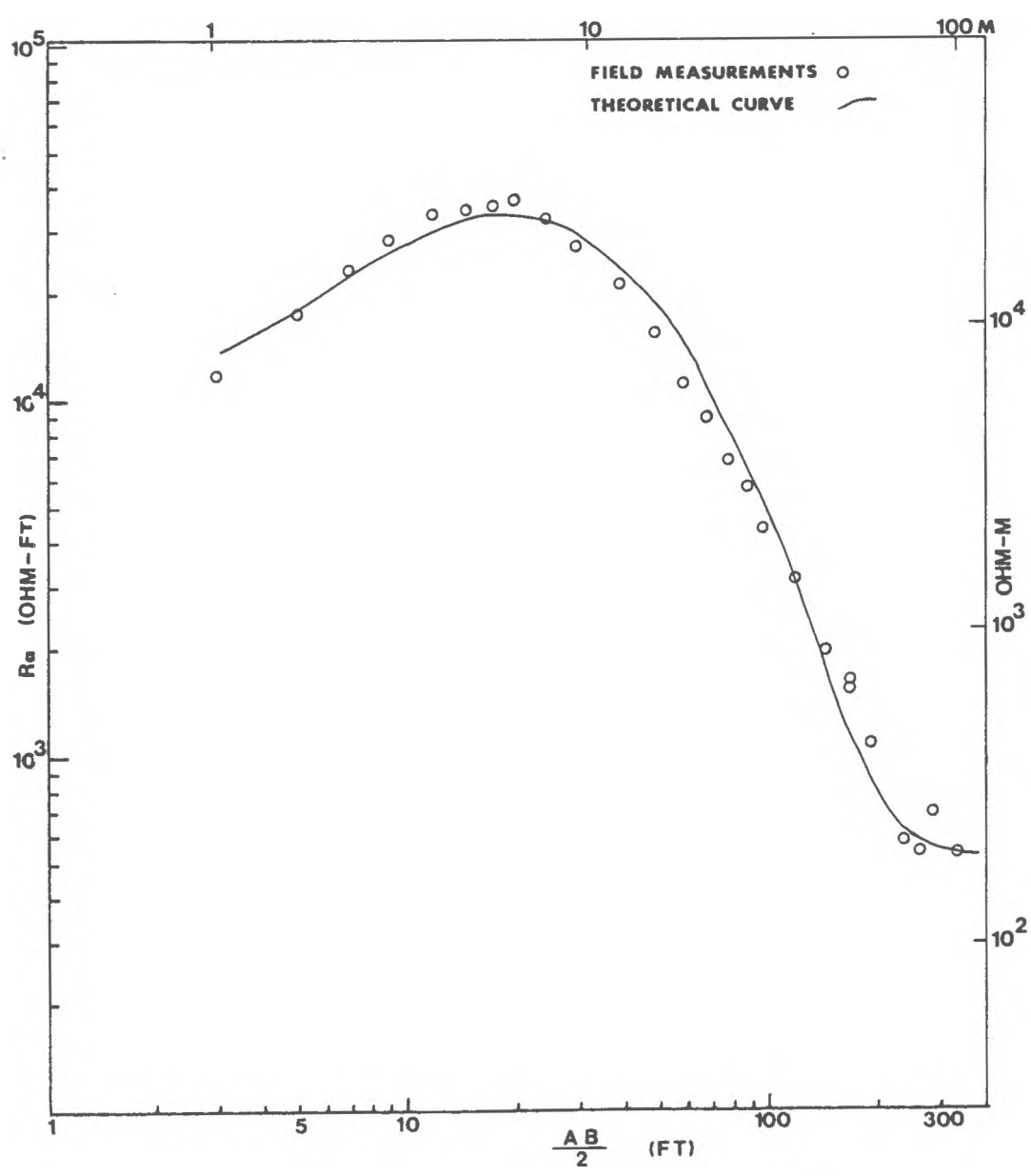


Figure 30a. Sounding 8 field data shown with the best match theoretical curve.

VES 8

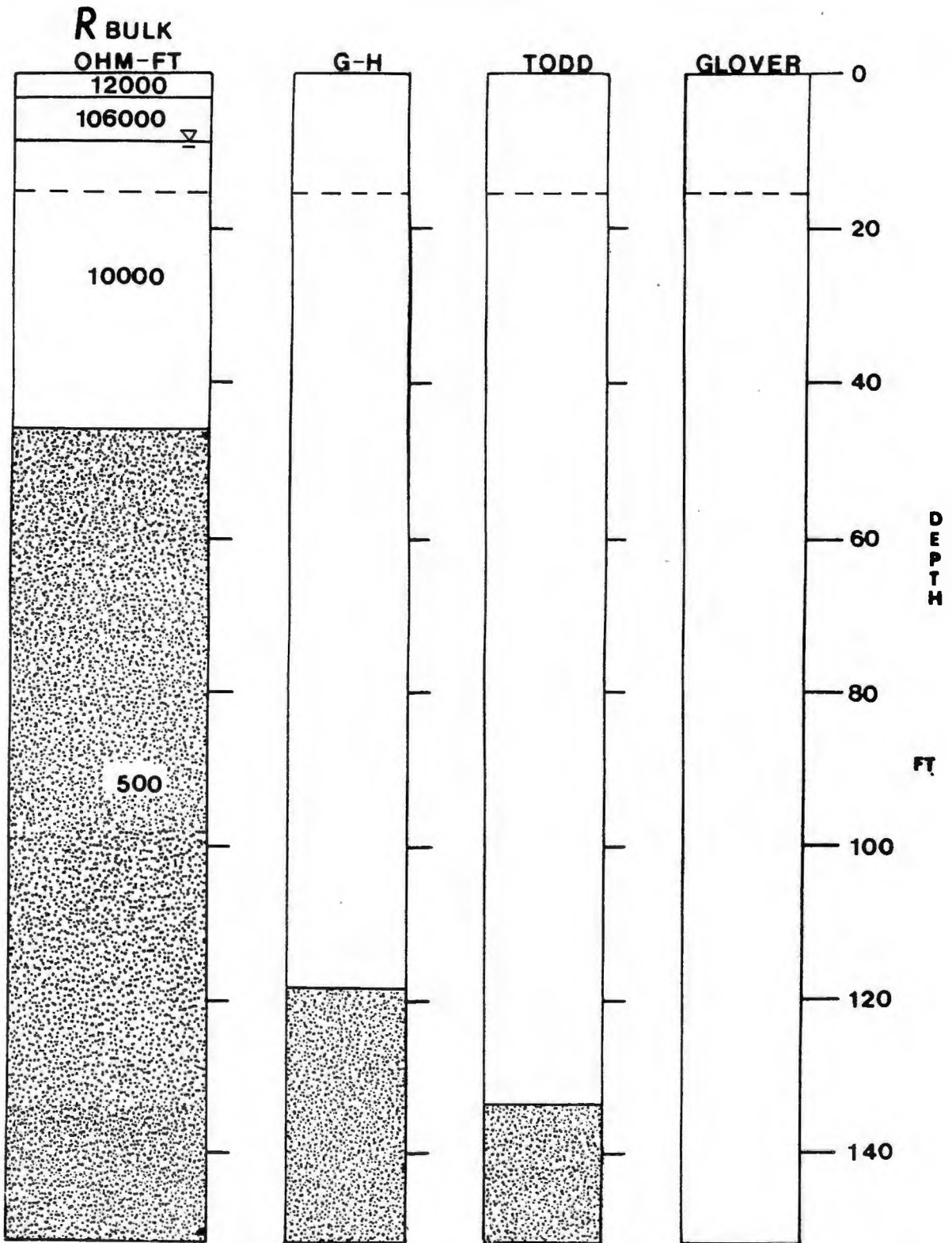


Figure 30b. The interpretation of the VES is shown in the left column. Two theoretical depths to the salt/fresh water interface are indicated in the two middle columns.

could range from a depth of 44.5 to 59.9 feet. Using the calculations previously shown, the bulk resistivities of the third (7000 ohm-ft) and fourth layer (500 ohm-ft) can be used to calculate the porewater specific conductivities of these two layers.

The resulting porewater specific conductivities are 450 micromhos/cm for the third layer and 6298 micromhos/cm for the fourth layer. The porewater specific conductivity of the third layer agrees fairly closely with the field measurements of fresh water specific conductivity in the nearby well. The porewater specific conductivity of the fourth layer (6298 micromhos/cm) indicates that only the top of the transition zone was detected in this area. The salinity of the water in the fourth layer is about 4 ppt.

Since the depth to the salt water in this area has probably been affected by the pumping of water from the aquifer it is expected that the theoretical depth to the salt water should be greater than that as detected by the Vertical Electrical Sounding. Figure 30b shows that the depth below the surface to the salt water has been calculated to be 118 and 133 feet by the Ghyben-Herzberg and the Todd methods respectively. In the Ghyben-Herzberg calculation Kashef's corrections could not be used because of a lack of sufficient data. It is important to note that the water level measurement used to calculate the depth to the interface with the Ghyben-Herzberg relation in this

location was obtained in a well with an active pump. Therefore, the depth of 118 feet to the interface reflects approximately the actual depth to the interface when the VES was performed in this location. Glover's method could also not be applied due to a lack of data.

5.9 Vertical Electrical Sounding #9

This sounding was conducted in the same general area as VES 7 but, at a slightly different orientation. Figure 22 shows the exact location of this sounding. The Center Point of this sounding was at a higher elevation than VES 7. The elevation of the center point was approximately 10 feet above mean sea level.

The field data for VES 9 and the computer generated match curve used to interpret the data are shown in Figure 31a. While the shape of this curve is similar to VES 7 and 8, the suppression of the fresh water layer in this curve was much greater. The depth-resistivity model used to produce the best match theoretical curve in Figure 31a is shown in Figure 31b. The layer sequence in this model was interpreted to represent the following: topsoil, 5000 ohm-ft (1524 ohm-m); unsaturated sand, 55000 ohm-ft (16770 ohm-m); fresh water saturated sand, 2000 ohm-ft (610 ohm-m); and salt water saturated sand, 100 ohm-ft (30.5 ohm-m). Due to suppression the thickness of the third (fresh water) layer could range from 0 to 20 feet. The resistivity of the porewater in the fourth layer would be 1.0 ohm-ft (0.32 ohm-m) with a corresponding specific conductance of 31475 umhos/cm.

The depth to the salt/fresh water interface from this VES curve interpretation was 26 feet. This compares favorably with the interpretation of VES 7 which indicated

VES 9

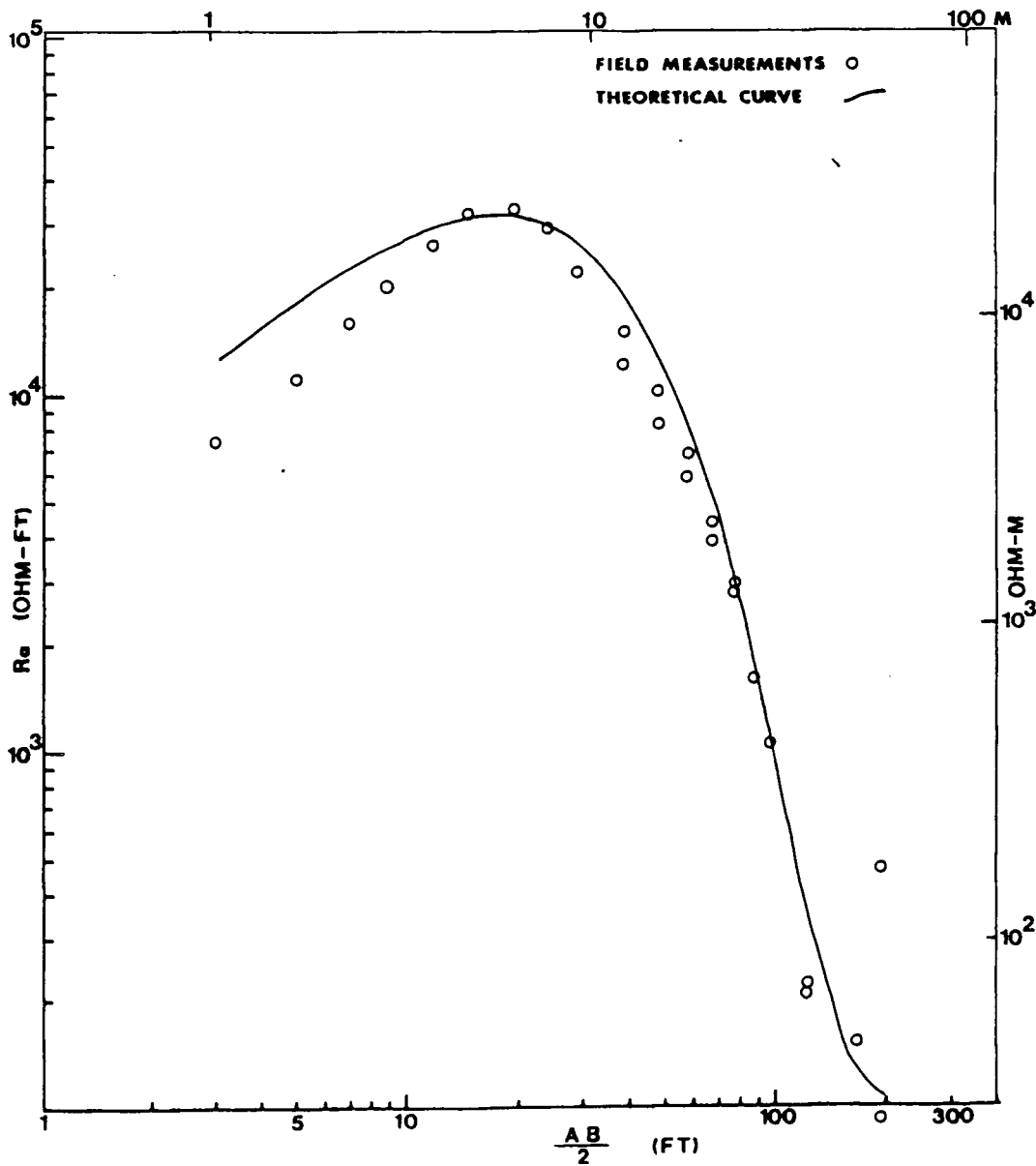


Figure 3la. Sounding 9 field data shown with the best match theoretical curve.

VES 9

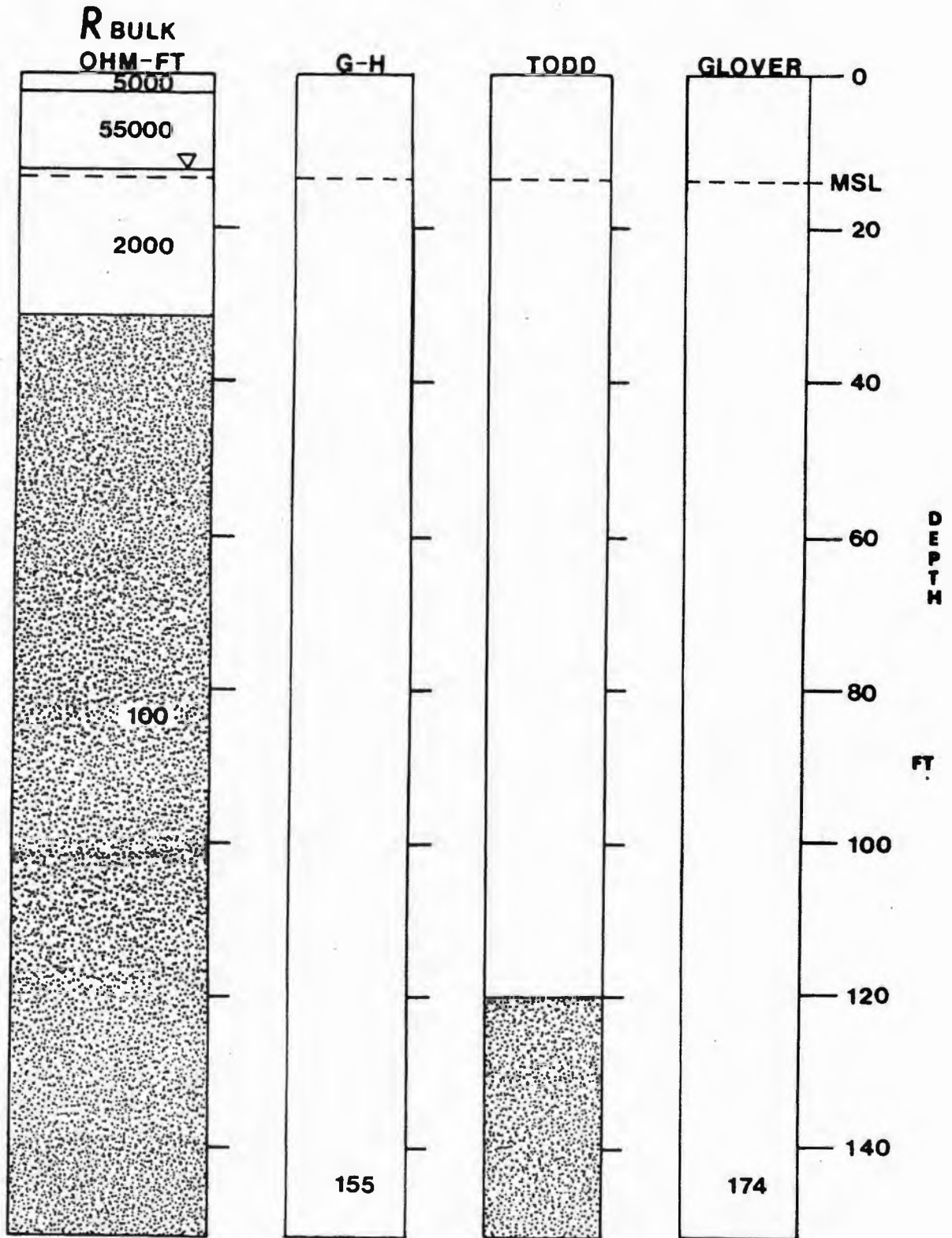


Figure 31b. The VES interpretation yielded a depth of 26 ft to the salt/fresh water interface versus a minimum depth of 120 ft for the theoretical calculations.

that the depth to the interface is about 30 feet. In Figure 31b the layer sequence interpretation for this curve was also compared to theoretical calculations performed with data obtained from nearby well #5.

5.10 Vertical Electrical Sounding #10

This Vertical Electrical Sounding was performed 135 feet north of VES 1 at a slightly higher elevation. The VES curve for this location could not be interpreted due to the wide scatter in the data points obtained at $L/2$ spacings greater than 70 feet (see Figure 32). The first part of the curve has a shape similar to VES curve 1, but with a higher resistivity second layer. The trend of the points on the ascending part of the curve seem to indicate that a minimum was detected.

The best estimate of the bulk resistivity of this minimum layer would probably be in the range from 500 to 800 ohm-ft (152 to 244 ohm-m). Using equation 16, the corresponding range in the specific conductivity of the porewater in this layer would be from 3900 to 6300 micromhos/cm. Therefore, it is very likely that salt water was detected by this sounding. However, it appears that only the top of the transition zone was detected in this location. This was expected since the depth to the salt water was anticipated to be much greater than at the site of VES 1 because VES 1 was much closer to the well which pumped salt water.

VES 10

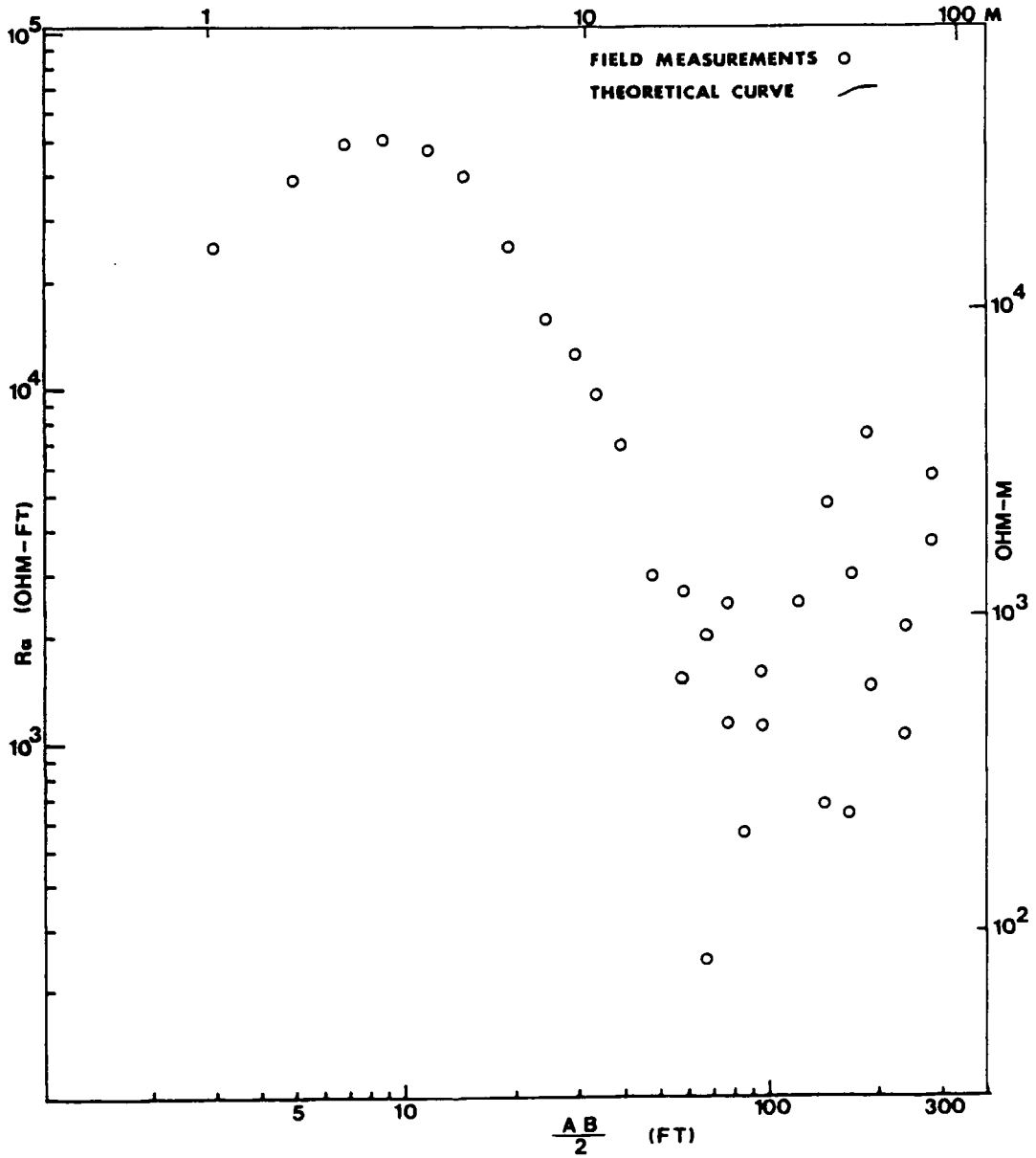


Figure 32. The wide scatter in the field data from sounding 10 precluded the interpretation of this field data.

5.11 Vertical Electrical Sounding #11

In an attempt to document the existence of a suspected abnormal conductance phenomena in the part of this aquifer occupied by salt water, a strip chart recorder was used to record the potential readings during the performance of a sounding. Special precautions were taken to insure that the anomalies in the curve could not be the result of current leakage from the equipment. All of the equipment was isolated from the ground by placing it in a van. The insulation on the current and potential wires were both checked for weak spots.

The sounding was performed in the same location as VES 1 so that the curve could be compared to the previous results. The VES curve produced is shown in Figure 33. The curve is very similar to VES 1 with the exception that the bulk resistivity or thickness of the second layer is larger. This was expected since the second layer in this case represents the unsaturated zone, which is usually thickest in October when the water table is at its lowest level.

The descending part of the curve is shown to split into two branches at an $AB/2$ of 70 feet. The two separate values were obtained by reversing the flow of current into the ground for each reading. It is evident that there is more resistance to the flow of the current in one direction

VES 11

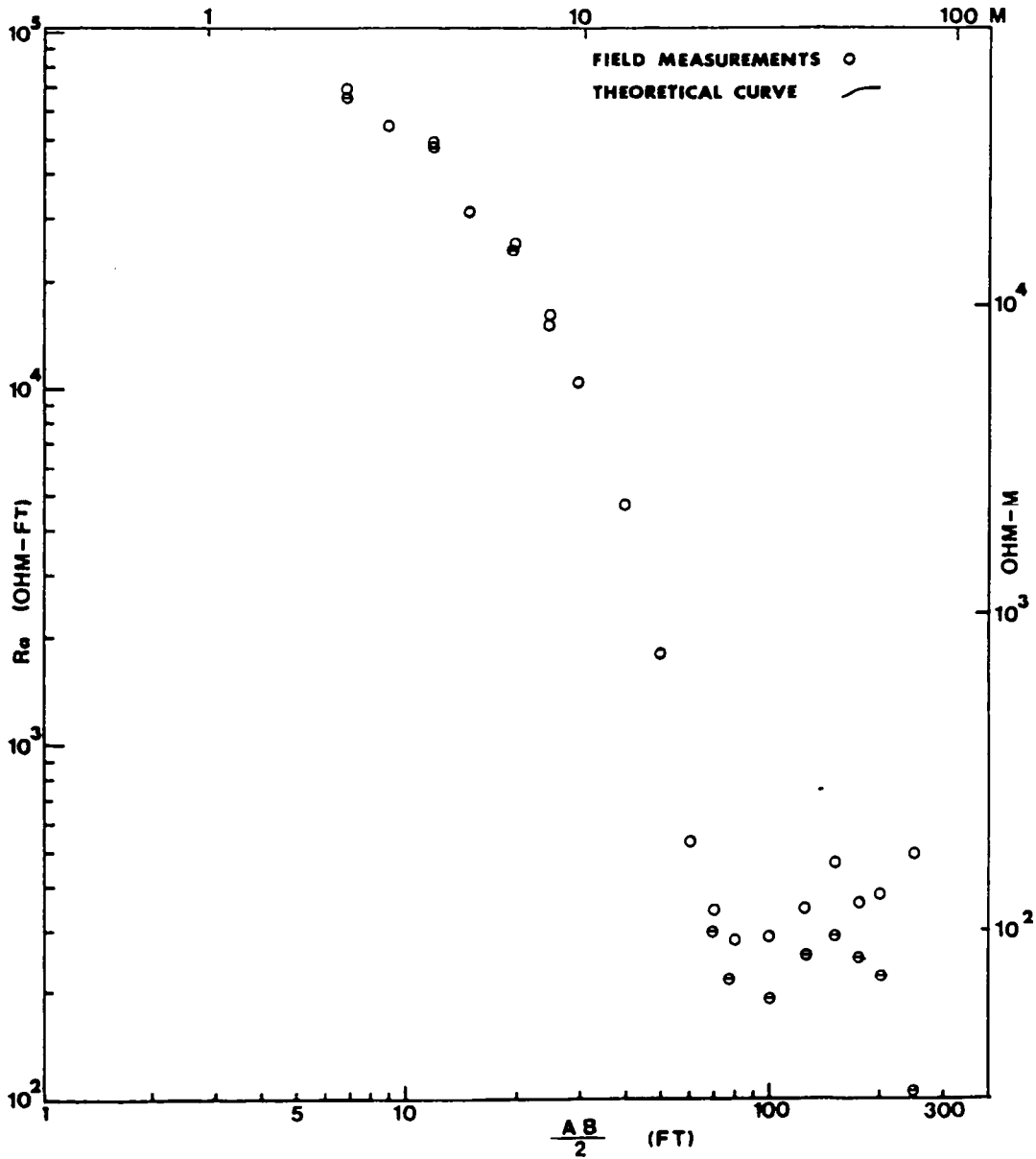


Figure 33. Potential readings taken with the current reversed produced the spread in the field data points shown above.

than in the other. There is no known explanation for this phenomena.

In order for this apparent anomaly to exist there either must be an unknown source of low level stray potentials in the area, some unique physical process or structure present or some unaccounted for equipment problem. This last possibility was the only one which could be virtually eliminated as a possibility. Of the remaining two, the first seems to be the most likely cause. It is hypothesized that low level electrical potentials could be created in the aquifer through the tidal movement of the salt water in the bedrock fractures.

6.0 SUMMARY

The results of this study have demonstrated that the depth to a salt/fresh water interface can be measured using the electrical resistivity method along with the use of only limited shallow borehole data. The relative amount of salt water intrusion resulting from the withdrawal of fresh groundwater from the study area was also determined. This determination was made by calculating the theoretical depth the salt/fresh water interface in the areas where electrical depth soundings were performed. The amount of intrusion was then obtained by subtracting the interface depth as measured in the sounding from the calculated theoretical depth to the interface. The depths to the interface across the study area, as determined by both the electrical depth sounding and the theoretical calculations, are shown in Tables 5, 6 and 7. Other significant findings of this study are listed below.

1. The use of a single deep borehole into bedrock made it possible to calibrate a Vertical Electrical Sounding (VES) curve performed adjacent to it. With this information the interpretation of the depth to the salt/fresh water interface on VES curves obtained in other areas without deep boreholes was successful.
2. The depths to the salt/fresh interface, as determined by the VES interpretation and the three theoretical methods employed, were in agreement in areas where the

TABLE 5

Theoretical and Measured Depths to a Salt/Fresh Water
Interface

Chaypee Hill

Location	VES 1	VES 5	VES 2
Ground Elevation (feet)	7.5	20.0	27.0
Mean Sea Level			
	24.8		
Depth to Salt/Fresh Water Interface (feet)		53.5	62.5 ?

***** 83 *****

***** 120 *****
***** 125 *****

- Notes:
- 24.8 -- is the depth to the salt/fresh water interface as measured by the VES.
 - *** 83 *** is the depth to the salt/fresh water interface as calculated using Todd's (1980) theoretical method (equation 14).

TABLE 6

Theoretical and Measured Depths to a Salt/Fresh Water Interface

Plummer and Berg Properties

Location	VES 9	VES 7	VES 8
Ground Elevation (feet)	10.0	5.0	16.0
Mean Sea Level	26.0	30.0	44.5
Depth to Salt/Fresh Water Interface (feet)			

***** 120 *****

***** 134 *****

Notes:

- 24.8 -- is the depth to the salt/fresh water interface as measured by the VES.
- *** 83 *** is the depth to the salt/fresh water interface as calculated using Todd's (1980) theoretical method (equation 14).

TABLE 7

Theoretical and Measured Depths to a Salt/Fresh Water Interface

Potomska Point

Location	VES 3	VES 6	VES 4
Ground Elevation (feet)	22.0	20.0	10.0
Mean Sea Level			
Depth to Salt/Fresh Water Interface (feet)			> 75
		***** 102 *****	
		----- ? ? -----	
		***** 120 *****	
	***** 129 *****		
	----- 145 -----		

- Notes:
- 24.8 -- is the depth to the salt/fresh water interface as measured by the VES.
 - *** 83 *** is the depth to the salt/fresh water interface as calculated using Todd's (1980) theoretical method (equation 14).

position of the salt/fresh water interface was not greatly affected by the pumping of water from the aquifer.

3. In areas where the position of the salt/fresh water interface was known to have been affected by the pumping of water from the aquifer, the depth to the interface interpreted from the VES curves was always less than predicted by the three theoretical methods.
4. The best method for calculating the theoretical depth to the salt/fresh water interface in this type of situation is with Todd's method.
5. The interpretation of the VES curves indicate that the depth to brackish water in this area ranges from just 10 feet to about 145 feet below the surface.
6. The shallow wells dug into the glacial till in this area are much more reliable as a source of fresh water than the deep 'artesian' wells drilled into bedrock. All three of the bedrock wells in this area penetrate the salt/fresh water interface.
7. The movement of the salt water through the aquifer may have produced an abnormal conductance phenomena as the low amperage direct current was introduced into the aquifer. Potential readings obtained were affected significantly by reversing the flow of the current through the ground.

REFERENCES

- Alger, R.P., 1966, Interpretation of electric logs in fresh water wells in unconsolidated formations: Trans. Soc. Prof. Well Log Analysts, 7th Ann. Logging Symposium, Tulsa, Okla., May 1966. pp661-662.
- Banks, H.O., and R.C. Richter, 1953, Sea-water intrusion into groundwater basins bordering the California coasts and inland bays: Trans. Amer. Geophysical Union, v.34, p.575
- Barksdale, H.C., 1940, The contamination of groundwater by salt water near Parlin, N.J.: Trans. Amer. Geophysical Union, v.21, p.471
- Bear, Jacob, 1979, Hydraulics of Groundwater, McGraw-Hill Inc., New York, 569 pp.
- Bear, J., and G. Dagan, 1964, Some exact solutions of interface problems by means of the hodograph method, J. Geophys. Res., v.69, no.2, pp.1563-1572.
- Bhattacharya, P.K., and H.P. Patra, 1968, Direct Current Geoelectric Soundings: Amsterdam, The Netherlands, Elsevier Press, 135pp.
- Bowles, J.E., 1976, Engineering Properties of Soils and Their Measurement, McGraw-Hill Book Co., New York
- Brown, J.S., 1925, A study of coastal groundwater with special reference to Connecticut: U.S.G.S. Water Supply Paper 537. 101 pp.
- Bugg, S.F., and J.W. Lloyd, 1976, A study of fresh water lens configuration in the Cayman Islands using Resistivity methods: Quarterly Journal of Engng. Geology, v.9, p.291
- Cooper, H.H., Jr., 1959, A hypothesis concerning the dynamic balance of fresh water and salt water in a coastal aquifer, Journal of Geophysical Research, v.64, no.4, p.971
- Cooper, H.H., Jr., 1964, Sea water in coastal aquifers, relation of salt water to fresh ground water: U.S. Geological Survey Water Supply Paper 1613-C, 84pp
- Dupuit, J., 1863, Etudes theoriques et pratiques sur la mouvement des eaux dans les canaux decouverts et a travers les terrains permeables, 2nd ed., Dunod, Paris, 304 p.

- Fetter, C.W., Jr., 1972, Position of the saline water interface beneath oceanic islands: Water Resources Research, v.8, no.5, p.1307
- Folk, R.L., 1974, Petrology of Sedimentary Rocks, Hemphill Publishing Company, Austin, Texas, pp.33-35.
- Fried, J.J., and P.O. Ungemach, 1971, Note: A dispersion model for a quantitative study of a ground water pollution by salt: Water Research, v.5, p.491
- Frohlich, R.H., 1974, Combined geoelectrical and drill-hole investigations for detecting fresh water aquifers in northwestern Missouri: Geophysics, v.39, no.3, p.340.
- Ghosh, D.P., 1971, The application of linear filter theory to the direct interpretation of geoelectrical resistivity sounding measurements: Geophysical Prospecting, v.19, pp. 192-217.
- Ghyben, B.W., 1888, Nota in verband met de voorgenomen putboring nabij Amsterdam (Notes on probable results of the proposed well drilling near Amsterdam): Tijdschrift van het Koninklijk Instituut van Ingenieurs, The Hague, P.21
- Ginzberg, A., and A. Levanon, 1976, Determination of a salt water interface by electrical resistivity depth soundings: Hydro. Sci. Bulletin, v.21, no.4 p.561
- Glover, R.E., 1959, The pattern of fresh-water flow in a coastal aquifer: J. Geophys. Res., v.64, no.4, p.439 .
- Henry, H.R., 1959, Salt intrusion into fresh water aquifers: Journal of Geophysical Research, v.64, no.11, p.1911
- Herzberg, B., 1901, Die wasserversorgung einiger Nordseebader (The water supply on parts of the North sea coast): J. Gas-beleuchtung und Wasserversorgung, v.44, pp.815-819, 842-844
- Hubbert, M.K., 1940, Theory of ground-water motion: J. Geol., v.48, no.8, p.785
- Kashef, A.-A. I., 1976, Theoretical developments and practical needs in the field of salt water intrusion: Advances in Groundwater Hydrology, American Water Resources Association, September.
- Kashef, A.-A. I., 1977, Management and control of salt water intrusion in coastal aquifers: Critical Reviews in Environmental Control, CRC Press Inc., pp.217-275.

- Kashef, A.-A. I., 1983, Harmonizing Ghyben-Herzberg interface with rigorous solutions: *Ground Water*, v.2, no.2, p.153
- Keller, G.V., and F.C. Frischknecht, 1966, Electrical Methods in Geophysical Prospecting: Oxford, Pergamon Press, 519pp.
- Kelly, W.E., 1976, Goelectrical sounding for delineating ground water contamination: *Ground Water*, v.14, no.1, p.6
- Kowalski, R.G., and D.S. Sanders, 1983, Introduction to hydrogeologic investigations of contamination in fractured rock: R.I. Water Resources Center Technical Report No.13, 71pp.
- Kunetz, G., 1966, Principles of Direct Current Resistivity Prospecting: Geopublication Associates, Berlin, 103pp.
- Lau, L.S., 1967, Seawater encroachment in Hawaiian Ghyben-Herzberg systems: Am. Water Resources Assoc., Proc. Symp. on Ground-Water Hydrology, San Francisco, Calif., pp.259-271
- Liu, C.C.K., L.S. Lau, and J.F. Fink, 1983, Groundwater model for a thick fresh water lens: *Groundwater*, v.21, no.3.
- Mundry, E., and J. Homilius, 1979, Three-Layer Model Curves for Goelectrical Resistivity Measurements, Schlumberger Array, Herausgegeben von der Bundesanstalt für Geowissenschaften und Rohstoffe und den Geologischen Landesämtern in der Bundesrepublik Deutschland, Hannover, log cycle 83.33 mm, with 615 sets of curves
- Patnode, H. W., and M.R.J. Wyllie, 1950, The presence of conductive soils in reservoir rocks as a factor in electric log interpretation: *Petroleum Trans., AIME*, T.P. 3541, v.189, pp.47-52.
- Pinder, G.F., and H.H. Cooper, Jr., 1970. A numerical technique for calculating the transient position of the saltwater front: *Water Res. Research*, v.6, no.3, p.875
- Pinder, G.F., and H. Page, Finite element simulation of salt water intrusion on the South Fork of Long Island, Proceedings Intern. Conf. on Finite Elements, Princeton Univ., Princeton, N.J., 1976.

- Sanders, D.P., 1983, Resistivity Methods Applied to Pollution Detection in a Crystalline Bedrock Aquifer at Little Compton, Rhode Island, Master's Thesis, University of Rhode Island.
- Shamir, U., and G.Dagan, 1971, Motion of the seawater interface in coastal aquifers: A numerical solution: Water Resources Research, v.7, no.3, p.644
- Shipman, W.D., 1978, Saltwater - Bearing Agifers at the Periphery of Narragansett Bay: Geoelectric and Geohydrological Characteristics: Master's Thesis, University of Rhode Island
- Spiegel, Z., Brief comments on the Hydrology of Suffolk County, Presentation to the County Legislature, Suffolk County, N.Y., May 27, 1971.
- Stefanescu, S.S., M. Schlumberger, and C. Schlumberger, 1930, The distribution of electrical potential about a point electrode in an earth of horizontal, homogenous and isotropic beds: The J. Physique et Radiul, ser. 7, vol. 1, pp. 132-141.
- Stollar, R.L., and P. Roux, 1975, Earth resistivity surveys - a method for defining ground water contamination: Ground Water, v.13, no.2, p.145
- Strahler, A.N., The Environmental Impact of Ground Water Use on Cape Cod: Impact Study III, Association for the Preservation of Cape Cod, Orleans, Mass, 68 pp, 1972.
- Swartz, J.H., 1937, Resistivity studies of some salt-water bound-aries in the Hawaiian Islands: Trans. Am. Geophy. Union, v.18, pt.2, p.387
- Todd, D.K., 1980, Ground Water Hydrology, John Wiley & Sons, Inc., New York, 336pp.
- Todd, D.K., and C.F. Meyer, 1971, Hydrology and geology of the Honolulu aquifer: Jour. Hydraulics Div., Am. Soc. of Civil Engineers, v.97, no.HY 2, p.233
- United States Geological Survey, 1983, Bedrock Geologic Map of Massachussetts, E-an Zen, Editor.
- Urish, D.W., 1980, Salt source sleuthing in a coastal environ-ment: a case study: Abs., EOS, Amer. Geo. Union, v.61, no.46, p.955
- Urish, D.W., 1982, The effect of beach slope on the fresh water lens in small oceanic landmasses: University of Rhode Island, work supported by NSF Grant No. ENG-7908084.

- Urish, D.W., 1983, (Personal communication)
- Van Dam, J.C., 1976, Possibilities and limitations of the resist-ivity method of geoelectric prospecting in the solution of geohydrological problems: Geoexploration, v.14, no.3/4, p.179
- Winsauer, W.O., H.M. Shearin, P.H. Masson, and M. Williams, 1952, Resistivity of brine saturated sands in relation to pore geometry: Bull. Amer. Assn. Petroleum Geology, v.36, no.2, pp. 253-277.
- Zohdy, A.A.R., 1974, A computer program for the calculation of Schlumberger sounding curves by convolution: U.S.G.S. Report USGS-GD-74-010, U.S. Dept. of Commerce, NTIS pub.
- Zohdy, A.A.R., G.P. Eaton and D.R. Mabey, 1974, Application of surface geophysics to groundwater investigations: Techniques of Water Resources Investigation of the USGS, Book 2, Chapter D1, U.S. Govt. Printing Office, 116p.

APPENDIX A

Kashef's Modification of the Ghyben-Herzberg Equation

In order to compensate for the movement of fresh water in a coastal aquifer, Kashef modified the basic Ghyben-Herzberg equation to allow for more precision within the zone close to the shoreline. The method employs two equations which yield values for the depth to a salt/fresh water interface below sea level assuming that either a horizontal or a vertical fresh water outflow face exists. The two equations are:

$$z_v/H_o = \sqrt{(H_f/aH_o)^2 + 0.1375 (1-\bar{x})/m^2} \quad (1A)$$

$$z_h/H_o = \sqrt{(H_f/a H_o)^2 + (0.25) m^2} \quad (2A)$$

where z_h and z_v are respectively, the depths of the interface below sea level assuming a horizontal and a vertical outflow face and H_o is the vertical distance between sea level and the underlying impervious boundary of an unconfined aquifer.

Before these equations can be applied in any situation, three factors must first be determined. The first one is the average hydraulic gradient (i) across the site. This is determined from field measurements of water levels above sea level in two or more wells in the area of interest.

The second factor which must be measured is the contrast in density between the fresh and salt water in the aquifer. This density contrast is designated by the symbol a , where: $a = (p_s - p_f)$. In this case the average density of the salt water in the surrounding estuary was used as the salinity of the water in the aquifer. The density of the fresh water was taken as 1.00 grams/cc. The average density of the salt water in the estuary was found to be 1.0185 grams/cc (see Appendix H).

The third factor which is needed is the depth to the impervious boundary of the unconfined aquifer below sea level. In this case the lower boundary is the depth in the bedrock at which there are no fractures open. This depth is usually between 200 and 300 feet below the surface. Therefore, most of the solutions are given in a range based on the use of these two depths. In summary, the three factors mentioned above used in this example are:

$$\begin{aligned}i &= 0.013 \\a &= 0.0185 \text{ g/cc} \\H_o &= 200 \text{ to } 300 \text{ feet}\end{aligned}$$

In order to illustrate the use of this method, the data from Well #2 will be used in the following sample calculation.

The first step in applying this equation is to calculate the theoretical maximum upstream fresh water head at the point of maximum landward extent of the salt water

wedge at $x = L$, as pictured in Figure 5. The maximum upstream head is:

$$a H_o / p_f$$

$$(0.0185 \text{ g/cc}) 200 \text{ ft} / 1.0 \text{ g/cc} = 3.70 \text{ ft}$$

or,

$$(0.0185 \text{ g/cc}) 300 \text{ ft} / 1.0 \text{ g/cc} = 5.55 \text{ ft}$$

Using these values the theoretical distance of the intruded salt water wedge from the shoreline (L) is calculated:

$$L = a H_o / 2 i p_f \quad (4A)$$

$$L = 3.70 / 2(0.013) = 142.3 \text{ ft}$$

or,

$$L = 5.55 / 2(0.013) = 213.5 \text{ ft}$$

In the next step the ratio between L and H_o is determined. This ratio is designated as m :

$$m = L/H_o \quad (5A)$$

$$m = 142.3/200 \quad \text{or} \quad 213.5/300$$

$$m = 0.7115$$

Now, since the water level in the well in this area (well 2) was 2.65 feet above mean sea level and this is less than the theoretical maximum upstream fresh water head of 3.7 feet, then this well must be located above the salt/fresh water wedge.

The next step is the calculation of the term \bar{x} , which is simply x/L and is equal to the square root of the ratio between the Ghyben-Herzberg depth to the interface (Z) and the thickness of the aquifer (H_o). The Ghyben-Herzberg depth, Z , is determined using the field measurement of the height of fresh water above sea level (H_f) in a borehole times the fresh water density divided by the density contrast (a) between the salt and fresh water:

$$Z = H_f \rho_f / a \quad (6A)$$

$$Z = 2.65 \text{ ft } (1.00 \text{ g/cc}) / (1.0185 \text{ g/cc} - 1.00 \text{ g/cc})$$

$$Z = 143.24 \text{ ft}$$

Now,

$$Z = H_o \sqrt{\bar{x}} \quad (7A)$$

$$\sqrt{\bar{x}} = (Z/H_o) \quad (8A)$$

$$\sqrt{\bar{x}} = (143.24 / 200) \text{ or } (143.24 / 300)$$

$$\bar{x} = 0.5130 \text{ or } 0.2280$$

All of the above values are now used to calculate the corrected depth to the salt/fresh water interface assuming either a vertical or horizontal fresh water outflow face.

$$Z_v/H_o = (0.5130) + 0.1375 (1 - 0.5130) / (0.7115)^2$$

or, if H_o is assumed to be 300 ft:

$$Z_v/H_o = (0.2280) + 0.1375 (1 - 0.2280) / (0.7115)^2$$

therefore,

$$Z_v = (0.8033) * 200 \text{ ft or } (0.6616) * 300 \text{ ft}$$

and

$$\begin{aligned} Z_v &= 160.7 \text{ to } 198.5 \text{ feet} \\ &= 49.0 \text{ to } 60.5 \text{ meters} \end{aligned}$$

If a horizontal outflow face is assumed to exist the following equation is employed:

$$z_h/H_o = \sqrt{(0.5130) + 0.25(0.7115)^2}$$

or, if H_o is assumed to be 300 ft:

$$z_h/H_o = \sqrt{(0.4068) + 0.25(0.7115)^2}$$

therefore,

$$z_h = (0.7997) * 200 \text{ ft} \quad \text{or} \quad (0.5954) * 300 \text{ ft}$$

and

$$\begin{aligned} z_h &= 159.9 \quad \text{to} \quad 178.6 \text{ feet} \\ &= 48.8 \quad \text{to} \quad 54.5 \text{ meters} \end{aligned}$$

In order to simplify the comparison between these values and the values obtained by the other methods, including the interpretation of the Vertical Electrical Soundings, an average of these values was obtained (174.4 ft or 53.2 m). To this value was added the height above sea level of the center point of the vertical electrical sounding performed adjacent to this well (6.5 ft or 1.98 m) for a final comparison value of 180.9 ft or 55.2 meters.

The result of applying this method in other locations in the study area is outlined below.

Well 1 Chaypee Hill

This well is located on Chaypee Hill at an elevation of 25.92 feet above mean sea level. However, the well is only 117 feet from the shoreline, and the hydraulic gradient between the well and the surrounding water level is very steep. As shown by the calculations below Kashef's

equations can not be applied when the hydraulic gradient is too great. Therefore, the hydraulic gradient between Wells 1 and 2 was used in this case. As the result of field measurements, the following terms were determined:

Hydraulic gradient (i)	0.013
Fresh water head	16.57 ft above msl
$P_s - P_f$	0.0185 g/cc

Applying the simple Ghyben-Herzberg relation (equation 1), the depth to the salt/fresh water interface was determined:

$$Z = 16.57 \text{ ft (1.0 g/cc) / (0.0185 g/cc)}$$

$$Z = 895.7 \text{ ft (273.1 m) below mean sea level}$$

When Kashef's equations are employed and the aquifer is assumed to be 200 feet thick, the depth to the interface was determined to be:

$$Z_v = 745.9 \text{ ft (227.4 m) below mean sea level}$$

$$Z_h = 868.4 \text{ ft (263.7 m) below mean sea level}$$

If the aquifer is assumed to be 300 feet thick, the depth to the interface changes to:

$$Z_v = 780.0 \text{ ft (237.8 m) below mean sea level}$$

$$Z_h = 901.8 \text{ ft (274.9 m) below mean sea level}$$

The average depth to the interface calculated from these values is 824.0 ft (251.2 m). Since this value is less than the depth determined by the simple Ghyben-Herzberg equation, it must be concluded that Kashef's equations can not be applied in certain situations. Apparently, the use of this equation is very sensitive to

small errors in hydraulic gradient measurements and can not be applied when the gradient becomes large. It is also important to note that all of the above depths to the interface indicate that there should be no salt water wedge below this measuring point since they are all below the bottom of the aquifer.

Well 6 Shattuck's New Well

In this location the following data was used in Kashef's equations:

Hydraulic gradient	0.0115
Fresh water head	3.06 ft above msl
$P_s - P_f$	0.0185 g/cc

Using the simple Ghyben-Herzberg equation, the depth to the salt/fresh water interface was calculated as:

$$Z = 3.06 \text{ ft (1.0 g/cc) / 0.0185 g/cc}$$

$$Z = 165.4 \text{ ft (50.4 m) below mean sea level}$$

When Kashef's equations were applied, assuming that the aquifer is 200 feet thick, the results were as follows:

$$Z_v = 173.3 \text{ ft (52.8 m) below msl}$$

$$Z_h = 183.9 \text{ ft (56.1 m) below msl}$$

If the aquifer is assumed to be 300 feet thick, the results are:

$$Z_v = 183.9 \text{ ft (56.1 m) below msl}$$

$$Z_h = 239.5 \text{ ft (73.0 m) below msl}$$

The average of these four values is 195.1 ft (59.5 m), or almost 30 ft (9.1 m) below the Ghyben-Herzberg interface.

Well 7 Shattuck's Old Well

This well is located near the center of Potomska Point at an elevation of 24.97 feet above mean sea level, the second highest in the area. From field observations and measurements the following data was obtained:

fresh water head: 19.27 ft (5.88 m) above msl
hydraulic gradient: 0.026
 $P_s - P_f$: 0.0185 g/cc

The Ghyben-Herzberg depth to the salt/fresh water interface using equation 1 is:

$$Z = 19.27 \text{ ft (1.0 g/cc) / (0.0185 g/cc)}$$

$$Z = 1041.6 \text{ ft (317.6 m) below msl}$$

Again, this solution implies that there is no salt water wedge below this well since the aquifer is only 200 to 300 feet deep. Normally there would be no need to apply Kashef's equations in this type of situation because those equations are supposed to yield solutions which are greater than the one given by equation 1. However, when Kashef's equations were applied in this case no solutions were obtained for Z_v because the square root of a negative number was encountered. The solutions for Z_h were as follows:

For a 200 foot thick aquifer:

$$Z_h = 1042.1 \text{ ft (317.7 m) below msl}$$

or, for a 300 foot thick aquifer:

$$Z_h = 1042.75 \text{ ft (317.9 m) below msl}$$

Comparing these with the simple Ghyben-Herzberg solution of 1041.6 ft, there is virtually no difference.

Well 8 Shattuck's Garden Well

This well is also located on Potomska Point, but is located much closer to the shoreline than Well 7. The application of Kashef's equations in this location also was not possible for the determination of Z_v for the same reason as above. The field data collected for this well is listed below:

hydraulic gradient:	0.038
fresh water head:	11.46 ft above msl
$P_s - p_f$:	0.0185 g/cc

The Ghyben-Herzberg depth to the interface was calculated as:

$$Z = 11.46 \text{ ft (1.0 g/cc) / (0.0185 g/cc)}$$

$$Z = 619.5 \text{ ft (188.9 m) below msl}$$

Again, in this case theoretical depth to the interface is below the bottom of the aquifer. As noted above, there is no solution for Z_v using Kashef's equation. The solution for Z_h when the aquifer is assumed to be 200 feet thick is:

$$Z_h = 619.9 \text{ ft (188.9 m) below msl}$$

or, if the aquifer is assumed to be 300 feet thick:

$$Z_h = 620.5 \text{ ft (189.2 m) below msl}$$

The small differences between the solutions from the Ghyben-Herzberg and Kashef's equations are insignificant. This was expected since all of the solutions indicate that this well is not located above the fresh/salt water interface.

Well 5

This well is located on the base of Potomska Point at an elevation of 14 feet above mean sea level, and 190 feet from the shore. The following data was used for this well:

Hydraulic gradient:	0.0087
Fresh water head:	1.66 feet
Density contrast:	0.0185

The application of the Ghyben-Herzberg equation gave the following depth to the salt/fresh water interface:

$$Z = 1.66 \text{ ft (1.0 g/cc) / (0.0185 g/cc)}$$

$$Z = 89.73 \text{ ft (27.4 m) below msl}$$

When Kashef's equations were applied, assuming the aquifer is 200 feet thick, the results were as follows:

$$Z_v = 109.4 \text{ ft (33.4 m) below msl}$$

$$Z_h = 138.9 \text{ ft (42.3 m) below msl}$$

If the aquifer is assumed to be 300 feet thick, the results change to:

$$Z_v = 134.5 \text{ ft (41.0 m) below msl}$$

$$Z_h = 182.6 \text{ ft (55.7 m) below msl}$$

The average of these four values is 141.4 feet or 43.1 meters below mean sea level. This average value is 51 feet greater than the normal Ghyben-Herzberg depth to the interface. For comparison purposes, the height of this well above mean sea level (14.2 ft, or 4.3 m) was added to the above average value for the depth to the salt/fresh water interface with a result of 155.6 ft (47.4 m) below mean sea level.

APPENDIX B

Glover's Solution for the Pattern of Fresh Water Flow in a Coastal Aquifer

A close representation of the flow conditions near a beach was obtained by modifying a solution previously obtained for the flow of ground water under gravity forces. With the use of flow net analysis, Glover plotted the interface between the fresh water and sea water from the following expression:

$$z^2 - 2Qx/aK - Q^2/a^2K^2 = 0 \quad (9A)$$

where:

K = hydraulic conductivity (ft/sec)

a = density difference between salt and fresh water

Q = fresh water flow per unit length of shoreline

x = distance measured horizontally landward from the shore

z = distance measured vertically downward from sea level

In order to apply this equation both Q and K had to be determined for the study area. The hydraulic conductivity of the bedrock aquifer was determined in Well #2 using the Tidal Method. The method and results of this procedure are described in Appendix G. Since the determination of the hydraulic conductivity of the bedrock depends on the porosity of the bedrock using this method, the results are given as a range. The range in hydraulic conductivity used was:

$$\begin{aligned} K &= 0.008 \text{ to } 0.0016 \text{ cm/sec} \\ &= 2.3 \text{ to } 0.47 \text{ ft/day} \end{aligned}$$

The corresponding range in porosity used to compute these hydraulic conductivities was:

$$n = 0.05 \text{ to } 0.01$$

The flow of fresh water per unit length of shore line (Q) was calculated in each area using this equation:

$$Q = K (H_o) i \quad (10A)$$

where:

H_o = the aquifer thickness

i = the aquifer hydraulic gradient

When the equation was applied using the range of hydraulic conductivities given above it was found that the difference in the calculated distance to the salt/fresh water interface using the two values was negligible. The solution to the equation was found to be much more sensitive to changes in the aquifer thickness. Since the aquifer thickness was estimated to be from 200 to 300 feet, the solution to the interface was given as a range according to the aquifer thickness. The following is an example calculation using this equation.

WELL # 2

This well is located near Chaypee Hill in the northern section of the study area. The well was drilled to a depth of 385 feet to supply water for a new home. The hydraulic conductivity of the bedrock was determined in this well by recording the changes in the water level in the well due to tidal fluctuations in the surrounding estuary. The well is

only 191 feet from the shoreline at an elevation of 6.5 feet above mean sea level.

The first step in applying Glover's equation is to calculate the flow of fresh water (Q) through the aquifer to the sea using equation 10A.

If the aquifer thickness (Ho) = 200 feet:

$$\begin{aligned} Q &= K (H_o) i \\ &= 2.3 \text{ ft/day} (200 \text{ ft}) 0.013 \\ &= 5.98 \text{ ft}^2/\text{day per ft of shoreline} \end{aligned}$$

This value is then substituted into Glover's equation which has been rearranged to solve for Z:

$$\begin{aligned} Z^2 &= [2 (5.98 \text{ ft}^2/\text{day}) 191 \text{ ft} / 0.0185 (2.3 \text{ ft/day})] - \\ &\quad [(5.98 \text{ ft}^2/\text{day})^2 / (0.0185)^2 (2.3 \text{ ft/day})^2] \\ Z^2 &= 34003.36 \text{ ft}^2 \\ Z &= 184.4 \text{ ft} \quad (56.2 \text{ m}) \end{aligned}$$

if the aquifer thickness (Ho) = 250 feet:

$$\begin{aligned} Q &= 2.3 \text{ ft/day} (0.013) 250 \text{ ft} \\ Q &= 7.47 \text{ ft}^2/\text{day} \end{aligned}$$

and

$$\begin{aligned} Z^2 &= [2 (7.47 \text{ ft}^2/\text{day}) 191 \text{ ft} / 0.04255] - \\ &\quad [(7.47 \text{ ft}^2/\text{day})^2 / 0.00181] \\ Z^2 &= 35490.7 \text{ ft}^2 \\ Z &= 188.4 \text{ ft} \quad (57.4 \text{ m}) \end{aligned}$$

if the aquifer thickness (Ho) = 300 feet:

$$\begin{aligned} Q &= 2.3 \text{ ft/day} (0.013) 300 \text{ ft} \\ Q &= 8.97 \text{ ft}^2/\text{day} \end{aligned}$$

and

$$z^2 = [2(8.97\text{ft}^2/\text{day}) 191 \text{ ft} / 0.042251] - \\ [(8.97 \text{ ft}^2/\text{day})^2 / 0.00181]$$
$$z^2 = 36183.3 \text{ ft}^2$$
$$z = 190.2 \text{ ft} \quad (58.0 \text{ m})$$

Therefore, the theoretical range in the depth below sea level to the salt/fresh water interface in this location is:

$$z = 184.4 \quad \text{to} \quad 190.2 \quad \text{feet}$$
$$= 56.2 \quad \text{to} \quad 58.0 \quad \text{meters}$$

For comparison, an average value of 187.6 ft (57.2 m) was used. To this value was added the surface elevation of this location above mean sea level (6.5 ft, 2.0 m) as determined in Appendices D and E, for a final comparison value of 194.1 ft or 59.2 meters.

The following table summarizes the results of the application of Glover's equation in other locations in the study area.

TABLE 8

Location	Depth to interface (Z)				
	Ho=200'	Ho=250'	Ho=300'	avg ft	avg m
Well # 1	114.6	101.2	70.3	92.3	28.1
VES # 5	266.8	277.3	303.2	282.4	86.1
Well # 7	320.8	322.3	308.2	317.1	96.7
Well # 6	225.0	241.5	253.1	239.9	73.1
Well # 5	163.9	175.6	183.5	174.3	53.2

This method could not be applied in some areas due to either a lack of sufficient data or to the existence of large hydraulic gradients. In some cases the solution was the square root of a negative number.

APPENDIX C

Todd's Solution For a Fresh Water Lens Under an Oceanic Island

Todd developed a solution for an approximate salt/fresh water boundary based upon the Dupuit assumptions and the Ghyben-Herzberg relation. In order to obtain a solution for the flow of water in an unconfined aquifer, Dupuit (1863) assumed (1) the velocity of the flow to be proportional to the tangent of the hydraulic gradient instead of the sine as for a confined aquifer, and (2) the flow is horizontal and uniform everywhere in a vertical section. Due to these assumptions, the actual water table will lie above the computed water table. Nevertheless, for flat water table slopes, where the sine and tangent are nearly equal, an equation based on the Dupuit assumptions closely predicts the water table position except near the outflow.

Todd assumed that a circular island of radius R , which receives an effective recharge from rainfall at a rate W , has an outward flow Q at radius r of:

$$Q = 2 \pi r K (Z + h) dh/dr \quad (11A)$$

where K is the hydraulic conductivity, and h and Z are as defined in Figure 34. Noting that $h = [(p_s - p_f)/p]z$ and that from continuity $Q = \pi r^2 W$, then:

$$Z dz = Wr dr/2K [1 + (p_s - p_f)/p_f] [(p_s - p_f)/p_f] \quad (12A)$$

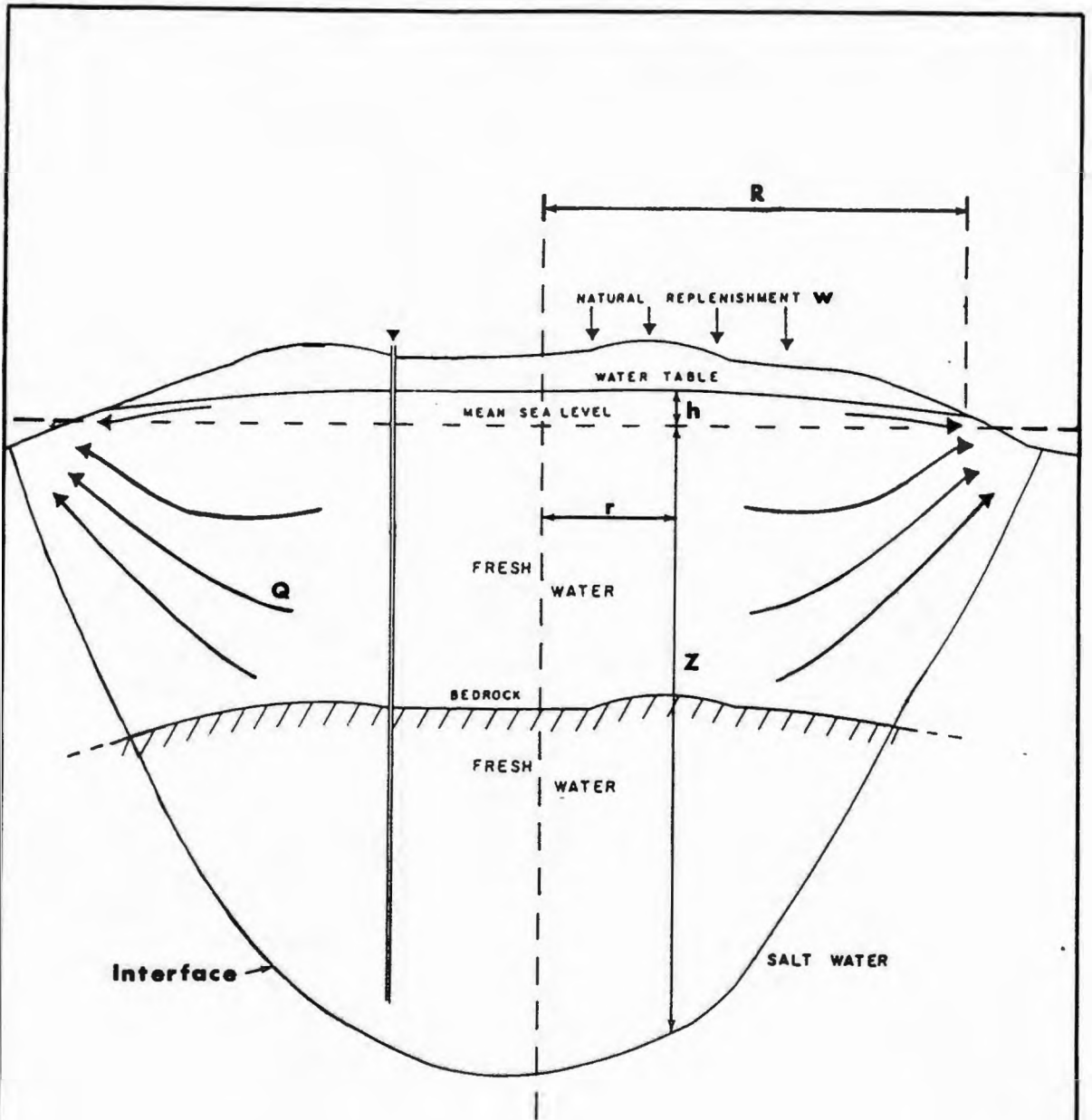


Figure 34. Explanation of the notation used by Todd for his solution for a salt/fresh water interface beneath an oceanic island.

Integrating and applying the boundary condition that $h = 0$ when $r = R$,

$$z^2 = \frac{W (R^2 - r^2)}{2 K [1 + (p_s - p_f)/p_f] [(p_s - p_f)/p_f]} \quad (12A)$$

Therefore, the depth to salt water at any location is a function of the rainfall recharge, the size of the island, and the hydraulic conductivity.

In order to apply Todd's equation it was necessary to make an estimate of the rate of recharge for the study area and to measure the radius of the island, in addition to the determination of the salt water density and the hydraulic conductivity of the aquifer.

The most common method of determining recharge is using an equation for the Hydrologic Budget of an aquifer. The following equation (Walton, 1970) represents the general hydrologic budget:

$$P = R + ET + U + Ss + Sg \quad (13A)$$

where:

- P = precipitation
- R = runoff and stream flow
- ET = evapo-transpiration
- U = subsurface underflow (or outflow)
- Ss = change in soil moisture
- Sg = change in ground water storage

The above symbols represent quantities for the period for which the balance is being made. In the equation, effective groundwater recharge would be the sum of U and

Sg. For a steady state condition recharge would be equal to subsurface underflow (U).

Direct rainfall data is not available for the South Dartmouth area. Average annual rainfall for New Bedford is 44.84 inches per year, based on 170 years of data. However, the yearly rainfall for 1983 was 59.16 inches. It should also be noted that the rainfall does vary considerably from the coast to locations further inland.

Because it was beyond the scope of this study, it was not possible to make direct evapo-transpiration estimates; nor was it feasible to directly apply the hydrologic budget. Therefore, to develop a reasonable estimate for the groundwater recharge, previously estimated evapotranspiration data for Block Island (Hansen and Shiner, 1964) Cape Cod (Strahler, 1972), Long Island (Speigel, 1971), and East Beach, Rhode Island (Urish, 1982) were evaluated. Based on an evaluation of this data a range for the rainfall recharge in this area was estimated to be from 16 to 20 inches per year.

The radius of the island was determined using aerial photographs of the area. Instead of using the nominal scale of the photo, a few large easily discernible features on the photos in the study area were measured in the field. These features were then measured on the photo to determine the true scale. When the radius of the island was determined it was necessary to divide the study area into a

few small segments. These segments were divided using apparent drainage divides and natural topographic barriers. Since most of these segments were not circles, the long and short axis of the segment was measured. The average of these two values was then used as the radius of the area. The following is a sample calculation using Todd's equation.

Well # 2 Glenn's Property

In applying Todd's equation the following data was used:

Island radius(R):	235	ft
Distance from shore(x):	191	ft
Recharge rate:	16	in/yr = 0.0036 ft/day
Hydraulic conductivity:	2.3	ft/day
Salt water - fresh water density contrast:	0.0185	g/cc

Before these values can be substituted into Todd's equation the value of r must be calculated:

$$r = R - x$$

$$r = 235 \text{ ft} - 191 \text{ ft} = 44 \text{ ft}$$

Now,

$$z^2 = \frac{0.0036 (235^2 - 44^2)}{2 (2.3) (1 + 0.0185) (0.0185/1.0)}$$

$$z^2 = \frac{0.0036 \text{ ft/day} (53289 \text{ ft}^2)}{4.6 \text{ ft/day} (0.01884)}$$

$$z^2 = 2237.9 \text{ ft}^2$$

$$z = 47.3 \text{ ft} \quad (14.4 \text{ m})$$

If the recharge is assumed to be 20 inches per year instead of 16 and the hydraulic conductivity is 2.3 ft/year:

$$Z = 53.0 \text{ ft} \quad (16.2 \text{ m})$$

These two values, 47.3 ft and 53 ft show that there is not much variation when the recharge rate is increased 20%. However, when the hydraulic conductivity of the aquifer is decreased from 2.3 ft/day to 0.47 ft/day there is a significant change in the value of Z as is shown below. This is in contrast to Glover's equations which were not greatly affected by this change in K. Although these two values (2.3 and 0.47 ft/day) may seem to represent a large range in hydraulic conductivity, it is actually not significant considering that values of hydraulic conductivity range over thirteen orders of magnitude from 10^{-13} to 1.0 meters per second.

If the aquifer hydraulic conductivity is assumed to be 0.47 ft/day and the recharge rate is 16 in/year:

$$Z = 104.0 \text{ ft} \quad (31.7 \text{ m})$$

and if the recharge rate is 20 in/year:

$$Z = 117.0 \text{ ft} \quad (35.7 \text{ m})$$

Taking the average of all four of the above values yields a figure of 80.3 ft (24.5 m) for the depth to the salt/fresh water interface below mean sea level. Although this gives a range of plus or minus approximately 35 ft (10.6 m) for the location of the interface, this range is

probably within reason considering that this method can give no indication for the thickness of a transition zone. For comparison purposes the height of this well above mean sea level was added to this average for a final value of 86.8 feet (26.5 m).

Presented below are the results of the application of Todd's method in other locations in the study area.

Well # 1

This well is located on Chaypee Hill at an elevation of 27.5 feet above mean sea level and 117 feet from the shore. The radius of the island for this well is 402 feet. The same salt/fresh water density contrast was used for this location as for the example above.

If the hydraulic conductivity is assumed to be 2.3 ft/day and the recharge rate is 16 in/year the depth to the interface is:

$$Z = 58.1 \text{ ft } (17.7 \text{ m})$$

If the recharge rate is changed to 20 in/year:

$$Z = 65.1 \text{ ft } (19.8 \text{ m})$$

Now, if the hydraulic conductivity is assumed to be 0.47 ft/day and the recharge rate is 16 in/year:

$$Z = 128.5 \text{ ft } (39.2 \text{ m})$$

Finally, if the $K = 0.47$ ft/day and the recharge rate is increased to 20 in/year:

$$Z = 144.0 \text{ ft } (43.9 \text{ m})$$

The average of these four values is 98.9 ft (30.2 m) for a range in the depth to the interface of approximately plus or minus 42 feet (12.8 m). For comparison purposes, the height of this well above mean sea level was added to this average for a final value of 126.4 ft (38.5 m).

Well # 4 Plummer's Property

This well is located in the study area where the radius was determined to be 340 feet. The well is located 320 feet from the shore. The depth to water in the well was about 13 feet when measured after the pump had been off for about a half hour. The water yielded from this well is of a good quality. The calculated depth to the salt/fresh water interface is as follows;

With $K = 2.3$ ft/day and recharge = 16 in/year:

$$Z = 69.6 \text{ ft (21.3 m) below msl}$$

With $K = 2.3$ ft/day and recharge = 20 in/year:

$$Z = 77.9 \text{ ft (23.8 m) below msl}$$

With $K = 0.47$ ft/day and recharge = 16 in/year:

$$Z = 153.9 \text{ ft (46.9 m) below msl}$$

With $K = 0.47$ ft/day and recharge = 20 in/year:

$$Z = 172.4 \text{ ft (52.6 m) below msl}$$

The average of these four values is 118.4 ft (36.1 m). The resulting range in the depth to the interface is approximately plus or minus 51 feet or 15.5 meters. Adding the height of the well above msl to this value for

comparison purposes yields 133.4 feet or 40.7 meters to the salt/fresh water interface.

Well # 5 Berg's Property

This well is located near the mouth of the Little River at an elevation of 14.2 feet above mean sea level and 190 feet from the shore. The depth to water in the well was an average of about 12.5 feet during the study period. The well was abandoned in 1983 due to brackish water. The calculated depth to the salt/fresh water interface is as follows;

With $K = 2.3$ ft/day and recharge = 16 in/year:

$$Z = 62.5 \text{ ft (19.1 m) below mean sea level}$$

With $K = 2.3$ ft/day and recharge = 20 in/year:

$$Z = 70.1 \text{ ft (21.4 m) below msl}$$

With $K = 0.47$ ft/day and recharge = 16 in/year:

$$Z = 138.3 \text{ ft (42.2 m) below msl}$$

With $K = 0.47$ ft/day and recharge = 20 in/year:

$$Z = 155.0 \text{ ft (47.3 m) below msl}$$

The average of these four values is 106.5 feet or 32.5 meters below msl. The resulting range for the depth to the interface is about plus or minus 45 ft (13.7 m). Adding the height of this well above mean sea level to this figure gives a final comparison value of 120.6 ft (36.8 m).

Well # 6 Shattuck's New Well

This well is located on Potomska Point 265 feet from shore at an elevation of 15.4 feet (4.7 m) above mean sea level. The water quality from this well has been good since it was first brought into service after a well closer to Buzzards Bay (well #7) pumped salty water about 40 years ago. The depth to the interface was calculated as follows;

With $K = 2.3$ ft/day and recharge = 16 in/year:

$$Z = 88.6 \text{ ft } (27.0 \text{ m}) \text{ below mean sea level}$$

With $K = 2.3$ ft/day and recharge = 20 in/year:

$$Z = 99.3 \text{ ft } (30.3 \text{ m}) \text{ below msl}$$

With $K = 0.47$ ft/day and recharge = 16 in/year:

$$Z = 195.9 \text{ ft } (59.7 \text{ m}) \text{ below msl}$$

With $K = 0.47$ ft/day and recharge = 20 in/year:

$$Z = 219.5 \text{ ft } (66.9 \text{ m}) \text{ below msl}$$

The average of these four values is 150.8 feet or 46.0 meters. The resulting range in the depth to the interface is about plus or minus 61 ft (18.6 m). Adding the height of the well above mean sea level to this value gives a final figure for comparison with the VES interpretations of 166.2 ft (50.7 m).

Well # 7 Shattuck's Old Well

This well is also located on Potomska Point, at an elevation of 25.0 ft (7.6 m) above mean sea level and 324 ft from the shore. This well has not been used in over

forty years since it pumped salty water. Salinity measurements of the water now in this shallow well indicate that the water is fresh with no trace of salt. The depth to the salt/fresh water interface in this location was calculated as follows:

With $K = 2.3$ ft/day and recharge = 16 inches/year;

$Z = 93.7$ ft (28.6 m) below mean sea level

With $K = 2.3$ ft/day and recharge = 20 in/year;

$Z = 105.0$ ft (32.0 m) below msl

With $K = 0.47$ ft/day and recharge = 16 in/year;

$Z = 207.3$ ft (63.2 m) below msl

With $K = 0.47$ ft/day and recharge = 20 in/year;

$Z = 232.3$ ft (70.8 m) below msl

The average of these four values is 159.4 ft (48.6 m) for a range in the depth to the interface of plus or minus 69 ft (21 m). The large range in the depth to the interface at this well as compared with the other locations indicates that for this method, with the range in hydraulic conductivities given, the greater the calculated distance to the interface is the larger the range in the depth to the interface will be. As for the other examples the height of the well above msl was added to the calculated depth to the interface for a final value of 184.4 ft or 56.2 meters to the interface.

Well # 8 Shattuck's Garden Well

This dug well on Potomska Point at an elevation of 21.9 ft (6.7 m) above mean sea level is only 88 ft (26.8 m) from the shore. The water in this well is fresh but is not equipped with a pump. The well is occasionally used to water a garden. The depth to the interface was calculated as:

With $K = 2.3$ ft/day and recharge = 16 in/year;

$$Z = 57.1 \text{ ft (17.4 m) below mean sea level}$$

With $K = 2.3$ ft/day and recharge = 20 in/year;

$$Z = 63.9 \text{ ft (19.5 m) below msl}$$

With $K = 0.47$ ft/day and recharge = 16 in/year;

$$Z = 126.3 \text{ ft (38.5 m) below msl}$$

With $K = 0.47$ ft/day and recharge = 20 in/year;

$$Z = 141.5 \text{ ft (43.1 m) below msl}$$

The average of these four values is 97.2 ft (29.6 m) for a range in the depth to the salt/fresh water interface of about plus or minus 42 ft (12.8 m) below mean sea level. Adding the height of the well above msl to this value yields a final comparison figure of 119.1 ft (36.3 m) for the depth to the interface.

APPENDIX D

Tide Gauge Data for Mean Sea Level Determination

In order to establish mean sea level in the area during the period of the study only, a tide gauge was installed on a dock in the Slocum River. For this purpose a Tsurumi-Seiki recording tide gauge was obtained from the Southeastern Massachusetts University Biology Department. Continuous tide gauge recordings were obtained from August 3, 1983 to September 15, 1983. A sample of a typical tide gauge recording is shown in Figure 35.

Figure 35 shows that periodic measurements were taken, at least one per chart, in order to calibrate the curve to a known distance to the water level. After all the recordings were complete it was necessary to determine the distance from the measuring point on the tide gauge base to all the high and low water levels as indicated on the charts.

The next step taken was the computation of mean sea level. In order to facilitate this calculation a short computer program written in Basic was used. This program was written so that mean sea level could be determined using any amount of consecutive high and low tide readings. This was done so that mean sea level could be determined for both the entire period and also for just one full cycle

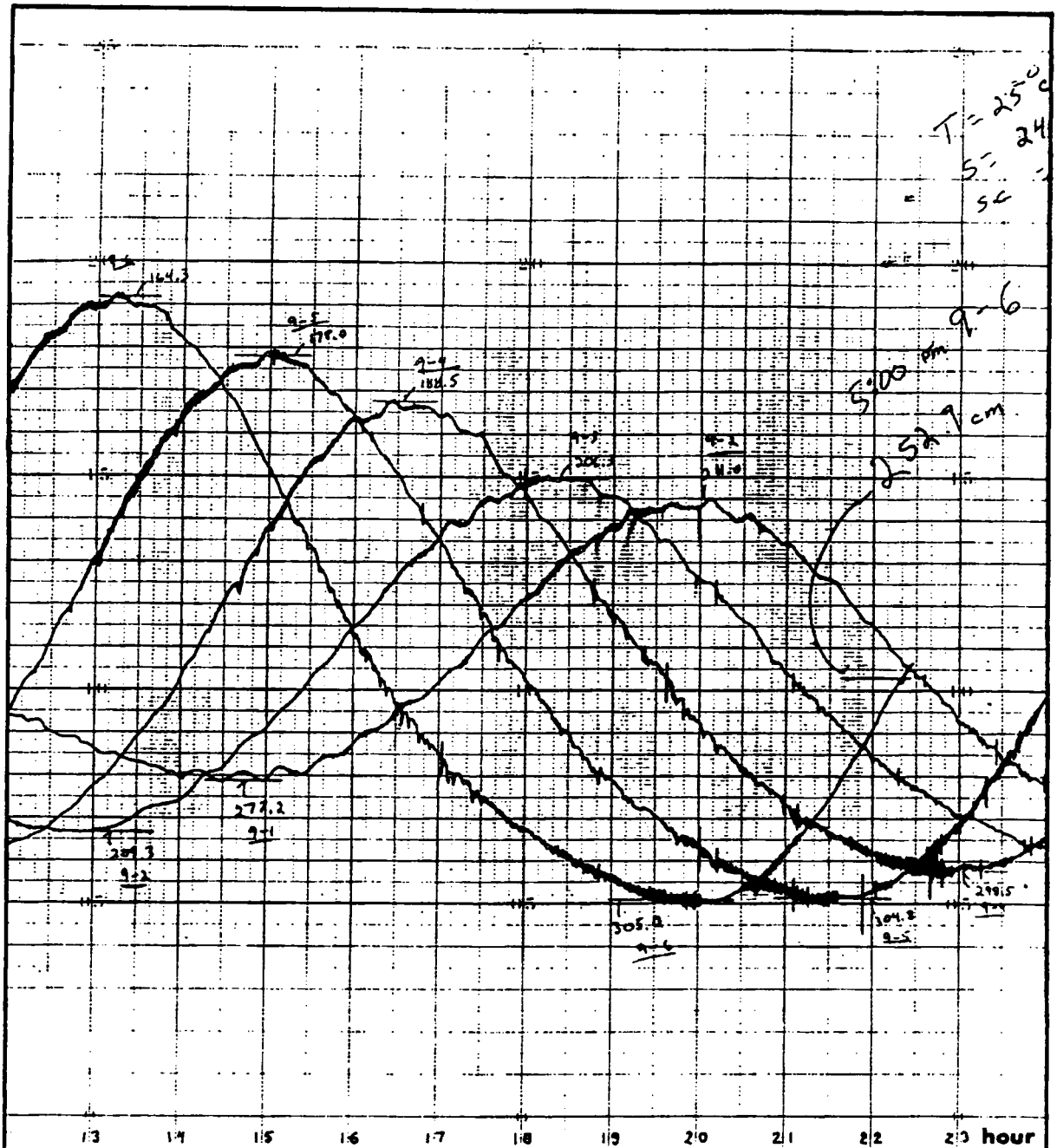


Figure 35. Tide gauge chart recording. The partial record for a five day period is shown. The reading in large print for Sept. 6 at 5 PM was taken in the field to calibrate the chart.

of the moon. A listing of the program and the tide gauge data is included at the end of this appendix.

The depth below the tide gauge base to mean sea level was calculated to be:

237.303 cm for the entire period

237.547 cm for only one full cycle of the moon

For the purpose of this study the difference between these two calculations is insignificant.

```

10     REM     THIS PROGRAM DETERMINES THE MEAN OF SEA LEVEL
20     REM     CHANGES
30     DIM A(171)
40     FOR I=1 TO 171
50     READ A(I)
60     NEXT I
70     SUMAVG = 0
80     PRINT "FIRST SAMPLE # ?"
90     INPUT M
100    PRINT "LAST SAMPLE # ?"
110    INPUT N
120    FOR I = M TO N
130    T = A(I) + A(I+1)
140    AVG = T/2!
150    SUMAVG = SUMAVG + AVG
160    NEXT I
170    ANS = SUMAVG/((N+1)-M)
180    PRINT "ANSWER ="ANS
190    REM     FIRST NO. IS DEPTH TO WATER AT HIGH TIDE,
191    REM     SECOND NO. IS DEPTH TO WATER AT LOW TIDE.
200    DATA 202!,287.5
210    DATA 225!,294.25
220    DATA 198.5,287.5
230    DATA 214.5,291!
240    DATA 189.5,290!
250    DATA 207.5,297!
260    DATA 180!,291!
270    DATA 191!,297!
280    DATA 164!,295.5
290    DATA 183!,301.5
300    DATA 157!,301.5
310    DATA 172!,302.25
320    DATA 147.5,302.75
330    DATA 162.0,304.5
340    DATA 143.5,309!
350    DATA 162!,305.0
360    DATA 154.5,305!
370    DATA 155!,295.25
380    DATA 141!,298.25
390    DATA 162.5,294!
400    DATA 172.75,286.5
410    DATA 163.5,282.5
420    DATA 179.5,288.5
430    DATA 176.75,283!
440    DATA 194.25,284.5
450    DATA 179.5,276!
460    DATA 206.5,285.5
470    DATA 190.25,278.5
480    DATA 215.5,284.5
490    DATA 196.5,279.5
500    DATA 210.75,278.5
510    DATA 190.25,274!

```


520 DATA 202.5,277.5
530 DATA 187!,277.5
540 DATA 202!,281.25
550 DATA 188.25,287!
560 DATA 202.75,284.75
570 DATA 187.75,285.75
580 DATA 194.5,283.5
590 DATA 179.5,285.5
600 DATA 195.5,286!
610 DATA 186!,291.75
620 DATA 198!,295.5
630 DATA 193.75,295!
640 DATA 196!,292.75
650 DATA 197.25,297.5
660 DATA 193!,290.25
670 DATA 197.5,292.5
680 DATA 190.25,287!
690 DATA 200.75,290!
700 DATA 187.75,280!
710 DATA 197.75,289!
720 DATA 188.5,277.5
730 DATA 200!,285.5
740 DATA 185.75,273.75
750 DATA 206.5,273.5
760 DATA 186!,271.5
770 DATA 206.5,280.25
780 DATA 186!,277.2
790 DATA 211.0,288.0
800 DATA 190!,289.3
810 DATA 206.3,294.8
820 DATA 184.8,295!
830 DATA 188.5,298.5
840 DATA 170.5,301!
850 DATA 178!,304.8
860 DATA 160.5,304.2
870 DATA 164.3,305!
880 DATA 150.7,304.2
890 DATA 153.2,305.7
900 DATA 159!,310.2
910 DATA 155.5,307.4
920 DATA 165.5,311.0
930 DATA 156.5,305.8

940 DATA 176.4,302.7
950 DATA 164!,296.8
960 DATA 184.2,292.7
970 DATA 161.2,277.4
980 DATA 189.5,291.5
990 DATA 178.5,278!
1000 DATA 200.4,287.2
1010 DATA 190.5,277.4
1020 DATA 200.4,281.2
1030 DATA 192.5,276!
1040 DATA 207.2,274.5
1050 DATA 195.3
1060 END

APPENDIX E

Well Elevation Survey Data (Chaypee Hill, Wells 1,2and 3)

Station	B.S.	H.I.	F.S.	ELEVATION
Well # 1	1.490	101.490		100.000 m
TP-1A	0.680	99.130	3.04	98.450
Well # 3	1.990	100.860	0.260	98.870
TP-1B	0.250	97.235	3.875	96.985
TP-1C	0.880	94.215	3.900	93.335
TP-1D	1.160	94.205	1.170	93.045
Tide Gauge			0.232	93.973
Well # 2	1.170	11.170		10.000 m
TP-1D	1.160	10.615	1.715	9.455
Tide Gauge			0.232	10.383

Therefore,

$$\begin{aligned} \text{Well \# 1} &= 100.000 - 93.973 \text{ m} \\ &= 6.027 \text{ m above the tide gauge base} \end{aligned}$$

$$\begin{aligned} \text{Well \# 2} &= 10.000 - 10.383 \text{ m} \\ &= 0.383 \text{ m below the tide gauge base} \end{aligned}$$

$$\begin{aligned} \text{Well \# 3} &= 98.450 - 93.973 \text{ m} \\ &= 4.477 \text{ m above the tide gauge base} \end{aligned}$$

Since the tide gauge data from Appendix D indicates that the depth to mean sea level below the tide gauge base = 2.375 m, the elevations of these wells above mean sea level are:

$$\text{Well \# 1} = 6.027 + 2.375 \text{ m} = 8.402 \text{ m} = 27.57 \text{ ft above msl}$$

$$\text{Well \# 2} = 2.375 - 0.383 \text{ m} = 1.992 \text{ m} = 6.53 \text{ ft above msl}$$

$$\text{Well \# 3} = 4.477 + 2.375 \text{ m} = 7.272 \text{ m} = 23.86 \text{ ft above msl}$$

Well Elevation Survey Data - Plumber's Well (#4)

Station	B.S.	H.I.	F.S.	ELEVATION
Well # 4	1.710	101.710		100.000 m
TP-5A	0.450	99.460	2.700	99.010
Dock			2.620	96.840

The tide gauge was too far away to attempt tying in this well with the other wells. Therefore, as an estimate the elevation of this well above the top of a low dock was determined. The top of this dock was estimated to be about four feet above mean sea level.

$$\begin{aligned}
 \text{Well \# 4} &= 100.00 - 96.84 \text{ m} \\
 &= 3.16 \text{ m (10.367 ft) above top of dock} \\
 &= 10.4 + 2.4 \text{ ft} = 14.4 \text{ ft (4.4 m) above msl}
 \end{aligned}$$

Well Elevation Survey Data - Potomska Point

(Wells # 6, 7, and 8)

Station	B.S.	H.I.	I.F.S.	F.S.	ELEVATION
Well # 7	2.515	102.515			100.000 m
TP-2A	1.045	101.960		1.600	100.915
TP-2B	0.790	101.005		1.745	100.215
Well # 8			1.950		99.055
TP-2C	0.190	97.385		3.810	97.195
TP-2D	0.980	95.215		3.150	94.235
TP-2E	0.685	94.705		1.195	94.020
TP-2F	1.660	94.995		1.370	93.335
Tide Gauge				0.232	94.763

Station	B.S.	H.I.	F.S.	ELEVATION
Well # 6	1.035	101.035		100.000 m
TP-3A	1.760	102.335	0.460	100.575
TP-3B	2.265	104.315	0.285	102.050
TP-3C	0.790	103.925	1.180	103.135
TP-2C	0.190	100.305	3.810	100.115
TP-2D	0.980	98.135	3.150	97.155
TP-2E	0.685	97.625	1.195	96.940
TP-2F	1.660	97.915	1.370	96.255
Tide Gauge			0.232	97.683

Therefore,

Well # 6 = 100.000 - 97.683 m
 = 2.317 m above the tide gauge base
 Well # 7 = 100.000 - 94.763 m
 = 5.237 m above the tide gauge base
 Well # 8 = 99.055 - 94.763 m
 = 4.292 m above the tide gauge base

Since the tide gauge base = 2.375 m above mean sea level:

Well # 6 = 2.317 + 2.375 m = 4.692 m = 15.39 ft above msl

Well # 7 = 5.237 + 2.375 m = 7.612 m = 24.97 ft above msl

Well # 8 = 4.292 + 2.375 m = 6.667 m = 21.87 ft above msl

APPENDIX F

Well Gauging Data

The depth to water in the wells in the study area was periodically measured with either a tape measure or with an Oil Recovery Systems' electronic interface probe. This probe uses a combination of optical and conductivity sensors to measure the depth to water and petroleum in observation wells. The depth to liquid measurement is accurate to 0.01 ft with this instrument. The tape measure was only used to determine the depth to water in wells where the surface of the water was very close to the top of the well casing.

The well gauging data coupled with the elevation survey and the tide gauge data was used to determine the height of the fresh water in the wells above mean sea level. In the case of Well #2 the depth to water was determined from the data provided by the continuous water level recording obtained for the Tidal Method. The average depth to water in Well #2 during this period was 3.93 feet (1.2 m). The height of the well above msl is 6.53 ft, therefore, the height of the water in this well above msl is 2.60 feet. However, since the water in well 2 had a salinity of about 9 ppt it was necessary to convert the height of the water column in this well to fresh water head ($H_f = p_s H_s / p_f$). The resulting fresh water head is 2.65 ft. The well gauging data is presented in Table 9.

TABLE 9

Well Gauging Data

Location	Date	Well Elevation	Depth to Water	Water Table Elevation
Well 1	7-14-83	27.57	23.96	3.61 ft
	3-16-84	"	11.01	16.56
Well 2	6-14-83	6.53	3.33	3.20 *
	6-14-83	"	3.96	2.57
	6-24-83	"	3.85	2.68
	6-27-83	"	3.88	2.65
	6-27-83	"	2.94	3.59
	7-14-83	"	2.54	3.99
	7-14-83	"	3.88	2.65
	7-15-83	"	2.79	3.74
	7-15-83	"	2.46	4.07
	7-29-83	"	3.08	3.45
	8-10-83	"	2.63	3.90
	9-1-83	"	3.94	2.59
	9-6-83	"	4.06	2.47
9-17-83	"	3.58	2.95	
10-22-83	"	3.69	2.84	
* Salt water head				
Well 3	* Not accesible for measurements			
Well 4	6-14-83	14.4	14.5	-0.10
	6-17-83	"	12.6	1.8
	6-17-83	"	12.5	1.9

TABLE 9continued

Location	Date	Well Elevation	Depth to Water	Water Table Elevation
Well 5	8-10-83	14.16	12.42	1.74 ft
	9-18-83	"	12.50	1.66
Well 6	6-17-83	15.39	12.33	3.06
Well 7	7-29-83	24.97	5.71	19.26
	8-10-83	"	6.31	18.66
	9-18-83	"	8.45	16.52
Well 8	6-17-83	21.87	9.00	12.87
	7-15-83	"	10.17	11.70
	7-29-83	"	10.79	11.08
	8-17-83	"	11.13	10.74

APPENDIX G

Determining Aquifer Hydraulic Conductivity by the Tidal Method

The tidal method is a technique of analyzing water level fluctuations in a well (that responds to changes in sea level) to determine the aquifer hydraulic characteristics (hydraulic conductivity and specific storage). According to Carr and Van Der Kamp (1969) the amplitude of the tidal fluctuations in a well is smaller than the fluctuations in the sea because only part of the change in load on the aquifer is carried by the water.

The ratio between the amplitude of the tidal fluctuations in the aquifer and the sea is defined as the true tidal efficiency of the aquifer $TE(\text{true})$ and is given as:

$$TE(\text{true}) = a / a + nB \quad (14A)$$

where:

- a = compressibility of the aquifer skeleton
- B = compressibility of the water
- n = porosity of the rock

The specific storage S_s , of an aquifer is defined as the volume of water released per unit volume of the aquifer per unit decline in head. In a confined aquifer it is given by:

$$S_s = s_w(a + nB) \quad (15A)$$

where s_w is the specific weight of water. Combining the

two above equations gives:

$$S_s = nBs_w / 1 - TE \text{ (true)} \quad (16A)$$

Since the values of s_w and B are known, and the porosity n can be either measured or estimated, then the specific storage can be calculated from the true tidal efficiency of the aquifer.

Generally, it is not possible to measure true tidal efficiency directly because wells tapping the subsea portion of confined aquifers are not available. Tidal efficiencies determined from wells inland from the coast must be classified as apparent tidal efficiencies $TE(\text{app})$ because the amplitudes of the tidal fluctuations are less than those for the subsea portion of the aquifer. Observations of tidal fluctuations from inland wells show that their amplitudes gradually decrease as they move inland.

The true tidal efficiency of an aquifer can be determined using a measurement of the apparent tidal efficiency $TE(\text{app})$ and the amount of lag time that is required for a particular tidal wave crest to travel the distance inland to the observation well. The time required for a particular crest to travel a distance x inland is given by:

$$\text{Lag} = x (t_o S_s / 4 \pi K)^{0.5} \quad (17A)$$

where: t_0 = period of the tidal fluctuation
 K = hydraulic conductivity of the aquifer

The amplitude of the fluctuation in freshwater potentiometric head at a distance x inland can be expressed in terms of the apparent tidal efficiency by:

$$TE(\text{app}) = TE(\text{true}) \exp \left[-x \left(\frac{\pi S_s}{t_0 K} \right)^{0.5} \right] \quad (18A)$$

This equation shows that $TE(\text{app}) = TE(\text{true})$ only for $x = 0$. Substituting into this equation for time lag gives:

$$TE(\text{true}) = TE(\text{app}) \exp \left[\left(\frac{2 \pi}{t_0} \right) \text{Lag} \right] \quad (19A)$$

This last equation shows that using measurements of time lag and the apparent tidal efficiency, the true tidal efficiency of the aquifer can be calculated. The calculated value of $TE(\text{true})$ is then used in equation 16A to determine the specific storage S_s of the aquifer.

In order to calculate the hydraulic conductivity of the aquifer equation 17A is rearranged and is solved for K :

$$S_s/K = \frac{4 \pi (\text{Lag})^2}{t_0 (x^2)} \quad (20A)$$

Since S_s is determined independently through equations 16A and 19A, the value of the hydraulic conductivity K can also be calculated from the value of S_s/K .

Corrections for the Effect of the Observation Hole

The water level in an observation well cannot respond immediately and fully to pore pressure changes in the aquifer. Since the tidal time lags and apparent tidal

efficiencies must be determined precisely, the observed time lag and observed tidal efficiency must be corrected for the delaying and damping effects of the observation hole.

Hvorslev (1951) studied this problem in great detail and developed a method of determining the effects of the observation hole. A measure of the inertia or basic time lag of the hole can be obtained by injecting water into the hole and recording the decline of water level with respect to time. The difference between the head of water in the hole and the undisturbed potentiometric head in the surrounding aquifer is called the active head. The basic time lag t_b is defined as the time required for the active head to drop by 63% from any convenient initial value.

The response of the water level in the hole to a sinusoidal fluctuation of potentiometric head in the surrounding aquifer depends on the period of the fluctuation t_o , and the basic time lag t_b of the hole. The response time t_r of an observation hole is defined by Hvorslev (1951) as:

$$t_r = (t_o / 2 \pi) \arctan (2 \pi t_b / t_o) \quad (21A)$$

The corrected tidal time lag (Lag) is given by subtracting the response time from the observed time lag.

Due to the limited amount of time for the response of the change in the water level in a borehole, the amplitude,

A' of the water level fluctuation in the well is smaller than the amplitude A of the potentiometric head fluctuation in the surrounding aquifer. To correct for this effect, Hvorslev (1951) developed the equation:

$$A/A' = [1 + (2 \pi t_b / t_0)^2]^{0.5} \quad (22A)$$

The observed tidal efficiency is multiplied by the factor A/A' to give the apparent tidal efficiency.

Application of the Tidal Method

Theoretically, the time required for a particular crest to travel a distance x inland can be expressed as:

$$\text{Lag} = x (t_0 S_s / 4 \pi K)^{0.5} \quad (23A)$$

The amplitude of the fluctuation at a distance x inland can be expressed in terms of the apparent tidal efficiency as:

$$\text{TE}(\text{app}) = \text{TE}(\text{true}) \exp [-x (\pi S_s / t_0 K)^{0.5}] \quad (24A)$$

This equation shows that TE(app) = TE(true) only for x = 0. Substituting into this equation for time lag gives:

$$\text{TE}(\text{true}) = \text{TE}(\text{app}) \exp [2 \pi \text{Lag} / t_0] \quad (25A)$$

This last equation shows that measurements of time lag and apparent tidal efficiency permit the calculation of a value of TE(true) and of specific storage, S_s through equation 16A. Using the calculated values of these two factors the

hydraulic conductivity of the aquifer may be calculated for by solving for K in equation 23A:

$$K = S_s t_o x^2 / 4 \pi \text{Lag}^2 \quad (26A)$$

Seven days of records of water level fluctuations for Well #2 were obtained (see Figure 36) and related to the tidal records from the gauge on Shattuck's dock. The tidal efficiency was calculated by determining the ratio of the rise or fall in water level in the well to the rise or fall of sea level producing the fluctuation. The time lag was determined by measuring the time between the occurrence of a high or a low water level in the well and the occurrence of the corresponding maximum or minimum in sea level. This data is listed in Table 10. These values are referred to as observed tidal efficiency and observed time lag.

From twenty-four values the average observed tidal efficiency is 28.7%, and the average observed time lag is 34 minutes.

The basic time lag of Well #2 was determined by filling it with water and measuring the decline in active head. Eighteen minutes were required for the head to fall through 63% of its original value. This gives the basic time lag of the well.

The response time of the well for a wave with a period of 750 minutes was calculated from equation 21A using a value of 18 minutes for the basic time lag:

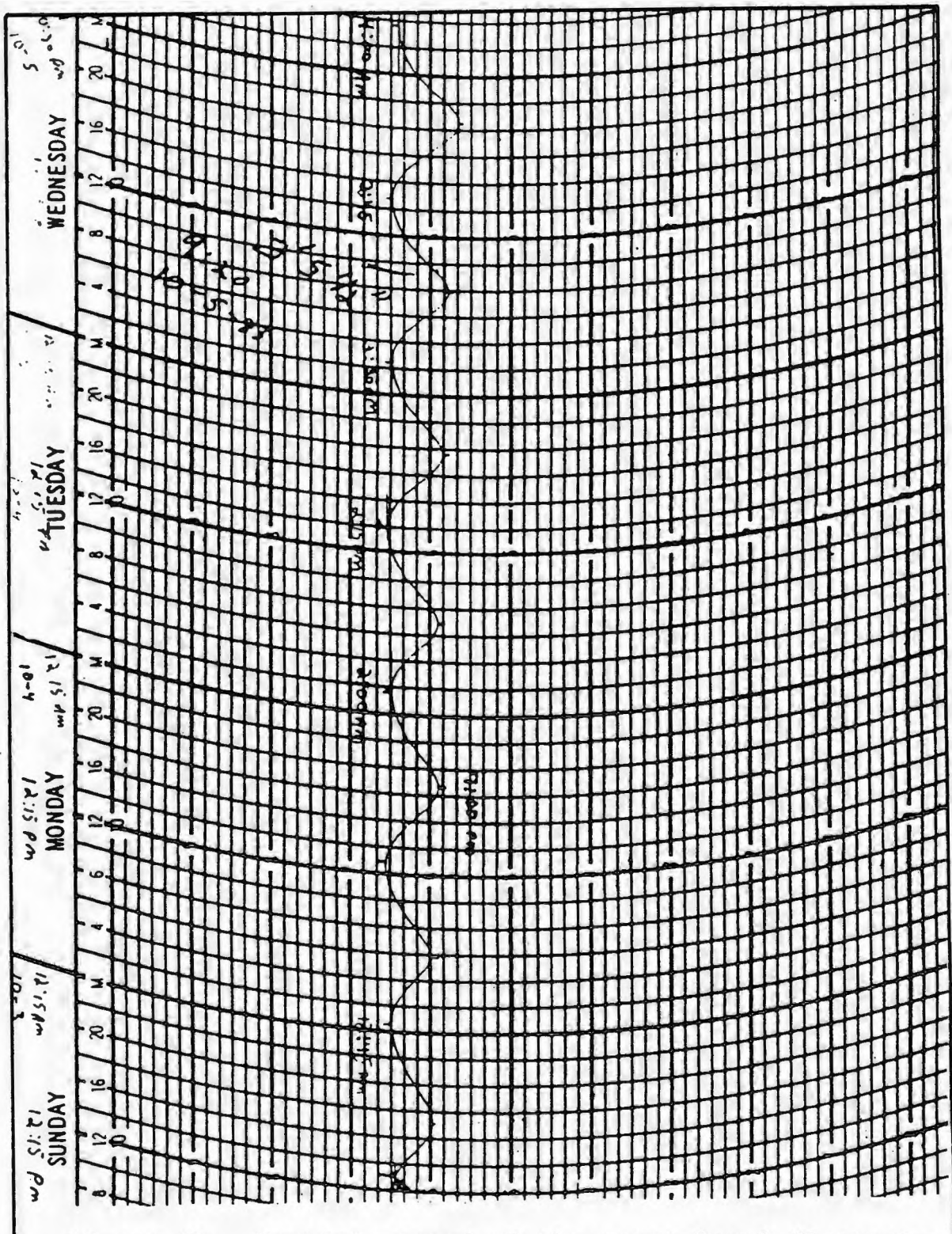


Figure 36. Partial record of the water level fluctuations in Well 2 due to the change in tide in the Slocum River.

$$t_r = (750/2 \pi) \arctan (2 \pi 18 / 750) = 17.8 \text{ minutes}$$

Therefore the corrected time lag of the tidal fluctuations is the observed time lag (34.3 minutes) minus the response time (17.8 minutes) which equals 16.5 minutes.

In order to obtain the apparent tidal efficiency at this site, the observed tidal efficiency was corrected for the damping effect of the well using equation 22A:

$$A/A' = [1 + (2 \pi 18 / 750)^2] = 1.01$$

Therefore TE(app) = 28.7 times 1.01 = 29.02%. If a perfect measuring device existed at Well #2, an apparent tidal efficiency of 29.02% and a time lag of 16.5 minutes would be measured.

TABLE 10

Date of Oct.	Max. or Min.	Tides		Well #2		Observed TE (%)	Time lag min
		Time	Change in water level cm	Time	Change in water level cm		
2	A	1715	113.0	1730	31.75	28.1	15
3	B	0015	111.8	0045	30.48	27.3	30
3	C	0555	114.2	0615	34.29	30.0	20
3	D	1215	127.7	1315	40.69	31.8	60
3	E	1815	128.3	1900	36.83	28.7	45
4	F	0050	127.3	0200	35.56	27.9	70
4	G	0640	131.7	0715	36.83	28.0	35
4	H	1245	140.8	1415	41.91	29.8	90
4	I	1906	136.1	2000	39.37	28.9	54
5	J	0140	144.9	0215	43.18	29.8	35
5	K	0740	145.4	0800	43.18	29.7	20
5	L	1400	156.5	1430	49.53	31.6	30
5	M	2000	149.7	2000	45.09	30.1	0
6	N	0210	145.9	0315	44.45	30.5	65
6	O	0750	157.0	0815	49.53	31.5	25
6	P	1420	139.0	1530	40.00	28.8	70
6	Q	2040	147.4	2040	40.64	27.6	0
7	R	0320	147.4	0345	41.28	28.0	25
7	S	0900	148.1	0900	41.91	28.3	0
7	T	1545	137.9	1630	33.02	23.9	45
7	U	2115	132.8	2115	33.02	24.9	0
8	V	0330	151.1	0345	43.18	28.6	15
8	W	0945	145.3	0945	39.37	27.1	0
8	X	1630	--	1745	--	--	75

Now, from equation 25A:

$$TE(\text{true}) = 29.02 \exp(2 \pi 16.5 / 750) = 33.32\%$$

This value of true tidal efficiency can be substituted into equation 5, but the porosity and compressibility must also be known. Groundwater at 10 degrees C has a compressibility of 2.11×10^{-8} feet squared per pound (Chow, 1964). Based on the yield of the well and on observations of bedrock fracture spacings in outcrops, the porosity of the bedrock was estimated to be in the range of from 1 to 5 percent (0.01 to 0.05). Substitution of these values into equation 16A gives:

$$\begin{aligned} S_s &= 62.4 (0.01) 2.11 \times 10^{-8} / 1.000 - 0.333 \\ &= 1.97 \times 10^{-8} \text{ per foot of aquifer} \end{aligned}$$

Since the distance between the well and the coastline is known to be 275 feet, equation 26A can be solved to obtain a value of K:

$$\begin{aligned} K &= S_s t_0 x^2 / 4 \pi L a g^2 \\ &= 1.97 \times 10^{-8} (750) 275^2 / 4 \pi 16.5^2 \\ &= 3.26 \times 10^{-4} \text{ ft/min} \\ &= 0.47 \text{ ft/day} \quad (0.14 \text{ m/day}) \end{aligned}$$

If the porosity is assumed to be 5% then the hydraulic conductivity of the aquifer would be 2.3 ft per day or 0.70 m per day.

APPENDIX H

Salinity, Temperature and Specific Conductivity Measurements

In order to determine the density of the salt water in the aquifer and in the wells, salinity readings were taken. Since the salinity of the water in the aquifer could not be measured directly, salinity readings were taken of the surface waters in various locations across the study area. It was assumed that the salinity of the water in the aquifer should be no more salty than the average salinity of the water in the surface waters.

Specific conductivity and temperature readings were also taken both as a check for the salinity readings and as a means of calibrating some of the Vertical Electrical Sounding curve interpretations. All readings were taken with a Yellow Springs Instrument Salinity/Specific Conductivity, Temperature meter, Model #33.

The instrument was calibrated according to the instruction manual before and after all the readings were taken. The calibration curve is shown in Figure 37. All salinity readings were corrected using this calibration curve. The readings are listed in Table 11.

The average salinity of the surface waters in the surrounding estuary was found to be 25.19 parts per

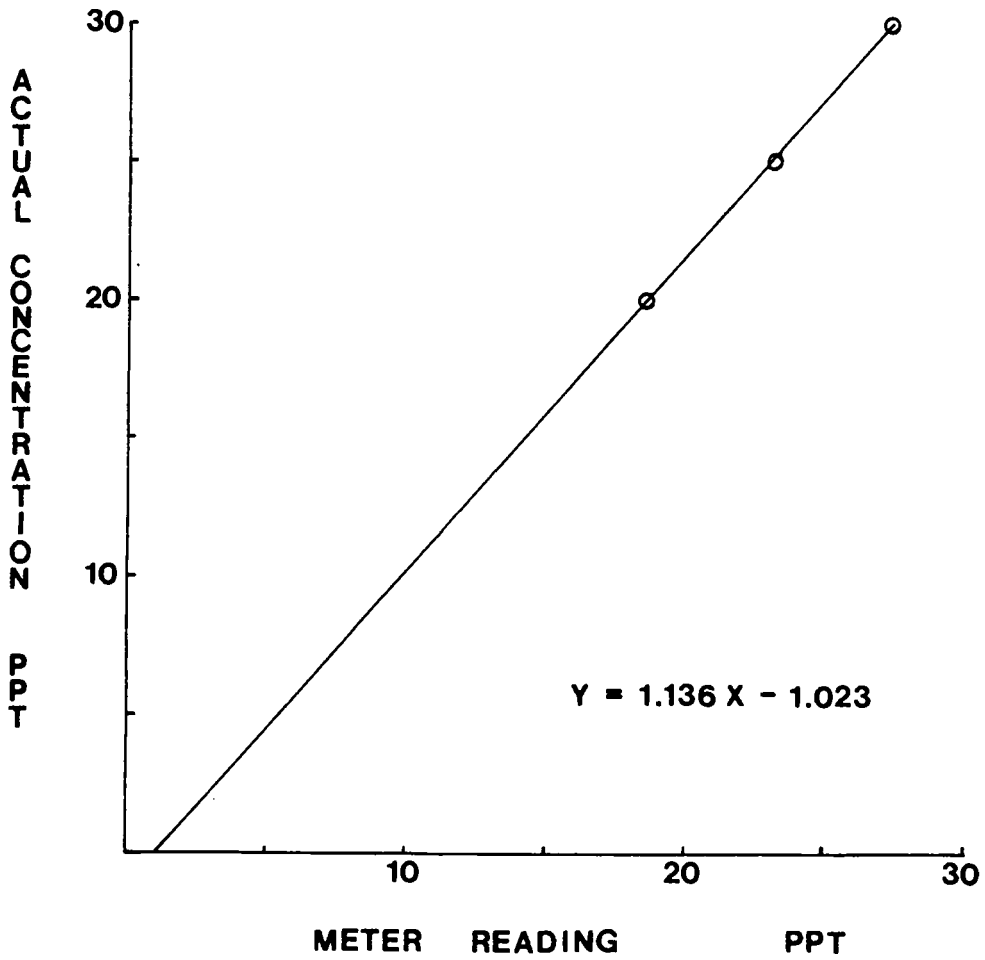


Figure 37. Calibration curve for the salinity meter.

thousand (ppt). Using a standard table the density of water, at 15 degrees C, with this salinity is 1.0185 grams/cc.

TABLE 11

Salinity, Temperature and Specific Conductivity
Measurements

Location	Date	Time	Temp. C	Spec. Cond. umhos/cm	Salinity ppt	Corrected Salinity ppt
Potter dock	4/13/84	1125	10.0	22800	18.83	20.38
Potter dock	4/13/84	1128	9.5	22800	19.10	20.66
Potter drive N	4/13/84	1140	19.0	28600	19.58	21.23
Potter drive S	4/13/84	1142	20.0	31500	21.40	23.27
Shattuck drive	4/13/84	1150	12.8	30000	24.09	26.35
Shattuck dock-top	4/14/84	1650	7.5	26900	23.91	26.57
Shattuck dock-bot.	4/14/84	1653	7.0	27900	25.69	28.17
Shattuck drive	4/14/84	1705	8.0	27000	24.08	26.34
Plummer bridge	4/22/84	1700	9.0	27700	24.33	26.63
Little River	4/22/84	1800	10.5	28000	23.82	26.05
Little River	5/20/84	1250	18.5	33000	23.58	25.78
Potter dock	5/20/84	1300	14.0	32200	25.22	27.64
Potter drive N	5/20/84	1321	15.5	31800	23.83	26.06
Shattuck drive	5/20/84	1327	14.8	33700	25.70	28.16

TABLE 11 Continued.....

Location	Date	Time	Temp. C	Spec. Cond. umhos/cm	Salinity ppt	Corrected Salinity ppt
Little River	5/29/84	1813	17.2	29600	20.79	22.60
Shattuck drive	5/20/84	1821	16.5	3330	24.58	26.91
Plummer bridge	5/20/84	1827	16.2	33800	24.89	27.26
Potter drive N	5/20/84	1843	17.2	30200	21.58	23.50
Well #2	6/17/83	950	10.5	11500	9.2	9.4
Well #1	6/17/83	1000	20.4	2680	2.2	2.2
Well #4	6/17/83	1050	17.5	115	0.0	0.0
Well #6	6/17/83	1130	20.0	222	0.0	0.0
Well #8	6/17/83	1539	12.0	120	0.0	0.0
Well #2	7/29/83	1120	15.5	11000	7.5	7.5
Well #7	8/2/83	1530	16.0	105	0.0	0.0
Well #8	8/2/83	1545	17.0	800	0.0	0.0
Well #5	8/10/83	1125	16.0	520	0.0	0.0
Well #2	9/1/83	930	15.0	9200	6.5	6.5
Well #2	5/20/84	1315	8.5	10000	8.0	8.1

APPENDIX I

Constant Head Permeability Test

The coefficient of permeability, or hydraulic conductivity (K) is a constant of porportionality relating to the ability of a fluid to pass through a porous medium. The constant head method is a laboratory method which is used to determine K directly. The method employs Darcy's Law:

$$v = Ki \quad (27A)$$

and the corresponding flow rate through the sample is:

$$q = KiA \quad (28A)$$

where:

- q = quantity of fluid flow in a unit time
- K = coefficient of permeability (units of velocity)
- i = hydraulic gradient = h/L
- h = differential head across the sample
- L = sample length across which h is measured
- A = cross-section area of soil mass under consideration

This method yields a value for K which will be less than the actual horizontal permeability of the soil in the field and greater than the actual vertical in place permeability. In an effort to obtain the best results possible the in place density of the samples were determined in the field. Then, when the soil samples were tested in the laboratory they were tested at a density both higher and lower than the in place density.

The test was performed according to the procedures outlined in Bowles (1976). The following is a short

description of the method;

1. The volume and cross sectional area of the permeameter was measured.

2. The soil was placed in the permeameter using a moderate compaction effort by hand. A piece of filter paper prevents the soil from escaping from the bottom of the apparatus.

3. A piece of filter paper is cut to size and is placed between the soil and the top cap of the apparatus.

4. The water inlet tube from the constant head reservoir is attached to the top of the permeameter and the exit tube is attached to the bottom and run to a sink. Two ports on the side of the permeameter allow for head measurement across the sample.

5. The sample is saturated by turning on the water supply slowly, so as not to disturb the sample. Water is run through the sample for a period to ensure saturation and to stabilize the conditions.

6. Once the test is begun a measurement of the head across the sample is taken.

7. The time is recorded to collect a specific quantity (Q) of water from the exit port.

8. Compute K from:

$$K = Q L / A h t \text{ cm/sec} \quad (29A)$$

Results

Permeameter:

inside diameter = 2.963" ; radius = 1.4815" = 3.763 cm

height = 8.0625"

volume = $\pi r^2 h = 3.1416 (1.4815)^2 8.0625$

= 55.593 in³

= 911.366 cc

L = 4.013" = 10.193 cm

area = $\pi r^2 = 3.1416 (3.763 \text{ cm})^2 = 44.486 \text{ cm}^2$

Sample #5

In place density = 1.729 grams/cc = 108.04 lb/ft³

Run #1

density = 1.67 g/cc

time to collect 1000 cc = 340 seconds

difference in head across the sample = 9.0 cm

$$K = Q L / A h t$$

$$= 1000\text{cc}(10.193 \text{ cm}) / 44.49 \text{ cm}^2(9.0 \text{ cm})340 \text{ sec}$$

$$= 0.0749 \text{ cm/sec} = 212.3 \text{ ft/day}$$

Run #2

density = 1.67 g/cc

time to collect 1000 cc = 338 seconds

difference in head = 8.6 cm

$$K = 0.0788 \text{ cm/sec} = 223.4 \text{ ft/day}$$

Run #3

density = 1.67 g/cc

time to collect 1000 cc = 340 sec

difference in head = 8.2 cm

$K = 0.0822 \text{ cm/sec} = 233.0 \text{ ft/day}$

Average K for sample #5 - first three runs = 0.0786 cm/sec
= 222.9 ft/day

Sample #5

Run #4

density = 1.78 g/cc

time to collect 1000 cc = 615 seconds

difference in head = 11.7 cm

$K = 0.0318 \text{ cm/sec} = 90.1 \text{ ft/day}$

Run #5

density = 1.78 g/cc

time to collect 1000 cc = 617 seconds

difference in head = 11.3 cm

$K = 0.0329 \text{ cm/sec} = 93.3 \text{ ft/day}$

Run #6

density = 1.78 g/cc

time to collect 1000 cc = 625 seconds

difference in head = 11.0 cm

$K = 0.0333 \text{ cm/sec} = 94.4 \text{ ft/day}$

Average K for sample #5 - second three runs = 0.0327 cm/sec
= 92.6 ft/day

Average K for sample #5 - all six runs = 0.055 cm/sec
= 157.7 ft/day

Sample #4

In place density = 1.918 g/cc = 119.78 lb/ft³

Run #7

density = 1.80 g/cc

time to collect 1000 cc = 695 seconds

difference in head = 24.2 cm

$$K = 0.0136 \text{ cm/sec} = 38.55 \text{ ft/day}$$

Run #8

density = 1.80 g/cc

time to collect 1000 cc = 680 seconds

difference in head = 24.8 cm

$$K = 0.0136 \text{ cm/sec} = 38.55 \text{ ft/day}$$

Run #9

density = 1.80 g/cc

time to collect 1000 cc = 680 seconds

difference in head = 25.2 cm

$$K = 0.0134 \text{ cm/sec} = 37.9 \text{ ft/day}$$

Average K for sample #4 - first three runs = 0.0135 cm/sec
= 38.33 ft/day

An attempt to determine the permeability of sample #4 at a higher density was unsuccessful. It was not possible to obtain a density greater than 1.8 g/cc in the permeameter. There is a possibility that there was an error made in determining the in place density of this sample. The value for the hydraulic conductivity given above for this sample must be assumed to be lower limit for the K of this sample.

APPENDIX J

Soil Porosity

Two soil samples were taken in the study area in order to determine the porosity of the unconsolidated aquifer material. To make this determination it was first necessary to determine the soil water content and the in-place soil density. With these two parameters it was then possible to calculate the void ratio (e) of the soil with the following equation:

$$e = [G_s D_w (1 + w) / D_s] - 1 \quad (30A)$$

where:

- G_s = Specific gravity of the soil (2.68)
- D_w = Density of water
- w = Water content of the soil
- D_s = In - place soil density

With the void ratio the porosity could then be determined with equation 31:

$$n = e / e + 1 \quad (31A)$$

The results of applying these procedures on the two soil samples are shown on the following pages.

Sample A

In - Place Soil Density

Soil volume = 1017 cc

Soil weight = 1950.9 grams

Soil density = $1950.9 \text{ g} / 1017 \text{ cc} = 1.918 \text{ g} / \text{cc}$
 $= 119.73 \text{ lb/cubic feet}$

Soil Water Content

$w/c = (\text{wt. moist soil} - \text{wt. dry soil}) / \text{wt. dry soil}$

$w/c = 0.028 = 2.8 \%$

Soil Void Ratio

$e = [(2.68) 62.4 \text{ lb/ft}^3 (1 + 0.028) / 119.73 \text{ lb/ft}^3] - 1$

$e = 1.436 - 1$

$e = 0.436$

Soil Porosity

$n = 0.436 / 1 + 0.436$

$n = 0.304$

Sample B

In - Place Soil Density

Soil volume = 1177 cc

Soil weight = 2035.1 grams

Soil density = $1950.9 \text{ g} / 1017 \text{ cc} = 1.729 \text{ g} / \text{cc}$
 $= 107.85 \text{ lb/cubic feet}$

Soil Water Content

w/c = (wt. moist soil - wt. dry soil) / wt. dry soil

w/c = 0.0275 = 2.75 %

Soil Void Ratio

$e = [(2.68) 62.4 \text{ lb/ft}^3 (1 + 0.0275) / 107.85 \text{ lb/ft}^3] - 1$

$e = 1.593 - 1$

$e = 0.593$

Soil Porosity

$n = 0.593 / 1 + 0.593$

$n = 0.372$

The average soil porosity from A and B above is 0.338

APPENDIX K

Vertical Electrical Sounding Field Data

TABLE 12

Field Data for VES 1

MN Potential Electrode Spacing (feet)	AB/2 Current Electrode Spacing (feet)	Current (mA)	Voltage Drop (mV)	Apparent Resistivity (ohm-ft)
2.0	3.0	34.0	31000.0	11460.9
2.0	5.0	36.0	14000.0	14777.8
2.0	7.0	33.0	7600.0	17364.8
2.0	9.0	32.0	4450.0	17474.6
2.0	12.0	30.0	2350.0	17595.2
2.0	15.0	38.0	1600.0	14815.1
2.0	20.0	28.0	500.0	11191.9
2.0	24.0	27.0	275.0	9199.4
2.0	30.0	26.0	160.0	8690.2
2.0	40.0	22.0	34.0	3881.7
2.0	50.0	20.0	6.2	1216.8
2.0	50.0	21.0	10.0	1869.2
2.0	60.0	27.0	4.2	879.4
2.0	80.0	44.0	1.9	434.0
4.0	80.0	45.0	2.4	267.9
4.0	80.0	45.0	3.2	357.2
4.0	90.0	42.0	1.2	181.6
4.0	100.0	55.0	1.1	314.1
4.0	100.0	52.0	0.4	60.4
4.0	100.0	54.0	1.7	247.2
4.0	130.0	41.0	0.6	194.2
4.0	160.0	38.0	0.5	264.5
4.0	160.0	38.0	0.4	211.0
4.0	200.0	56.0	0.45	252.4

TABLE 13

Field Data for VES 2

MN Potential Electrode Spacing (feet)	AB/2 Current Electrode Spacing (feet)	Current (mA)	Voltage Drop (mV)	Apparent Resistivity (ohm-ft)
2.0	3.0	92.0	18000.0	2459.3
2.0	5.0	92.0	10000.0	4130.4
2.0	7.0	85.0	6600.0	5854.6
2.0	9.0	87.0	5200.0	7510.7
2.0	12.0	86.0	3700.0	9663.8
2.0	15.0	80.0	2800.0	12314.7
2.0	20.0	79.5	1950.0	15373.1
2.0	25.0	76.0	1300.0	16766.2
2.0	30.0	82.0	1050.0	18082.4
2.0	40.0	77.0	600.0	19571.7
2.0	50.0	68.0	360.0	20781.5
2.0	60.0	62.5	230.0	20804.1
2.0	70.0	56.0	135.0	18551.3
2.0	75.0	49.0	96.0	17307.8
2.0	80.0	40.0	62.0	15579.8
2.0	100.0	36.0	25.5	11125.0
2.0	125.0	65.0	30.0	11327.1
2.0	150.0	58.0	20.0	12186.5
2.0	175.0	48.0	11.0	11023.8
2.0	200.0	44.5	4.5	6353.6
2.0	230.0	20.0	1.15	4778.0

TABLE 14

Field Data for VES 3

MN Potential Electrode Spacing (feet)	AB/2 Current Electrode Spacing (feet)	Current (mA)	Voltage Drop (mV)	Apparent Resistivity (ohm-ft)
2.0	3.0	42.0	15000.0	4489.3
2.0	5.0	29.5	3700.0	4766.0
2.0	7.0	2.3	137.5	4507.6
2.0	9.0	5.3	215.0	5097.5
2.0	12.0	4.5	115.0	5740.2
2.0	15.0	2.4	43.0	6303.9
2.0	20.0	2.8	32.0	7162.8
2.0	25.0	6.3	52.0	8090.4
2.0	30.0	33.0	210.0	8986.4
2.0	40.0	24.0	86.0	9000.3
2.0	50.0	46.0	105.0	8960.1
2.0	60.0	34.0	41.0	6817.2
2.0	80.0	39.0	26.0	6701.0
2.0	90.0	30.0	16.0	6785.6
2.0	100.0	34.0	17.0	7853.0
2.0	125.0	17.0	4.3	6207.8
2.0	150.0	40.0	7.9	6979.8
2.0	175.0	22.0	2.7	5903.7
2.0	200.0	32.5	2.5	4833.1
2.0	250.0	27.0	0.62	2254.4
2.0	300.0	24.5	0.32	1846.5
4.0	300.0	33.0	1.05	2249.0
2.0	350.0	28.0	0.3	2061.7
4.0	350.0	28.0	0.72	2473.9
4.0	400.0	23.5	0.3	1604.2
6.0	400.0	24.0	0.49	1710.3
6.0	500.0	19.0	0.18	1240.0

TABLE 15

Field Data for VES 4

MN Potential Electrode Spacing (feet)	AB/2 Current Electrode Spacing (feet)	Current (mA)	Voltage Drop (mV)	Apparent Resistivity (ohm-ft)
2.0	3.0	38.0	16000.0	5292.6
2.0	5.0	28.0	4250.0	5767.8
2.0	7.0	26.0	2400.0	6960.0
2.0	9.0	26.0	1700.0	8216.2
2.0	12.0	28.0	1100.0	8824.4
2.0	15.0	32.5	990.0	10717.8
2.0	20.0	36.5	720.0	12363.3
2.0	25.0	28.0	370.0	12952.4
2.0	30.0	38.0	380.0	14121.5
2.0	40.0	38.0	220.0	14541.4
2.0	50.0	40.0	150.0	14720.3
2.0	60.0	34.0	88.0	14632.1
2.0	80.0	42.5	54.5	12889.6
2.0	100.0	32.5	25.0	12081.5
2.0	125.0	30.0	13.5	11043.9
2.0	150.0	30.5	9.1	10544.4
2.0	175.0	38.5	8.8	10995.2
2.0	200.0	14.5	2.3	9966.1
2.0	250.0	53.0	4.4	8150.2
2.0	290.0	29.0	1.35	6149.6
2.0	300.0	42.5	1.8	5987.4
2.0	350.0	29.0	0.87	5805.8
2.0	400.0	35.0	0.8	5744.6

TABLE 16

Field Data for VES 5

MN Potential Electrode Spacing (feet)	AB/2 Current Electrode Spacing (feet)	Current (mA)	Voltage Drop (mV)	Apparent Resistivity (ohm-ft)
2.0	3.0	52.5	16000.0	3830.8
2.0	5.0	56.5	8600.0	5784.1
2.0	7.0	55.0	4600.0	6306.2
2.0	8.0	51.0	5600.0	10866.2
2.0	9.0	41.0	4200.0	12872.5
2.0	12.0	32.0	1850.0	12985.8
2.0	15.0	46.0	1950.0	14915.4
2.0	18.0	58.0	1900.0	16620.7
2.0	20.0	66.0	1900.0	18042.8
2.0	25.0	65.5	1400.0	20950.4
2.0	30.0	67.0	1250.0	26346.1
2.0	40.0	56.0	620.0	27808.1
2.0	50.0	36.0	262.0	28568.2
2.0	60.0	60.0	317.0	29868.2
2.0	80.0	36.0	91.0	25407.9
2.0	90.0	43.0	73.0	21599.5
2.0	100.0	33.5	37.5	17581.3
2.0	125.0	48.0	25.0	12782.3
2.0	150.0	47.0	10.25	7707.3
2.0	175.0	43.0	5.5	6152.8
2.0	200.0	35.5	2.7	4778.6
2.0	300.0	16.0	0.20	1767.1

TABLE 17

Field Data for VES 6

MN Potential Electrode Spacing (feet)	AB/2 Current Electrode Spacing (feet)	Current (mA)	Voltage Drop (mV)	Apparent Resistivity (ohm-ft)
2.0	3.0	44.5	10000.0	2824.7
2.0	5.0	58.0	5950.0	3898.3
2.0	7.0	54.5	3400.0	4703.8
2.0	9.0	44.0	1900.0	5426.2
2.0	12.0	59.0	1800.0	6852.2
2.0	15.0	62.0	1400.0	7945.0
2.0	20.0	42.0	640.0	9550.5
2.0	25.0	46.0	510.0	10867.2
2.0	30.0	42.0	345.0	11599.8
2.0	40.0	48.0	235.0	12296.8
2.0	50.0	34.0	100.0	11545.3
2.0	60.0	38.0	62.0	9223.8
2.0	70.0	43.0	54.0	9663.8
2.0	80.0	36.0	35.5	9911.9
2.0	90.0	33.0	24.0	9253.1
2.0	100.0	43.5	24.5	8845.9
2.0	125.0	26.0	8.6	8117.7
2.0	150.0	42.0	9.6	8077.9
2.0	175.0	38.5	5.9	7371.8
2.0	200.0	50.0	5.4	6785.6
2.0	225.0	42.5	3.2	5987.4
2.0	250.0	25.5	1.45	5582.3

TABLE 18

Field Data for VES 7

MN Potential Electrode Spacing (feet)	AB/2 Current Electrode Spacing (feet)	Current (mA)	Voltage Drop (mV)	Apparent Resistivity (ohm-ft)
2.0	3.0	20.0	19000.0	11941.5
2.0	5.0	20.0	7000.0	13300.0
2.0	7.0	20.0	3600.0	13572.0
2.0	9.0	23.0	2650.0	14438.2
2.0	12.0	15.0	1025.0	15347.7
2.0	15.0	16.0	650.0	14293.9
2.0	20.0	13.0	270.0	13017.1
2.0	25.0	12.5	131.0	10272.3
2.0	30.0	14.0	73.5	7413.8
2.0	35.0	12.0	29.0	4646.4
2.0	40.0	8.8	9.3	2654.4
2.0	50.0	14.5	4.85	1312.9
2.0	60.0	11.0	3.1	1593.2
2.0	70.0	18.5	1.25	519.9
2.0	80.0	12.0	0.46	385.3
2.0	80.0	12.0	0.80	670.1
4.0	80.0	12.0	1.5	627.9
4.0	100.0	22.5	0.30	104.7
2.0	100.0	23.0	0.16	109.2
4.0	125.0	13.5	0.08	72.7
4.0	125.0	13.5	0.22	199.9
6.0	150.0	7.2	0.08	130.8
6.0	175.0	12.0	0.12	138.2
6.0	200.0	13.0	0.12	193.3
4.0	200.0	13.0	0.08	193.3

TABLE 19

Field Data for VES 8

MN Potential Electrode Spacing (feet)	AB/2 Current Electrode Spacing (feet)	Current (mA)	Voltage Drop (mV)	Apparent Resistivity (ohm-ft)
2.0	3.0	24.0	22500.0	11784.4
2.0	5.0	26.0	12000.0	17538.5
2.0	7.0	24.0	7400.0	23248.3
2.0	9.0	22.5	5100.0	28482.9
2.0	12.0	21.75	3200.0	33047.5
2.0	15.0	17.0	1650.0	34150.1
2.0	18.0	22.0	1525.0	35169.9
2.0	20.0	20.5	1200.0	36687.8
2.0	25.0	21.5	710.0	32368.7
2.0	30.0	20.5	400.0	27554.1
2.0	40.0	23.5	200.0	21376.2
2.0	50.0	22.0	86.0	15344.7
2.0	60.0	22.5	44.0	11055.3
2.0	70.0	30.0	35.0	8977.8
2.0	80.0	14.0	9.3	6677.1
2.0	90.0	8.5	3.8	5687.9
2.0	100.0	18.0	4.9	4275.5
2.0	125.0	5.2	0.66	3114.9
4.0	125.0	5.1	1.3	3127.3
4.0	150.0	20.0	2.15	1899.4
2.0	150.0	20.0	1.15	2032.1
2.0	175.0	26.0	0.87	1609.6
4.0	175.0	26.0	1.65	1526.2
4.0	200.0	19.0	0.66	1091.2
6.0	250.0	12.5	0.22	575.9
8.0	275.0	16.0	0.29	538.2
10.0	300.0	6.9	0.17	696.4
10.0	350.0	18.0	0.25	534.4

TABLE 20

Field Data For VES 9

MN Potential Electrode Spacing (feet)	AB/2 Current Electrode Spacing (feet)	Current (mA)	Voltage Drop (mV)	Apparent Resistivity (ohm-ft)
2.0	3.0	49.5	28200.0	7161.1
2.0	5.0	50.0	14500.0	10933.0
2.0	7.0	44.0	9000.0	15422.7
2.0	9.0	40.0	6300.0	19797.8
2.0	12.0	42.0	4800.0	25668.6
2.0	15.0	27.75	2500.0	31702.7
2.0	20.0	15.0	770.0	32173.1
2.0	25.0	5.5	160.0	28514.9
2.0	30.0	18.75	285.0	21463.9
2.0	40.0	8.2	38.0	11930.0
2.0	40.0	8.2	46.0	14442.0
2.0	50.0	23.0	46.0	7850.0
2.0	50.0	23.0	58.0	9899.0
2.0	60.0	19.3	19.3	5653.0
2.0	60.0	19.3	22.8	6678.0
2.0	70.0	26.5	13.0	3775.0
2.0	70.0	26.5	14.5	4210.0
2.0	80.0	7.0	1.8	2585.0
2.0	80.0	7.0	2.0	2871.0
2.0	90.0	11.5	1.4	1548.8
2.0	100.0	11.5	0.76	1037.9
2.0	125.0	22.5	0.20	218.2
4.0	125.0	22.5	0.37	205.0
4.0	100.0	9.0	1.17	1024.9
8.0	175.0	16.0	0.10	75.0
8.0	175.0	16.0	0.20	150.0
8.0	200.0	17.0	0.10	92.0
8.0	200.0	17.0	0.50	462.0

TABLE 21

Field Data for VES 10

MN Potential Electrode Spacing (feet)	AB/2 Current Electrode Spacing (feet)	Current (mA)	Voltage Drop (mV)	Apparent Resistivity (ohm-ft)
2.0	3.0	20.5	40000.0	24526.8
2.0	5.0	18.0	18000.0	38000.0
2.0	7.0	16.5	10500.0	47981.8
2.0	9.0	16.0	6200.0	48693.3
2.0	12.0	18.5	3800.0	46138.2
2.0	15.0	21.5	2400.0	39276.3
2.0	20.0	19.0	750.0	24740.1
2.0	25.0	28.0	440.0	15403.1
2.0	30.0	25.0	220.0	12426.9
2.0	35.0	44.0	215.0	9394.5
2.0	40.0	36.5	100.0	6881.3
2.0	50.0	26.5	19.5	2888.5
2.0	60.0	34.0	9.0	1496.0
2.0	60.0	34.0	16.0	2660.0
2.0	70.0	25.5	0.8	241.0
2.0	70.0	25.5	6.6	1991.0
2.0	80.0	12.5	1.4	1126.0
2.0	80.0	12.5	3.0	2412.0
2.0	100.0	14.0	0.9	1010.0
2.0	100.0	14.0	1.4	1571.0
2.0	125.0	14.0	1.4	2454.2
2.0	150.0	22.5	0.42	660.0
2.0	150.0	22.5	3.0	4712.0
2.0	175.0	37.0	0.48	624.0
2.0	175.0	37.0	2.3	2990.0
2.0	200.0	19.5	0.44	1417.0
2.0	200.0	19.5	2.3	7410.0
2.0	250.0	56.0	0.6	1052.0
2.0	250.0	56.0	1.2	2104.0
2.0	300.0	34.5	0.9	3688.0
2.0	300.0	34.5	1.4	5737.0

TABLE 22

Field Data for VES 11

MN Potential Electrode Spacing (feet)	AB/2 Current Electrode Spacing (feet)	Current (mA)	Voltage Drop (mV)	Apparent Resistivity (ohm-ft)
2.0	7.0	16.5	14100.0	64432.7
2.0	7.0	16.5	13800.0	63061.8
2.0	9.0	16.0	65400.0	51363.0
2.0	9.0	16.0	66000.0	51834.8
2.0	12.0	15.5	3200.0	46373.0
2.0	12.0	15.5	3100.0	44924.0
2.0	15.0	7.3	620.0	29883.2
2.0	15.0	7.3	620.0	29883.2
2.0	20.0	13.5	510.0	23677.2
2.0	20.0	13.5	525.0	24373.6
2.0	25.0	12.0	190.0	15519.5
2.0	25.0	12.0	180.0	14702.7
2.0	30.0	16.0	114.0	10061.6
2.0	30.0	16.0	112.5	9929.2
2.0	40.0	15.5	29.0	4699.3
2.0	40.0	15.5	28.3	4585.9
2.0	50.0	15.5	7.2	1823.4
2.0	50.0	15.5	7.05	1785.4
2.0	60.0	24.5	2.4	553.7
2.0	60.0	24.5	2.3	530.7
2.0	70.0	36.0	1.65	352.7
2.0	70.0	36.0	1.42	303.5
2.0	80.0	42.0	1.2	287.2
2.0	80.0	42.0	0.94	224.9
2.0	100.0	33.0	0.63	299.8
2.0	100.0	33.0	0.42	199.9
2.0	125.0	41.0	0.60	359.2
2.0	125.0	41.0	0.44	263.4
2.0	150.0	39.0	0.53	480.3
2.0	150.0	39.0	0.33	299.0
2.0	175.0	59.0	0.45	370.9
2.0	175.0	59.0	0.32	260.9
2.0	200.0	60.0	0.37	387.5
2.0	200.0	60.0	0.22	230.4
2.0	250.0	27.0	0.14	509.0
2.0	250.0	27.0	-0.01	-36.4

Note: The double readings recorded for each AB/2 were obtained by taking a reading with the current flowing in one direction and then in the other.

APPENDIX L

Computer Program For VES Curve Interpretation

```
10 REM PROGRAM TO CALCULATE APPARENT RESISTIVITIES FOR
20 REM SCHLUMBERGER VES CURVES
30 REM THIS PROGRAMS ALSO READS FIELD VALUES FROM AN ARRAY
40 REM AFTER THE RESISTIVITY IS GIVEN AND THEN COMPUTES THE
50 REM RESIDUAL BETWEEN THE COMPUTED VALUE AND THE FIELD VALUE
51 REM
58 DEFINT Z
60 DIM R(10),D(9),T(35),H(11,20)
70 FOR I = 1 TO 11
80 FOR J=1 TO 20
90 READ H(I,J)
100 NEXT J
110 NEXT I
120 DEF FN A(X) = INT (X * 10 ^2)/10^2
130 F = EXP (LOG (10)/8)
140 PRINT "GIVE NUMBER OF LAYERS"
150 INPUT I9
160 I8 = I9 - 1
170 PRINT "GIVE RESISTIVITIES"
180 FOR I = 1 TO I9
190 INPUT R(I)
200 NEXT I
210 PRINT "GIVE THICKNESSES"
220 FOR I = 1 TO I8
230 INPUT D(I)
240 NEXT I
250 PRINT "CASE DESCRIPTION"
260 INPUT N$
270 LPRINT "CASE: ";N$
280 PRINT "CASE:";N$
290 PRINT "LAYER"; TAB(16); "RESISTIVITY"; TAB(32); "THICKNESS"
300 FOR I = 1 TO I8
310 PRINT I,R(I),D(I)
320 LPRINT I,R(I),D(I)
330 NEXT I
340 PRINT I9,R(I9)
350 LPRINT I9,R(I9)
360 LPRINT " "
370 PRINT "ENTER CURVE NUMBER"
380 INPUT CN
390 PRINT "GIVE FIRST ABSCISSA"
400 INPUT X1#
410 PRINT "FIRST ABSCISSA";X1#
420 PRINT "NUMBER OF SAMPLES";
430 INPUT N
440 PRINT "NUMBER OF SAMPLES";N
450 PRINT "APPARENT RESISTIVITY"
460 Y = X1#/822.8
470 FOR J = 1 TO 34
```

```

480 GOSUB 730
490 T(J) = B
500 Y = Y*F
510 NEXT J
520 FOR M = 1 TO N
530 GOSUB 730
540 T(35) = B
550 Y = Y*F
560 S = 42*T(1) - 103 * T(3)+144*T(5)-211*T(7)+330*T(9)-574*T(11)
570 S = S+1184*T(13)-3162*T(15)+10219*T(17)-24514*T(19)
580 S = S+18192*T(21)+6486*T(23)+1739*T(25)+79*T(27)+200*T(29)
590 S = (S-106*T(31)+93 * T(33)-38*T(35))/10000
600 FOR J = 1 TO 34
610 T(J) = T(J+1)
620 NEXT J
630 X = X1# *F^(M-1)
640 X# = FN A(X)
650 S = FN A(S)
667 REM LINE 670 ACCESSES THE FIELD CURVE DATA FOR
668 REM COMPARISON WITH THE POINTS GENERATED BY THE PROGRAM.
669 REM LINE 680 COMPUTES THE DIFFERENCE.
670 HH=H(CN,M)
680 Z=HH-S
690 PRINT TAB (3);"M="M; TAB(15);"X='X!"; TAB(29);"S=";S
      TAB(45) "DELTA ="Z
700 LPRINT TAB(2)"M="M; TAB(15)"X="X!"; TAB (29)"S="S;
      TAB(50)"D= "Z; TAB(64) M
710 NEXT M
720 GOTO 950
730 B = R(I9)
740 FOR K = 1 TO I8
750 I = I9-K
760 U = D(I)/Y
770 IF (5-U) > 0 THEN 800
780 B = R(I)
790 GOTO 830
800 A1 = EXP(U)
810 A2 = (A1-1/A1)/(A1+1/A1)
820 B = (B+A2*R(I))/(1+A2*B/R(I))
830 NEXT K
840 RETURN
849 REM CURVE 1
850 DATA 11460,13000,15000,17400,17500,17000,13500,9500,8700,3900
860 DATA 1200,460,160,185,240,260,0,0,0,0
869 REM CURVE 2
870 DATA 2460,3300,4400,5900,7900,10000,13800,16100,18080,19570
880 DATA 20900,18500,12800,11300,11500,4790,0,0,0,0
889 REM CURVE 3
890 DATA 4490,4600,4700,4500,5200,5800,6600,7600,8990,9000
900 DATA 8250,6700,6790,6900,6400,3200,2000,1600,0,0
909 REM CURVE 4

```

910 DATA 5290,5450,5990,6990,8450,9225,11800,12400,14120,14540
920 DATA 14700,13500,12100,11000,10900,9000,5990,5745,0,0
929 REM CURVE 5
930 DATA 3831,4900,5900,6400,12875,13100,15800,19600,26350,27800
931 DATA 29000,28500,20000,12780,6400,3400,1770,0,0,0
939 REM CURVE #6
940 DATA 3000,3500,4000,5000,5800,7000,8500,10200,11600,12300
941 DATA 10800,9600,9000,8100,7500,6000,0,0,0,0
949 REM CURVE #7
950 DATA 11940,12800,13400,13570,15000,15300,14000,11750,7400,2650
951 DATA 1200,700,260,135,137,220,0,0,0,0
959 REM CURVE #8
960 DATA 11780,15000,18200,23500,29500,34000,35000,35000,27550,21375
961 DATA 14000,8500,4800,3100,1500,750,540,0,0,0
969 REM CURVE #9
970 DATA 24500,30000,38000,48000,48500,46000,32000,19500,12425,6880
971 DATA 2450,1200,1300,2450,2900,3800,4700,0,0,0
979 REM CURVE #12
980 DATA 7160,8800,11200,15450,18800,26500,32000,31500,21460,13190
981 DATA 8000,3900,1300,210,110,47,0,0,0,0
989 REM CURVE #15 601 POTOMSKA RD.
990 DATA 11340,15000,19500,24000,31000,35000,42000,44000,39700,31600
991 DATA 21500,13500,9000,4500,2100,1250,1140,1240,1700,0
1000 END